We thank the editor and reviewers for the timely handling of our manuscript, particularly during these difficult corona times. Please find below our point-by-point responses to each of the reviewer comments, including descriptions of the modifications we have made to the manuscript. Reviewer comments are in black text and our responses are given in blue text. Line numbers refer to the modified version of the manuscript with track changes highlighted.

Anonymous Referee #1

General comments:

This study presents the mass absorption cross-section of BC and the related parameters based on observation at background site. They showed that clear correlation between coating thickness and mass absorption cross-section of BC. One of the relations between lensing effect and mass ratio of BC was well corresponding with simply relation based on recent simulation study which considered some morphological factors. These main results based on observation measurements are of interest and useful to the community. I found that the measurements were conducted and analyzed well carefully. However, some evaluations for factors which concluded as "minor role" seemed to be biased and insufficiently. I felt that measurements and discussions was partly different from that expected in abstract and introduction. I recommend publication of their study after the following expressions are improved.

We thank the referee for his careful review and constructive comments, which we addressed as explained in the responses given below.

Specific comments:

1) "Mixing morphology" in abstract and introduction: "Morphology" sets reader expectation for shape factor, such as aggregation or chain, core-shell or non-spherical, attached or coating, and etc. However, this study did not investigate morphology itself (e.g. microscopic observation) and parameters well-relevant with shape (e.g. particle density and light polarization). In discussion, I found that authors used ratio of inorganic to organic in place of morphology, based on previous knowledge. However, as authors mentioned in discussion, ACSM data contains none of single particle information relating external and internal mixed. Also, organic species in a particle and the phase (liquid or solid) of the particle in the atmosphere relates to formation of the morphology. Therefore, it would be impossible in their measurements to infer and evaluate morphology. I recommend to replace the word into direct expression of measurements such as "ratio of inorganic to organic (in balk particles)" simply. For whole manuscript, some "morphology" relating with mixing states should be revised. "mixing morphology" were used in introduction relating a hypothesis by Cappa et al. (2019), but I could not find the word the literature. The word is not general and gives confusion.

We agree with the referee that "morphology" was used in an imprecise manner in some places. All instances of "morphology" where checked and where needed replaced with more specific terms.

2) Introduction explained that maximal MAC depends on particle morphology and size. Although increase of coating thickness of BC can enhance the lensing effect, the lensing effect of atmospheric

aerosols would be less than that expected by spherical coreshell shaped particles. In addition, coating thickness and morphology (morphology of individual particles and distribution of different morphological variation of particles) can alter in combination by aging process. These are not independent parameter. Inhibition of lensing effect by morphology and size can affect to not only correlation but also slope of relation between MAC and coating thickness. Therefore, the minor or major roles should not be defined by only correlation. The observation period was short. It is unclear that morphological factors in the period changed such to have given variation of the EMAC.

Figures 4 and 7 show that different air mass transport patterns and a considerable range in BC particle properties and sources were observed, suggesting that a fair amount of variability expected in winter time at this rural background site was likely covered during the observation period. We added the qualifier "…rural background site…" in the abstract:
"These results for ambient BC measured at Melpitz during winter show that the lensing effect caused by coatings on BC is the main driver of the variations in MAC_{BC} and E_{MAC}, while changes in other BC particle properties such as source, BC core size or coating composition play only minor roles at this rural background site."
and in the conclusions
"…No evidence was found for cases with absence of lensing effect despite internally mixed BC, as reported in other previous studies. Additional potential drivers of MAC_{BC} variations including dominant BC source, average BC core size and coating composition were also investigated. None of these was found to have a substantial effect at the rural background site Melpitz. However, such effects could potentially be obscured by the lack of single particle information required for more quantitative assessment….".

To what extent can morphology and size effects on the MAC potentially be hidden in a reduction of the slope of the correlation between MAC and coating thickness? Figure 7b suggests that the MAC is largely independent of the modal diameter of the BC core mass size distribution for a constant coating thickness (points of similar color are approximately horizontally aligned). By contrast, MAC varies systematically with coating thickness (the darker the points the higher up). Therefore, we retain our statement that the effects of coating thickness variations on MAC variations clearly dominate the effects of BC core size variations. As for the morphology: lacking particle morphology measurements we cannot directly exclude that BC particle morphology effects strongly affect the slope of the correlation between MA C and coating thickness. However, there is indirect evidence, as explained in the revised manuscript:

In Section 3.5: "Nevertheless, the agreement of the observation of this study with a model based on coated BC particles with morphologies favorable for occurrence of the lensing effect provides indirect evidence that dampening of the lensing effect due to particle shapes with unfavorable morphologies was only minor or negligible for the rural background aerosol at Melpitz in winter."

In the abstract and conclusions: "Indirect evidence suggests that potential dampening of the lensing effect due to unfavorable morphology was most likely small or even negligible."

3) All parameters for aerosols seemed to be measured after passing drier in the study. This point should be noted in abstract, discussion and conclusion. For example, hygroscopicity of BC-containing particle depends on coating composition. If the coating thickness strongly affect the lensing effect, the

deliquescence relative humidity and growth factor depending on the composition can influence on the lensing effect.

Important point. We have made additions to abstract, conclusions, captions of Figures 5&6 and in Section 3.3 in order to emphasize that all measurements are done for ambient aerosol dried to low RH.

4) I could not understand what specific cause and process was expected to different BC source as factor affecting to MACBC. Coating thickness usually increases with aging process. If MACBC is different according to BC source, the difference will be clearer freshly BC before aging. The coating thickness as shown in Fig. S7 was not bi-modal distribution which often found in urban sites, suggesting the BC observed in the site was almost well-aged. It is not surprising that effect by property of BC core in source decrease with increase coating thickness. I think that discussion of BC source should be mentioned with property of the observation site and the aging level of BC.

"…Central European Background site…" is already mentioned in the title and we have added the qualifier "…at this rural background site with a large fraction of aged particles…" to abstract and conclusions in order to emphasize the aged nature of the aerosol.

We also added the following paragraph at the end of Sect. 3.4:
"Despite the fact that atmospheric aging processes tend to make aerosols more homogeneous during transport away from sources, e.g. by increasing the degree of internal mixing, some dependence of MAC_{BC} on BC source could be retained. Possible drivers for such source dependence include differences in BC core size and morphology, in chemical microstructure of the BC, in morphology of the coated BC due to differences in coating processes and/or coating composition. The MAC_{BC} of denuded aerosol samples exhibited very limited variability (Fig. S4b) suggesting that potential differences in MAC_{BC} of bare cores from different sources are small. The analyses presented above further suggest that BC source related differences in MAC_{BC}, which may or may not exist close to sources, largely disappear during transport to the rural background site. The only exception are variations in coating thickness, which have been shown to drive MAC_{BC} variations, and which may have retained some residual relation with BC source."

5) How was relation of MACBC after denuded BC coating to AAE and diameter of rBC? As commented above, I thought that it would be difficult to evaluate these relations after aging proceed.

See response to previous comment.

Technical comment and minor issues:

Abstract:

As commented in specific comments, abstract should be improved for reader to understand contents which were directly used in measurement and evaluation. The conclusion should be limited adequately for atmospheric condition, considering the method and the property of observation site.

We have modified the abstract and conclusions as suggested so that the statements are limited appropriately to the measurement site and methods.

P2L54 “The maximal MAC enhancement factor that can be reached for a particle depends on particle morphology and size, with greater values for smaller particles.” Which are these “particle” meaning “BC core/BC particle” or “BC-containing particle”? The sentence sound not right if they are BC-containing particle because particle morphology and size can alter by aging process.

The statement refers to BC cores. We have modified the sentence on L65 to clarify this: “The maximal MAC enhancement factor that can be reached for a BC core depends on particle morphology and size, with greater values for smaller cores”

Figure S1: What does mean the “all particles”? I wondered about their inconsistence with sum of BC-free particle and BC-containing particle.

‘All particles’ indeed refers to the sum of the BC-free and BC-containing particles. The confusion results from the fact that the BC-free distributions are not shown completely because they overlap with the BC-containing distributions. This was also commented on by Reviewer 2. We have replaced Fig. S1 with a version that makes this more clear by making the distributions semi-transparent so that the entire BC-free size (blue) size distributions can be seen. In addition, we modified the legend so that it is explicitly stated that the ‘all particles’ distributions are the sum of the corresponding ‘BC-free’ and ‘BC-containing’ distributions.

New version of Fig. S1:

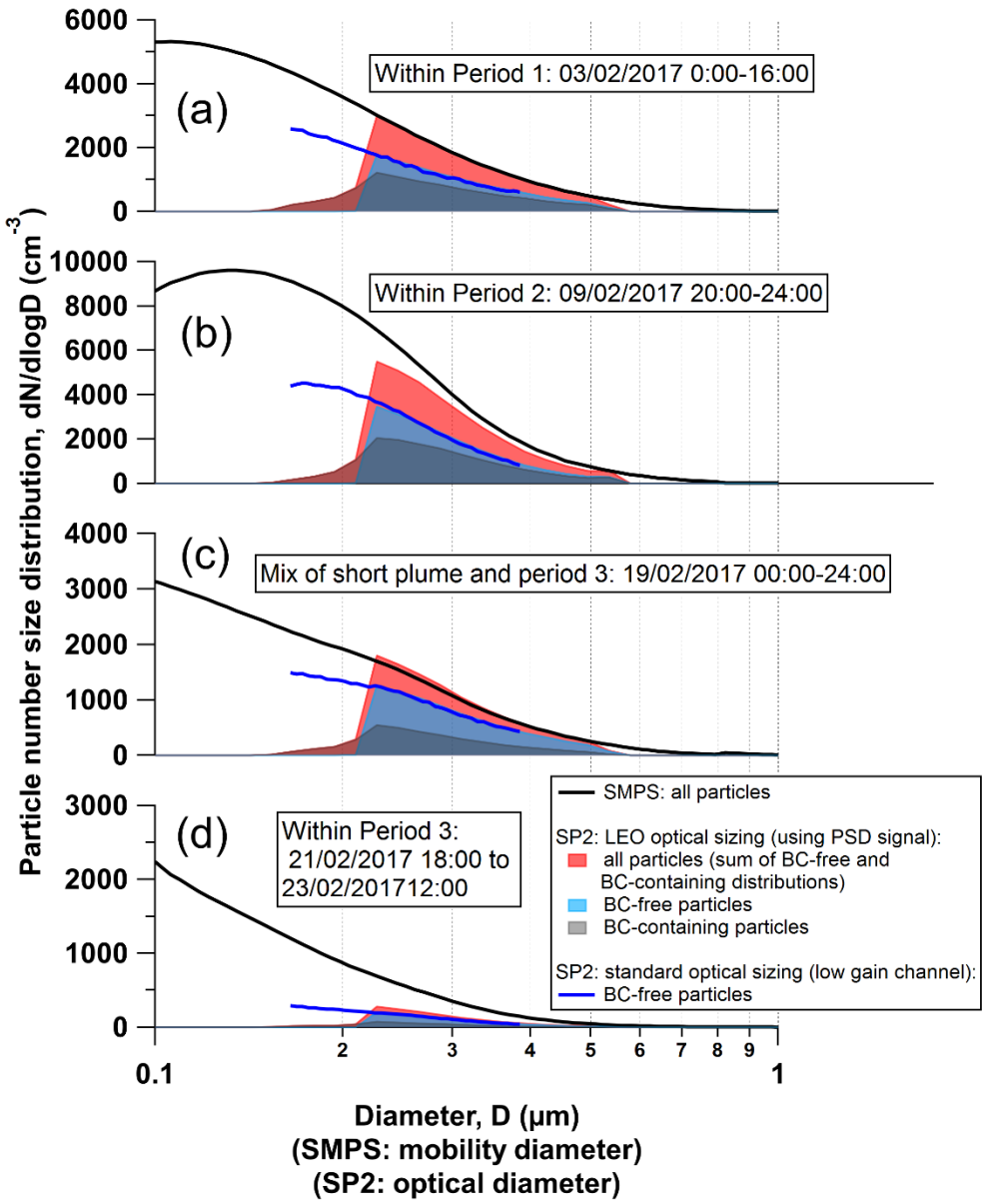

P9L1 “choosing it in this manner ensures bias-free measurements of the coating thickness of uncoated bare BC particles.” I could not understand this sentence until section 2.4.3. (I confused why “uncoated bare BC” have coating?). Also, in this paragraph, “bare BC”, “BC core”, and ”uncoated BC” was used, but their difference was unclear.

We have modified the text in this paragraph to clarify and make consistent the use of the term ‘bare BC core’.

Specifically, on L303 we have changed ‘BC core’ to ‘bare BC core’.

And on L309 we have added a statement in parentheses to clarify the meaning of the sentence: “However, choosing it in this manner ensures bias-free measurements of the coating thickness of bare

BC particles (i.e., this choice results in coating thickness histograms for bare BC particles that are centered around 0 nm)."

P11L309 "Since the MAAP is more robust as an absolute reference,: : :" I cannot agree with this sentence. MAAP measure absorption of cumulative particles on filter. Therefore, the absorption might include more inaccurate lensing effect comparing to that by photo-acoustic spectroscopy.

Section 2.4.2.2 was entirely rewritten in order to clarify our approach to measure the absorption coefficient at high time resolution:
"The absorption coefficient was quantified with a combination of PAX, MAAP and AE33 data. The absorption coefficient measured by the MAAP at λ=637 nm was adjusted to λ=870 nm, using the AAE obtained from the AE33:

$$b_{\mathrm{ap,MAAP,870nm}} = b_{\mathrm{ap,MAAP,637nm}} \times (637/870)^{\mathrm{AAE}(637,870)} \quad (7)$$

The correlation between wavelength-adjusted MAAP data and PAX data is excellent in the range above ~1 Mm^{-1} (Fig. 2). However, the $b_{ap,PAX,870nm}$ measurements are biased systematically lower than the $b_{ap,MAAP,870nm}$ measurements by 31%, which is most likely a result of imprecise and hence inaccurate PAX calibration (Section 2.4.2.1). The MAAP demonstrated good accuracy in several intercomparison studies and it has been shown to have a low instrument-to-instrument variability of less than 5 % (Müller et al., 2011). Therefore, we decided to scale the PAX data by a constant scaling factor of 1.44 [=1/(1-0.31)]. to match $b_{ap,MAAP,870nm}$ as shown in Fig. 2. Application of this constant scaling factor brings the scaled PAX and MAAP measurements into good agreement at absorption coefficients greater than ~15 Mm^{-1}, while the scaled PAX measurements are up to 10% lower than the corresponding MAAP measurements in the range down to 1 Mm^{-1} (as shown by the green crosses in Fig. 2). The scaled PAX data provide absorption coefficients with high time resolution and for both ambient and denuded inlets, with absolute calibration referenced to the MAAP."

Table S1, _P12L330 Please specify instrument information of SO2, NOx and aerosol concentration, and species measured by ACSM, in Table S1 or section 2.2.

We have modified the relevant parts of Sect. 2.2 to include this information.

L180: "The ACSM (Aerodyne Research, MA, US; Ng et al., 2011) measured the near-PM1 bulk chemical composition of non-refractory aerosol species including organics (Org), nitrate (NO_3), sulfate (SO_4), ammonium (NH_4) and chloride (Chl). The ACSM measurements are described as near-PM1 since the instrument inlet has an upper cut-off at an aerodynamic diameter of around 1 µm."

L194: "Concentrations of SO_2 were measured with a UV-Fluorescence instrument (Type APSA 360A, HORIBA Jobin Yvon GmbH, Germany) and NO and NO_2 (NO_x) concentrations were measured with a Trace Level NOx Analyzer (Type 42i-TL, Thermo Fischer Scientific GmbH, Germany)."

P15L394 Probably, “Fig. 05b” is “Fig. S5b”.

Yes, thanks for picking this up. Change made as suggested.

P20LL498 “It is seen that the denuded-MACBC values all fall in the range from 5.6 to 6.0 m2 g-1: : :” However, some yellow dots seem to be >7 m2 g-1, which were probably in gray period of Figure 5. Does the MACBC of denuded BC depend on coating of denuded BC coating?

Firstly, we incorrectly stated that all values fall within the range from 5.6 to 6.0 m2 g-1 (as also noted by Reviewer 2). We have modified the statement to state “…that most of the denuded-MAC_{BC} values fall…” in the stated range (L618).

Secondly, we added a new figure to the supplementary information (Fig. S4) to explicitly show the relationship between the denuded MAC_BC values and the coating thickness of the denuded particles. It is seen that there is no clear correlation between these two variables (Pearson r = -0.29).

The full statement beginning L618 now says: “It is seen that most of the denuded-MAC_{BC} values fall in the range from 5.6 to 6.0 $m^2\ g^{-1}$ (median= 5.8 $m^2\ g^{-1}$) and that the values are largely independent of the original coating thickness, with a Pearson correlation coefficient of only 0.02 (the denuded-MAC_{BC} values are also largely independent of the coating thickness of the denuded particles as shown in Fig. S4, with a Pearson correlation coefficient of -0.29).”

P20LL461 Although authors inferred short residence time as a cause of incomplete remove coating. However, some residuals such as incomplete charring of organic compounds can also remain after passing denuder at 350 degC. The absorption of such charring organics would be slight at 870 nm. However, I think that lensing effect by residuals can appear as some bias of MACBC of denuded BC coating when such residuals presence on BC core.

Actually there is no lensing effect apparent when plotting the denuded-MAC_BC values against the coating thickness of the denuded particles, as discussed in the comment above. We made the statement that the residual coatings on the denuded particles “might still be responsible for a lensing effect” not because we have direct evidence for it, but because we cannot rule it out.

We have modified the statement in question on L628 to try and clarify these points: “The denuded particles retain thin coatings which might still be responsible for a lensing effect. However, such a lensing effect is not apparent when plotting the denuded-MAC_{BC} values against the coating thickness of the denuded particles (Fig. S4). In any case, we consider the median denuded MAC_{BC} of 5.8 $m^2\ g^{-1}$ to represent an upper limit estimate of $MAC_{BC,bare}$”

P26L616 Sorry If I miss the point. Is upper limit of EMAC are MACBC,ambient/5.8? Which is upper limit of EMAC, MACBC,ambient/5.0 (constant) or MACBC,ambient/ MACBC,denuded (time variable)? I recommend to show equations.

Thanks for pointing this out we agree it is useful to clarify explicitly how these quantities were calculated. We have modified the statement on L767 as follows: “Two sets of data points from this study are shown in Fig. 8a: lower limit estimates of E_{MAC} that were obtained with constraining the MAC_{BC} of

bare BC cores by the denuding method (i.e., E_{MAC} = $MAC_{BC,amb}$/5.8 m^2 g^{-1}), and upper limit estimates of E_{MAC} that were obtained with constraining the MAC_{BC} of bare BC cores by the correlation method (i.e., E_{MAC} = $MAC_{BC,amb}$/5.0 m^2 g^{-1}), as described in Sect. 3.3."

P28L668 Which instruments measured the Mtotal and MBC? What particle dose "total" contain? BC-containing particles or whole partilces?

Different instruments were applied in different studies. We only considered studies that quantified non-BC matter internally mixed with BC and BC mass. See next item for clarification of M_{total}.

Figure 8 Please remove "BC mixing state" of x-label because of above confusion.

M_{total} refers to the total particle mass of BC-containing particles. Reviewer 2 also had comments about this quantity and other clarification issues with respect to Fig. 8b. In response to these comments we have made the following modifications to make clarify precisely what this quantity represents and how it related to Rcoat-BC plotted in Fig. 8a.

The caption of Fig. 8 now states: "Figure 8. Summary of E_{MAC} values and their dependence on BC mixing state from this study compared with literature data measured at wavelengths from 532 nm to 870 nm. The E_{MAC} values are plotted versus the ratio of coating to BC core mass (a) and versus the ratio of total particle mass to BC core mass (only considering BC-containing particles) (b). Panel (a) is an updated version of a figure from Cappa et al. (2019), while in panel (b) the abscissa has been changed to M_{total}/M_{BC} to additionally include the simple power-law parameterization of the lensing effect proposed by Chakrabarty and Heinson (2018), which uses M_{total}/M_{BC} as the input parameter to represent BC mixing state (where M_{total} refers to the total mass of the BC-containing particle, such that M_{total}/M_{BC} = 1 + $R_{coat\text{-}BC}$**)**. The two approaches applied to obtain the lower and upper limit E_{MAC} values presented for this study are discussed in Sect. 3.3). Note: the data points from the study of Liu et al. (2015a) deviate marginally from those in the original figure by Cappa et al. (2019), as the abscissa values were recalculated from the original data using material densities for BC and coating material of 1.8 and 1.6 g cm^{-3}, respectively, as applied in this study."

And on L830 of the main text: "The E_{MAC} results from this study and selected ambient literature studies are plotted against BC mixing state expressed as M_{total}/M_{BC} in Fig. 8b (where M_{total}/M_{BC} = 1 + $R_{coat\text{-}BC}$)."

Anonymous Referee #2

General comments:

The authors report on measurements of the relationship between absorption by black carbon and the extent to which the BC particles are coated. Overall, I find this is a nice addition to the existing literature on this topic, and the results appear to be of high quality. I have a number of comments that I think the authors should address before this is accepted for publication. I would ask that they pay particular attention to the comments regarding Fig. 8 as there are a number of aspects that I find unclear about the data presented in this figure.

We thank the reviewer for his/her assessment of our manuscript and the comments provided. We have endeavoured to suitably address each of these comments. We believe this has helped greatly to improve the manuscript by clarifying some important aspects. We took particular care with Fig. 8 and hope the discussion around this figure is now clearer.

Specific comments:

L40: The authors might more accurately state that when BC is freshly emitted it "may be" separated from other species. Some combustion processes emit BC already internally mixed with some other components (e.g. organics). Also, in the next sentence I suggest it would be more precise to say that "particles" coagulate (not "species").

We agree that this is an important qualifier. We have added the word 'often' to indicate that this is not always the case. We also modified the sentence following this to further clarify that we are referring to particles coagulating.

L50: "During the atmospheric aging of BC, non-BC particles coagulate (e.g. particulate sulfate, nitrate, organics) with or gaseous species condense onto BC particles to form a variety of internal mixing states."

L47: I'm not certain that Mie theory deals with "refraction" of light, as the authors state. "Refraction" is more of a geometric optics concept.

We agree that the use of the term 'refraction' here is potentially confusing given the precise definition of the term in geometric optics. We have changed 'refracted' to 'focused' on L58.

L70: The authors might note that the results of Qiu et al. (2012) are outliers among the now numerous lab experiments that indicate notable enhancements occur for size selected BC.

Agreed. We have added the following sentence to the end of this paragraph (L86): "It should be noted that the results of Qiu et al., (2012) are outliers among the more numerous laboratory studies showing notable absorption enhancements."

L80: It seems a bit of a stretch to me to simply state that the SP-AMS is not quantitative owing to variability in detection efficiency, with citing only of the Taylor et al. (2015) paper. This effect has been noted by others in papers that focused on this issue (Willis et al., 2014) and others have used this knowledge to account for the variability in the detection efficiency (e.g., Collier et al., 2018). (I'll also note that Taylor et al. show the SP-AMS/SP2 BC ratio versus the absolute concentration of inorganic species measured by the SP-AMS, not versus the coating-to-BC ratio as implied by the authors use of the term "mixing state" here.) I suggest the authors temper the statement here a bit to indicate that quantification is challenging and care must be taken to account for changes in detection efficiency that might occur as the coating state of the BC changes. Also, it would be useful if the authors would clarify whether they are using "absolute" here to mean the absolute concentrations or the absolute coating

thickness. I believe they mean the latter, based on the discussion in the next paragraph. However, this seems to contradict, somewhat, the authors statement that the SP-AMS does well with the coating-to-core ratio, which is the primary determinant of the coating thickness (if one translates from a mass ratio to a coating amount).

We thank the reviewer for these suggestions and apologize for omitting the relevant references in our initial submission. We have tempered the original statement as suggested by the reviewer, added the suggested references, and clarified that we are referring to absolute mass concentrations of BC cores and their coating material. The revised statement now says (L95): "However, the detection efficiency of BC cores in an SP-AMS is sensitive to BC mixing state, since coatings affect the focusing of BC-containing particles within the instrument, and consequently the degree of overlap between the instrument's laser and particle beams (Taylor et al., 2015; Willis et al., 2014). This complicates the quantification of absolute BC core and coating mass concentrations with the SP-AMS, particularly in ambient campaigns where a wide variety of BC mixing states might be encountered (e.g. Collier et al., 2018)."

L87: Given the citation of the Taylor et al. (2015) paper above, it seems appropriate that the authors here might acknowledge some of the challenges in extracting absolute measures of the coating thickness that result from having to make particular assumptions regarding the BC material properties. (This does come up later, briefly.) Additionally, the SP2 interpretation method inherently assumes spheres yet the particles may not be spherical (as the authors note above), which will affect the accuracy of the method; it seems this should be noted. Also, the authors cite here Laborde et al. (2012a) as justification for "quantitative" coating thickness determination. It is unclear where in that paper coating thickness determination is shown to be quantitative; the paper seems to actually be quite qualitative in terms of coatings. As such, I suggest this reference be clarified, removed, or replaced with a more appropriate reference.

We agree this is a good place to raise this point, especially given its importance. We have modified the statement to make this point and then direct the reader to Sect. 2.4.1, where a detailed discussion of the required assumptions is already provided (we would argue this discussion can't be classified as 'brief', as is also seemingly acknowledged later by the reviewer in their comment on 'SP2 coating determination'). Regarding the Laborde et al., (2012a) citation, it is included here not for justification purposes, but rather as a reference for how such coating thickness calculations can be performed (i.e., for the same reason Gao et al., 2007 is cited). In particular, Section 2.2.1 from Laborde et al. (2012a) details an important modification to the original Gao et al. (2007) procedure for determining coating thicknesses that requires less assumptions on the laser beam profile. That discussion covers some of the key quantitative aspects in determining the scattering cross section required for the coating thickness determination. Therefore, we believe the reference is appropriate and choose to leave it in place.

The modified statements now read (L105): "In addition, incandescence measurements are combined with optical measurements of particle size in the SP2, allowing quantitative measurement of the BC coating thickness under the assumptions of a core-shell morphology for BC-containing particles as well as certain material properties (Gao et al., 2007; Laborde et al., 2012a). The derived coating thickness values are sensitive to these assumptions as discussed in detail below in Sect. 2.4.1 and by Taylor et al. (2015), which necessitates the exercise of considerable care when using the SP2 to perform quantitative coating thickness measurements".

L115: Is it quite correct to state that the MAC is compared to the "BC particle mixing state?" Coating thickness is not exactly mixing state. At minimum, the authors should clarify that they mean "internal mixing state" per their discussion earlier. But I suggest that rather than using "mixing state" here and "infer[ring]" mixing state from coating thickness they just state that they compare with mean coating thickness for particles in a particular size range from the SP2. I feel that the use of the term "mixing state" here serves to confuse rather than clarify, at least for me. The same I find true when the authors state that they determine "mixing state" by thermodenuding. I suggest just stating what specifically was measured, for example (L120) that the authors aim to infer a causal relationship between the lensing effect and the "coating amount" rather than "mixing state."

Although we agree that 'mixing state' is a broader concept then 'coating thickness' alone, we believe that our use of the term 'mixing state' is generally consistent with the relevant literature. For example, in a recent, comprehensive review of aerosol mixing state (Riemer et al., 2019), SP2 measurements of coating amounts are discussed at length with respect to previous studies in a section titled "Other Mixing State Metrics for Measurements and Models" (Sect. 5.3). Therefore, we consider it as accepted usage to refer to such measurements as a metric of BC mixing state. To clarify this point we have added reference to the aforementioned mixing state review on L142: "The relationships between this specific metric of BC mixing state and more general measures of aerosol mixing state (e.g. the mixing state index χ) are discussed in the review of Riemer et al. (2019)".

Riemer, N., Ault, A. P., West, M., Craig, R. L. and Curtis, J. H.: Aerosol Mixing State: Measurements, Modeling, and Impacts, Reviews of Geophysics, 57(2), 187–249, doi:10.1029/2018RG000615, 2019.

L192: The authors note that the SP2 "missing mass correction" will be detailed in a separate paper that is not available for review at this time. Therefore, I suggest that the authors provide at least a short summary of the correction method. For example, was a single campaign average value applied, or did the authors determine a missing mass correction based on three hour averages (as this is their averaging time for the various measurements)? If the latter, noting min/max values (as percents) would seem appropriate. It seems to me that the latter is more appropriate. Certainly, based on the mean values given the missing mass correction details should have small effect, but they should nonetheless be noted here.

Originally a single missing mass percentage was calculated based on the campaign averaged size distribution. Since this value was very low a correction factor was not applied to account for the missing mass. This was not stated clearly in the original manuscript and indeed the opposite was even implied. We apologize for this mistake and the confusion it caused.

As insightfully noted by the Reviewer in their comment on line 562, it is important to consider potential differences in missing mass between the four main periods highlighted during the campaign (described in Sect. 3.1), in order to be able to examine to what extent these differences might contribute to the trends seen in e.g. Fig. 6. Therefore, we have now calculated missing mass percentages for each of the four main periods identified during the campaign. Further, the reviewer also noted in their comment on L562 that a single fitted lognormal mode might potentially underestimate the fraction of missed mass.

We agree that this is a possibility. Therefore, we fitted lognormal modes separately to the upper and lower portions of the mass size distributions to produce more conservative estimates of the missed mass percentages.

We have added a new paragraph at L234 to explicitly discuss each of these points and to explain the full process more clearly (note the cited paper by Pileci et al. has since been made available online in AMTD):
"As discussed by Pileci et al. (2020), there are a number of different methods for quantifying and correcting for the mass of BC outside the SP2 size detection limits (if the user decides to apply a correction at all). These methods are based on extrapolation of SP2-measured BC core mass size distributions. In this study we used the lognormal fit approach. Further, to better represent the upper portion of the size distributions where most of the missing mass appeared to lie (Fig. S5), we fitted lognormal functions separately to the lower ($80 < D_{rBC} < 300$ nm) and upper portions ($230 < D_{rBC} < 600$ nm) of the measured size distributions. The extrapolated portions of these two types of fits are displayed in Fig. S5 for each of the four main periods of the campaign (which are introduced and described in Sect. 3.1). From the extrapolated sections of the fitted curves we estimate the missing mass percentages below the lower LOQ were 1.1, 0.4, 1.6, and 0.8 % for periods 1, 2, 3, and the short plume case, respectively. The corresponding percentages for the missing mass above the upper LOQ were 1.3, 4.9, 4.0, and 26%. Since these estimated percentages are low (less than 5% excepting the small portion of the dataset represented by the short plume case), we chose not to apply correction factors to account for the BC mass potentially missed by the SP2. The possible consequences of this decision are discussed in Sect. 3.3."

We have also replaced Fig. S5 with a new version that displays the extrapolated portions of the lognormal fitted lines that were used to calculate the missing mass percentages. The caption of this figure has also been updated accordingly.

New version of Fig. S5:

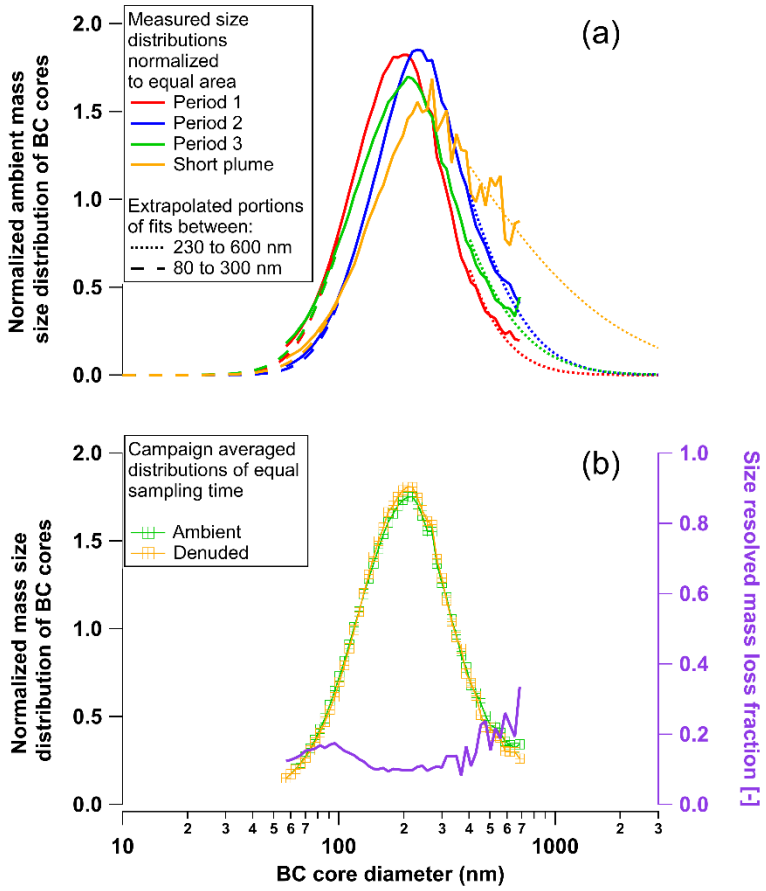

SP2 coating determination: While the details provided here are most certainly important, the authors could probably move most of these details to the supplemental and then note more succinctly in the main text the method used and the key uncertainties.

Although it is a lengthy discussion it was a deliberate decision on our part to include these details in the main text. Our reasoning is that we believe these details are often overlooked in SP2 studies and that, consequently, the complexity of this analysis and the sensitivity of derived coating thicknesses to the various underlying assumptions is often overlooked. We believe it is very important to highlight this complexity and sensitivity, as also suggested by the reviewer in their comment on L87 above. For this reason we would like to keep these details in the main text rather than moving them to the supplemental.

L211: It is unclear to me how Fig. S1 shows that optical diameters are within “a few percent” of the mobility diameters. Are the authors making this statement based on some general similarity in shape? Also, in Fig. S1 I find it unclear whether the red curve is the sum of the blue and the black, as it should be based on the definitions provided. If it is the sum, this means that the entirety of the blue curve is not shown. The authors might consider visual ways to clarify.

The ‘few percent’ stated in the original submission was a mistake on our part. We thank the reviewer for identifying this. As can be seen in Fig. S1 the agreement between the optical and mobility size distributions is clearly not within a few percent. We have recalculated this and find the two distributions generally agree to within 20%, except for the case shown from the end of the campaign with low aerosol loadings where the agreement was within 60%.

We have modified the statement so that it accurately reflects the actual level of agreement. L268 now states: “The refractive index of the particles is assumed to be 1.50+0i, which typically provides optical size distributions that agree within 20 % with corresponding mobility size distributions, excepting some outlying cases when the total aerosol load was very low (Fig. S1)”.

The reviewer is also correct that the red curves are the sum of the corresponding blue and the black curves. The hidden portions of the blue curves also caused confusion for Reviewer 1. To clarify this visually as suggested, we have replaced Fig. S1 with a version where the distributions are semi-transparent so that the entire BC-free size (blue) size distributions can now be seen. In addition, we modified the legend so that it is explicitly stated that the ‘all particles’ distributions are the sum of the corresponding ‘BC-free’ and ‘BC-containing’ distributions.

New version of Fig. S1:

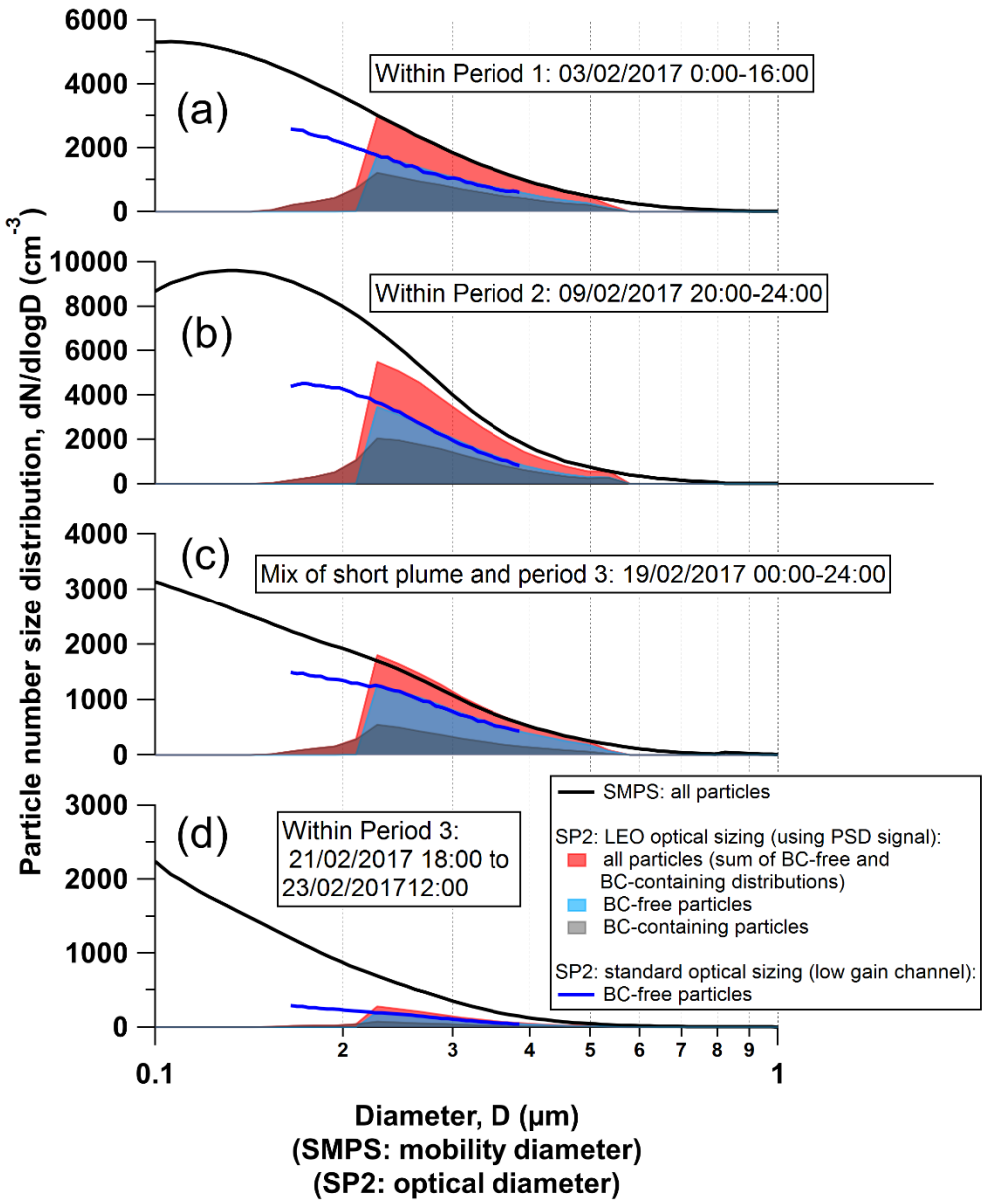

The minimum detectable coating thickness seems to come from Fig. S3b. I suggest that the authors report the +/- 10% and the 10th and 90th percentile bounds as diameter equivalent. I think the +/- 10% line is nominally 10 nm and the 10th/90th percentile is 30 nm.

We're not sure if we have understood this comment correctly, but It is a challenge to report these bounds in diameter units as they will then be a function of size. For example, yes the +/- 10% line corresponds to +/- 10 nm at an equivalent diameter of 100 nm on the 1:1 line, but it is +/- 20 nm at an equivalent diameter of 200 nm, and so on. The same goes for 10/90th percentile bounds, even though these are different in that they are calculated statistics. The primary purpose of the plot is to be able to compare the calculated statistics for each period (medians and 10/90th percentiles) with the 1:1 line and associated +/- 10% bounds. We believe the plot manages to achieve this so elect to leave it as is.

L305: A minor issue, but the authors might clarify whether the AAE values here are the concurrently measured 3-h averages.

Section 2.4.2.2 has been rewritten in response to several comments:
"The absorption coefficient was quantified with a combination of PAX, MAAP and AE33 data. The absorption coefficient measured by the MAAP at λ=637 nm was adjusted to λ=870 nm, using the 3h-averaged AAE data obtained from the AE33:

$$b_{\mathrm{ap,MAAP,870nm}} = b_{\mathrm{ap,MAAP,637nm}} \times (637/870)^{\mathrm{AAE}(637,870)} \quad (7)$$

The correlation between wavelength-adjusted MAAP data and PAX data is excellent in the range above ~1 Mm^{-1} (Fig. 2). However, the $b_{\mathrm{ap,PAX,870nm}}$ measurements are biased systematically lower than the $b_{\mathrm{ap,MAAP,870nm}}$ measurements by 31%, which is most likely a result of imprecise and hence inaccurate PAX calibration (Section 2.4.2.1). The MAAP demonstrated good accuracy in several intercomparison studies and it has been shown to have a low instrument-to-instrument variability of less than 5 % (Müller et al., 2011). Therefore, we decided to scale the PAX data by a constant scaling factor of 1.44 [=1/(1-0.31)] to match $b_{\mathrm{ap,MAAP,870nm}}$ as shown in Fig. 2. Application of this constant scaling factor brings the scaled PAX and MAAP measurements into good agreement at absorption coefficients greater than ~15 Mm^{-1}, while the scaled PAX measurements are up to 10% lower than the corresponding MAAP measurements in the range down to 1 Mm^{-1} (as shown by the green crosses in Fig. 2). The scaled PAX data provide absorption coefficients with high time resolution and for both ambient and denuded inlets, with absolute calibration referenced to the MAAP."

L308: It would be helpful if the authors clarify how a 31% bias translates to a scaling factor of 1.44. Why not 1.31?

See new Section 2.4.2.2 provide in response to the previous comment.

Fig. 2: Visually, it appears that the difference between the 1:1 line and the scaled measurements is largest at intermediate absorption values. It would be useful if the authors were to consider the percent difference as a function of absolute absorption, and comment on how this might (or might not) impact their conclusions here.

Thanks for this suggestion. We have replaced Fig. 2 with a version that displays the residual percentages between the scaled PAX and MAAP measurements. The caption of Fig. 2 has been modified accordingly and on L382 we have added the following sentence: "Application of this constant scaling factor brings the scaled PAX and MAAP measurements into good agreement at absorption coefficients greater than ~15 Mm^{-1}, while the scaled PAX measurements are up to 10% lower than the corresponding MAAP measurements in the range down to 1 Mm^{-1} (as shown by the green crosses in Fig. 2)."

To consider the potential impact of a loading-dependent scaling factor on our conclusions we have added a new supplementary figure to the manuscript, Fig. S10. Panel a) of this figure is equivalent to Fig. 6a, panel b) displays the same quantities but with an additional correction factor of 1.1 applied to the MAC of BC values corresponding to absorption coefficients less than 15 Mm^{-1}, panel c) displays the same quantities but with period-dependent missing mass correction factors applied to the MAC of BC values (as suggested by the reviewer in their comment on L562), and panel d) displays the same quantities but with both the loading-dependent absorption scaling factors and period-dependent missing mass correction factors applied to the MAC of BC values. It is seen that although the spread in the data points increases when the different types of scaling factors are applied to the MAC of BC data, the clear positive relationship between the MAC of BC and mean coating thickness remains. Therefore, these changes have no impact on the main conclusions of the manuscript.

We have added the following sentences on L598 to introduce Fig. S10 and discuss these implications: "To investigate the robustness of the results of the correlation method, Fig. S10 displays versions of Fig. 6a with different scaling factors applied to the underlying quantities used to calculate MAC_{BC}. In particular, we investigated the effect of applying a loading-dependent absorption scaling factor in Fig. S10b (as motivated by Fig. 2 and the discussion in Sect. 2.4.2.2), as well as the effect of applying separate missing rBC mass correction factors for each time period of the campaign in Fig. S10c (as discussed in Sect. 2.4.1). In these cases (as well as the case when both types of scaling factors are applied, Fig. S10d), the positive correlation between MACBC and the mean coating thickness remains, supporting the evidence for an observed lensing effect."

L322: Since the losses are size dependent, and since coating-to-BC ratios are likely size dependent as is the SP2 detection efficiency, the authors might instead state that the losses likely introduced minimal bias, rather than stating categorically that they introduced no bias.

We agree it cannot be categorically proven that no bias was introduced. We have tempered the statement as suggested. L414 now states: "The losses likely introduced only negligible bias in the MAC_{BC} values since the absorption measurement by the PAX was also behind the CS."

L323: The shapes of the particles may have changed upon denuding. Might this impact the determination of coating thickness, as the method assumes spherical particles (even for the BC)?

Coating thickness was exclusively quantified by SP2 data. Denuded data were only used to obtain an upper limit for the MAC_{BC} of the bare BC core. The MAC_{BC} of the bare BC core could be slightly affected by denuding compaction (which could potentially add up to the condensation compaction that already occurred during coating acquisition). However, the systematic bias introduced by residual coatings after denuding is likely larger and this is accounted for by using the denuding and the correlation approaches to obtain upper and lower limits of the MAC_{BC} of bare BC cores (and respective lower and upper limits of the absorption enhancement factor). We added the following statement at the end of Sect. 2.4.3: "Denuding could potentially cause some compaction of the BC cores. However, the denuded sample data were only used to determine the MAC_{BC} of the bare BC cores – more precisely an upper limit of it

due to residual coating – and hence such compaction does not significantly affect the interpretation of our results."

L416: It is not clear to me how Fig. 2 indicates the lower limit of quantification for the PAX. It just shows the relationship between the PAX and MAAP. The limit of quantification typically comes from consideration of the instrument noise when sampling zero particles over the time period of the instrument zeros.

Agreed. The value of ~1 Mm^{-1} is the value quoted by the manufacturer. Our intention was to indicate that Fig. 2 is at least consistent with that. We have modified the sentence on L517 as follows: "(the manufacturer-reported sensitivity of the PAX is <1 Mm^{-1} at 60 secs averaging time, which is consistent with instrument performance demonstrated in Fig. 2)".

L438: It would be helpful if the authors could clarify why they are not considering emissions from biomass combustion, which tend to also produce larger BC cores, instead focusing on coal as the major BC source.

Our original focus on coal emissions stemmed from the discussion in the previous section (Sect. 3.1), where we demonstrated that period 2 was characterized by air mass transport from Poland where high-sulfur content coal is still burned for industrial and domestic purposes. Elevated SO_2 to NO_x ratios were also measured during period 2, supporting the hypothesis that coal emissions were indeed an important source of BC during this period. However, we agree that biomass burning (e.g. wood) emissions might also be explain the larger BC cores observed during this period.

We have modified the discussion on L542 to explicitly mention this alternative (and not mutually exclusive) hypothesis: "The larger BC particles measured in period 2 might be related to coal burning emissions (e.g. lignite coal burning in Poland): while the burning of hard coal briquette emits particles that lie mostly in the nuclei and Aitken mode (20-100 nm), the number size distribution of lignite emissions peaks in the accumulation mode (100-1000 nm) (Bond et al., 2002). Therefore, it is possible that BC cores from lignite burning are larger than BC from other common sources such as traffic. Wood burning emissions from domestic heating are also expected to generate larger BC cores than those emitted by traffic, and thus could also be partly responsible for the generally larger BC cores observed during period 2."

L468: Do the results here change if the authors instead use the median values (rather than the mean)? Or, what if the authors use a geometric average rather than an arithmetic average. The former is typically more appropriate for distributions that are bounded on one side. Here, the coating thickness cannot be <0 nm (within error), and thus the distributions are inherently non-Gaussian but instead more log normal. (Also, Fig. S7 reports the medians. It would be good to see things reported in a common way.)

In general we agree that the median or geometric mean would be a more appropriate statistic for summarizing the coating thickness distribution itself. However, in this case our aim was to calculate an

'ensemble mean' coating thickness value that could be related to the measured absorption enhancement factors (which are ensemble averages by virtue of the way they are measured). Ideally, this would be done by weighting the calculated coating thickness average with the true coating-dependent enhancement factors. However, the true relationship between enhancement factor and coating thickness is unknown (indeed we seek to measure it). Nevertheless, our results suggest that this relationship is linear in fair approximation (Fig. 6a). Therefore, we chose to apply an arithmetic rather than geometric mean to represent the 'ensemble mean' coating thickness values.

In any case, the results do not change substantially regardless of the statistic used. To demonstrate this and to report things more consistently as suggested by the reviewer we have added the arithmetic mean values to the legends in both Figs. S7 and S8. These figures now report both the median and mean values so that the reader is able assess the difference between the two different measures.

Fig. 6: Given that the authors use the standard error of the mean to show their uncertainties here, it would be helpful if they would report the typical instrumental averaging times so that the reader can know how many points go into the 3-h averages. (In other words, are these averages of 1s data? 1 min? 10 min?)

The MAC of BC averages were calculated with 1 min resolution data, while the mean coating thicknesses were calculated with 1 sec resolution data. We have added this information to the caption of Fig. 6, although we note that the standard error of the mean is of course a meaningful quantity on its own. Knowledge of the number of points that go into its calculation is only required if one wished to interpret the standard deviation which is affected by increasing time resolution at the expense of increased random noise of underlying data points.

Fig. 6b: Given that the denuded particles appear to still have coatings, I suggest that it would be helpful to show also a composite plot with the ambient particles versus their coating thickness and the denuded particles versus their coating thickness so that the continuity between these can be seen.

We agree that some readers might find this plot useful (particularly because Reviewer 1 also asked to see it). We have added it as a new figure in the supplementary information (Fig. S4). The figure shows that there is no clear correlation between the denuded MAC_BC values and the coating thickness of the denuded particles

We have modified the statement beginning on L619 to refer to the new Fig. S4: "It is seen that most of the denuded-MAC_{BC} values fall in the range from 5.6 to 6.0 $m^2\ g^{-1}$ (median= 5.8 $m^2\ g^{-1}$) and that the values are largely independent of the original coating thickness, with a Pearson correlation coefficient of only 0.02 (the denuded-MAC_{BC} values are also largely independent of the coating thickness of the denuded particles as shown in Fig. S4, with a Pearson correlation coefficient of -0.29)."

Here is the Fig. S4:

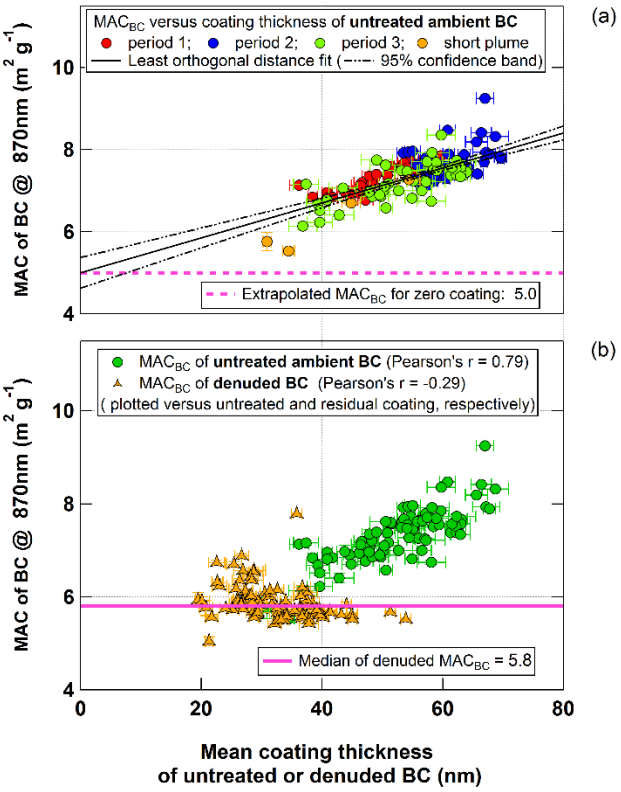

L497: It is not accurate to state that "all" the denuded MAC values fall in the stated range. There are some points that are outside this range. "Most" of the denuded MAC values fall in the stated range.

Agreed. We apologize for the careless wording in the original statement (as also noted by Reviewer 1). We have modified the statement to state "…that most of the denuded-MAC_{BC} values fall…" in the stated range (L619).

L549: Biomass burning emissions also exhibit a wide range of AAE values. Thus, it is not clear why apportionment is appropriate in the biomass burning assumption above but not for coal. It is also not clear why the biomass burning method would provide an "upper limit estimate" for the contributions. How is it specifically known that this is an upper limit?

The difference is that in the case of biomass burning previous studies indicated that the AAE of the typical central European mix of biomass burning aerosol is reasonably constant (e.g. Zotter et al., 2017). To the best of our knowledge no such studies have been performed for central European coal emissions as BC from biomass burning dominates over BC from coal burning in most areas. We have modified the sentence on L676 to include this explanation: "Given the wide range of observed AAE for coal burning emissions, and the lack of knowledge regarding a specific value that is appropriate for central Europe (e.g. as is the case for biomass burning aerosols; Zotter et al., 2017), it is not possible to use measured AAE values to apportion a specific fraction of equivalent BC to coal emissions."

Regarding the upper limit, we suggest these values are upper limits since if a third source was included in the aethalometer model than the contributions from the original two sources would most likely be lower. We have added this explanation to the sentence of L684: "In this case, the contributions of wood burning and traffic to BC as calculated with the aethalometer model and displayed in Fig. S9b should be considered as upper limit estimates, since these contributions would likely be lower if a third source was included in the model."

L 562: I suggest it would be useful for the authors to calculate and report the R2 value when the two clear outlier points are excluded. These correspond to the short period when the BC source was quite different. The Rˆ2 in this case would definitely be >0.01, although still not as large as the relationship with the coating thickness shown previously. Also, I find it a little awkward to note that variability in the BC diameter over the range 150 nm to 250 nm is a "narrow range" but the coating thicknesses, that only varied from _40-60 nm is not "narrow." Also, visually there appears some correlation between the BC diameter and the coating thickness from Fig. 5 (excluding the short plume). Finally, from the size distributions shown in Fig. S5, it would seem that any missing mass correction would be larger for period 2 than for period 3 than for period 1. To what extent might uncertainty in the missing mass correction contribute to the relationships shown? The distributions are close to log-normal, but not quite and thus use of a single mode fit might underestimate the correction that is necessary.

Taking each of the questions in this comment in turn:

The R^2 value with the two outlying points removed is 0.09. The corresponding Pearson correlation coefficient is 0.31. As predicted by the reviewer this is well below the correlation coefficient for the MAC of BC relationship against coating thickness (Fig. 6; 0.79). In addition, the relatively even spread of data points across the full range of measured coating thicknesses lends greater confidence to the latter measurement of correlation. In contrast, the clustering of the data points into two main clouds when plotted against the modal diameter of rBC indicates that the calculated correlation coefficient of 0.31 should be interpreted with caution. Therefore, removing the two outliers has no effect on the conclusions drawn. Nevertheless, we have added the additional measure of R^2 to the parentheses on L694: ". Figure 7b shows that there was no clear relationship between MAC_{BC} and BC core diameter (R^2=0.01, or 0.09 with the two outlying points with the largest modal diameters removed), which indicates that the variation in BC size was not responsible for the MAC_{BC} variability."

Regarding the use of the word narrow, we are not sure at which part of the manuscript the reviewer is referring where the range of measured coating thickness values is described as "not narrow". In any case, we would argue such a description could indeed be appropriate, depending on the context. For example, the range of coating thicknesses measured during this study are broad relative to those that have been measured in other studies using the same technique (e.g. this can be seen by comparing the ambient data shown in Fig. S8 with the compilation of coating thickness histograms presented in Fig. S6 of Motos et al., 2020). In contrast, we consider the rBC core diameter range from 150 to 250 nm to be "relatively narrow" in the context of the discussion that immediately follows on from this sentence. To summarize this discussion, this diameter range corresponds to size parameters from 0.5 to 0.9 at a wavelength of 870 nm, which is not wide enough to extend into the Rayleigh regime at the lower end and the geometric regime at the upper end. In this context, which is already outlined in the paragraph in question, we believe the use of the phrase "relatively narrow" is appropriate.

As described in the response to comment on L192 above, the potential missing mass correction is indeed greater in period 2 than in period 1 (though not greater than in period 3, considering also the potentially missed mass below the lower detection limit). As described above since these missing mass corrections are small (excepting the short plume case) and can't be known with any certainty (since they are calculated from extrapolated curves) we elected not to apply them. To consider the potential impact on the results if these period-dependent correction factors were applied, we added a new supplementary figure (Fig. S10) to the manuscript as described in our response to the comment on Fig. 2 above. This figure shows that although the spread in the data points increases when the different types of scaling factors are applied to the MAC of BC data, the clear positive relationship between the MAC of BC and mean coating thickness remains

We have added the following sentences on L598 to introduce Fig. S10 and discuss these implications: "To investigate the robustness of the results of the correlation method, Fig. S10 displays versions of Fig. 6a with different scaling factors applied to the underlying quantities used to calculate MACBC. In particular, we investigated the effect of applying a loading-dependent absorption scaling factor in Fig. S10b (as motivated by Fig. 2 and the discussion in Sect. 2.4.2.2), as well as the effect of applying separate missing rBC mass correction factors for each time period of the campaign in Fig. S10c (as discussed in Sect. 2.4.1). In these cases (as well as the case when both types of scaling factors are applied, Fig. S10d), the positive correlation between MACBC and the mean coating thickness remains, supporting the evidence for an observed lensing effect."

Motos, G., Corbin, J. C., Schmale, J., Modini, R. L., Bertò, M., Kupiszewski, P., Baltensperger, U. and Gysel-Beer, M.: Black Carbon Aerosols in the Lower Free Troposphere are Heavily Coated in Summer but Largely Uncoated in Winter at Jungfraujoch in the Swiss Alps, Geophysical Research Letters, 47(14), e2020GL088011, doi:10.1029/2020GL088011, 2020.

L567: The authors might note that this is the theoretical result of Mie theory, which might not be fully applicable to fractal-like particles for which absorption by the individual spherules might dominate.

We disagree with this comment. The inverse relationship between MAC of BC and BC diameter for size parameters much greater than 1 is not strictly a result of Mie theory. For example, it also emerges from geometric optics (e.g. Moosmüller and Sorensen, 2018). In addition, the inverse relationship is also observed in numerical computations of the MAC of BC for soot aggregates (Fuller et al., 1999; Mackowski, 1994). Therefore, we think it is appropriate to leave this general statement as is.

Fuller, K. A., Malm, W. C. and Kreidenweis, S. M.: Effects of mixing on extinction by carbonaceous particles, Journal of Geophysical Research: Atmospheres, 104(D13), 15941–15954, doi:10.1029/1998JD100069, 1999.

Mackowski, D. W.: Calculation of total cross sections of multiple-sphere clusters, J. Opt. Soc. Am. A, JOSAA, 11(11), 2851–2861, doi:10.1364/JOSAA.11.002851, 1994.

Moosmüller, H. and Sorensen, C. M.: Small and large particle limits of single scattering albedo for homogeneous, spherical particles, Journal of Quantitative Spectroscopy and Radiative Transfer, 204, 250–255, doi:10.1016/j.jqsrt.2017.09.029, 2018.

L578: I would suggest the authors go a bit further and argue that it is very likely that the coating amounts differed, as no attempt was made in that study to ensure that the particles had the same amount of coating.

Agreed. We have modified this sentence slightly to reflect this (L716): "However, it should be noted that the amount of coating could not be quantified conclusively in these experiments, and therefore it must be considered likely that the coating volume fractions differed for the different coating compositions."

Fig. 8 and origin of Ueda et al. (2016) data: The authors show results from Ueda et al. (2016) in this figure. In their caption they note that the points shown might differ from those shown in Cappa et al. (2019). However, in looking at Cappa et al. (2019) the Ueda et al. data are not included. As such, it is unclear where these data come from. Looking at the Ueda et al. (2016) paper directly, there is no indication that values of R_coat-BC are available in a general sense. At best, it would seem that up to four data points might be included, corresponding to the periods A-D in Ueda et al. (2016). It looks like the authors used the mean volume fraction of soot for particles in varying size ranges and with varying number of particles analyzed (per Ueda et al., Table 3) to calculate the volume fractions. For one of these periods (C), only 6 particles were analyzed, calling into question the statistical significance of any volume fraction. As for the Eabs values, did the authors use the 400 degC results reported? Or did they calculate an estimated Eabs based on the reported [BC] and absorption at 781 nm? I suspect the former, but it might be noted that if one assumes a constant MAC for uncoated BC and calculates an Eabs from the reported measurements, the thus derived Eabs does not match with the value derived from heating to 400 degC in terms of their apparent dependence on the coating volume fraction.

We agree with these concerns about the Ueda et al., data as represented in this plot. The reviewer is correct that for one of the data points only 6 BC particles (with diameters < 600 nm) are included in the calculation. As suggested, this makes it difficult to determine a representative BC volume fraction that corresponds to the overall absorption. For the Eabs calculation, the 400 degC results at 781 nm were indeed used (Table 2 of Ueda et al.), and we agree that the elevated temperature needs to be taken into consideration. Including all these caveats in the description of Fig. 8 obscures the overall message of the figure without adding any additional insight. Therefore, we decided to remove the Ueda et al., data from Fig. 8 in the revised manuscript.

Fig. 8b: It is unclear whether the x-axis is really the total NRPM-to-BC ratio for all studies shown. For some of the studies, the x-axis values in panel b appear the same as in panel a, which cannot be the case unless all NRPM is internally mixed with BC. But for other studies the relationship differs. Additionally, it is also not clear for the current measurements that the x-axis is correct. Looking at Fig. 2, the BC fraction ranges from about 0.04 to 0.22, excluding the short plume. The NRPM/BC ratio should just be (1-BCfraction)/BCfraction, and so should range from approximately 3.5 to 24. But the data shown in Fig. 8b only range from 2-4 for the current study. I suggest that clarification is needed. Perhaps I am just

misunderstanding the relationship between the R_coat-BC and M_total/M_BC as used here. Or misunderstanding what the authors mean in the figure caption when they note that the M_total/M_BC is a "free parameter." Free in what way? (As a minor note, inclusion of ticks between 1 and 2 on the y-axis would be helpful to the reader.)

We thank the reviewer for pointing out these points where clarification is required. The quantity plotted on the x-axis of Fig. 8b is the ratio of the mass of the total particle to the mass of BC in the BC-containin particle, not the NRPM or coating to BC mass ratio. This is quantity is related to $R_{coat\text{-}BC}$ (from Fig. 8a) according to: $M_{total}/M_{BC} = 1 + R_{coat\_BC}$. It was described as the 'free parameter' in the Chakrabarty and Heinson parameterization in the sense that it is the independent, input parameter to this function. We agree the use of the word 'free' can be confusing. To clarify these points we have made the following additions:

The caption of Fig. 8 now states: "Figure 8. Summary of E_{MAC} values and their dependence on BC mixing state from this study compared with literature data measured at wavelengths from 532 nm to 870 nm. The E_{MAC} values are plotted versus the ratio of coating to BC core mass (a) and versus the ratio of total particle mass to BC core mass (b). Panel (a) is an updated version of a figure from Cappa et al. (2019), while in panel (b) the abscissa has been changed to M_{total}/M_{BC} to additionally include the simple power-law parameterization of the lensing effect proposed by Chakrabarty and Heinson (2018), which uses M_{total}/M_{BC} as the input parameter to represent BC mixing state (where M_{total} refers to the total mass of the BC-containing particle, such that $M_{total}/M_{BC} = 1 + R_{coat\text{-}BC}$). The two approaches applied to obtain the lower and upper limit E_{MAC} values presented for this study are discussed in Sect. 3.3). Note: the data points from the study of Liu et al. (2015a) deviate marginally from those in the original figure by Cappa et al. (2019), as the abscissa values were recalculated from the original data using material densities for BC and coating material of 1.8 and 1.6 g cm^{-3}, respectively, as applied in this study."

And on L830 of the main text: "The E_{MAC} results from this study and selected ambient literature studies are plotted against BC mixing state expressed as M_{total}/M_{BC} in Fig. 8b (where $M_{total}/M_{BC} = 1 + R_{coat\text{-}BC}$)."

We have verified the correctness of the x-axis values in Fig. 8b. We believe confusion resulted from the fact that Mtotal/MBC was not adequately defined as being equal to 1 + Rcoat-BC. Due to the log x-axis, this means Rcoat-BC values greater than 10 don't seem to have moved much by eye when transformed to the Mtotal/MBC axis. The change is more noticeable, however, for the smaller Rcoat-BC values between 1 and 10, and even more so for values less than 1.

Regarding the measurements from this study specifically, we have also verified that these calculations are correct. The reviewers reasoning is essentially correct. However, confusion was caused by a mistake in Fig. 5d. The y-axis label of this figure mistakenly described the BC volume fraction as a percentage, not a fraction. Thus, the volume fractions from 0.2 to 0.4 correspond to Mtotal/MBC values of ~2 to 4 (assuming coating and BC core material densities of 1.6 and 1.8 g/cm3, respectively). We have corrected Fig. 5 so that the '%' symbol has been removed from the axis label.

Finally, we have added minor ticks between 1 and 2 on the y-axis of Fig. 8 as suggested by the reviewer.

L638: I suggest it would be helpful for the authors to be more explicit about the SP-AMS here. The introduction section does not indicate that the coating-to-core ratio from the SP-AMS should depend strongly on the coating amount but instead notes that absolute quantification of concentrations depends on the coating amount. How does a change in the collection efficiency affect the ratio, rather than the absolute values? Also, they might note that the laboratory studies that have looked at this effect find that above a coating-to-core ratio of _3 that the collection efficiency is effectively constant, and some of the studies shown do have coating-to-core ratios this large.

We agree that these are important clarifications and that our initial statement was overly simplistic. A change in collection efficiency could affect the ratio Rcoat-BC if the change in apparent efficiency was different for the non-refractory coating material and the BC core (e.g. as appears to be the case for organic coatings as shown in Fig. 2 of Willis et al., 2014, a reference mentioned by the reviewer above). Regarding the point that collection efficiency of the SP-AMS appears to be constant for Rcoat-BC values greater than 3, we believe the reviewer is referring to the same Fig. 2 of Willis et al., 2014. If so, this statement is then only based on 2-3 data points. Therefore, we do not feel comfortable generalizing this result to all the measured values greater than 3 displayed in Fig. 8a.

All in all, we feel that such detailed discussions of SP-AMS measurements are beyond the scope of this manuscript, given that the study is based on SP2, not SP-AMS measurements. We believe the most important point is that some differences are indeed observed between the two types of studies shown in Fig. 8b, which motivates the conclusion that dedicated, follow-up intercomparison studies are required. To focus on this point we have removed the sentence about SP-AMS collection efficiency. L789 now simply states: "It is noteworthy that the majority of SP-AMS-based studies observed only a weak lensing effect".

L640: This is a really great point, that I suggest the authors re-emphasize specifically in their conclusions.

As suggested we have re-emphasized this point in the conclusions section. L869: "In addition to this challenge, follow up studies should aim to intercompare different techniques for measuring BC volume fractions (e.g. SP2 versus SP-AMS measurements of $R_{coat\text{-}BC}$)."

In their discussion of physical explanations for the differences between studies, the authors might note that some of the studies are more likely to be impacted by local sources and some by particles that have undergone long-range transport. The latter might tend to homogenize the population, which could affect the observable absorption enhancement.

As suggested we have added a sentence about this on L813: "The interplay of these different effects and the resulting observable enhancement are likely to depend on the ratio of fresh to aged BC particles in a given air mass, and will therefore vary from site to site."

L681: The sentence beginning "The enhancement: : :" does not seem to be a complete sentence.

Thanks for picking this up. We have changed this sentence L847 to: “The enhancement of light absorption by BC due to coatings varied from 1.0 to 1.6 (lower limit estimates), or 1.2 to 1.9 (higher limit estimates), for mean BC volume fractions that varied from 46 to 22 % (for BC core sizes from 200 to 220nm)”.

L691: It is not overly clear to me how “such effects” might be obscured here. What do the authors mean when they indicate “a more quantitative assessment?” Do they mean calculated across the entire size distribution?

We have modified this sentence to clarify that we are referring to quantitative assessment on the single particle level, L861: “However, such effects could potentially be obscured by the lack of single particle composition and morphology information that would be required for a single-particle level quantitative assessment.”

References

Collier, S., Williams, L. R., Onasch, T. B., Cappa, C. D., Zhang, X., Russell, L. M., Chen, C.-L., Sanchez, K. J., Worsnop, D. R., and Zhang, Q.: Influence of emissions and aqueous processing on particles containing black carbon in a polluted urban environment: Insights from a soot particle – aerosol mass spectrometer, Journal of Geophysical Research-Atmospheres, 123, 6648-6666, https://doi.org/10.1002/2017JD027851, 2018.

Taylor, J. W., Allan, J. D., Liu, D., Flynn, M., Weber, R., Zhang, X., Lefer, B. L., Grossberg, N., Flynn, J., and Coe, H.: Assessment of the sensitivity of core / shell parameters derived using the single-particle soot photometer to density and refractive index, Atmos. Meas. Tech., 8, 1701-1718, https://doi.org/10.5194/amt-8-1701-2015, 2015.

Willis, M. D., Lee, A. K. Y., Onasch, T. B., Fortner, E. C., Williams, L. R., Lambe, A. T., Worsnop, D. R., and Abbatt, J. P. D.: Collection efficiency of the soot-particle aerosol mass spectrometer (SP-AMS) for internally mixed particulate black carbon, Atmospheric Measurement Techniques, 7, 4507-4516, https://doi.org/10.5194/amt-7- 4507-2014, 2014.

Variability in the mass absorption cross-section of black carbon (BC) aerosols is driven by BC internal mixing state at a central European background site (Melpitz, Germany) in winter

Jinfeng Yuan[1], Robin Lewis Modini[1], Marco Zanatta[2], Andreas B. Herber[2], Thomas Müller[3], Birgit Wehner[3], Laurent Poulain[3], Thomas Tuch[3], Urs Baltensperger[1] and Martin Gysel-Beer[1]

[1]Laboratory of Atmospheric Chemistry, Paul Scherrer Institute, Forschungsstrasse 111, 5232 Villigen PSI, Switzerland
[2]Helmholtz Center for Polar and Marine Research, Alfred-Wegener-Institute, Am Handelshafen 12, 27570 Bremerhaven, Germany
[3]Leibniz Institute for Tropospheric Research, Permoserstraße 15, 04318 Leipzig, Germany

Corresponding author: Robin Lewis Modini (robin.modini@psi.ch)

Abstract. Properties of atmospheric black carbon (BC) particles were characterized during a field experiment at a rural background site (Melpitz, Germany) in February 2017. BC absorption at a wavelength of 870 nm was measured by a photoacoustic extinctiometer and BC physical properties (BC mass concentration, core size distribution and coating thickness) were measured by a single-particle soot photometer (SP2). Additionally, a catalytic stripper was used to intermittently remove BC coatings by alternating between ambient and thermo-denuded conditions. From these data the mass absorption cross section of BC (MAC_{BC}) and its enhancement factor (E_{MAC}) were inferred for essentially water-free aerosol as present after drying to low RH. Two methods were applied independently to investigate the coating effect on E_{MAC}: a correlation method (ambient MAC_{BC} vs BC coating thickness) and a denuding method ($MAC_{BC,amb}$ vs $MAC_{BC,denuded}$). Observed E_{MAC} values varied from 1.0 to 1.6 (lower limit from denuding method) or ~1.2 to 1.9 (higher limit from correlation method) with the mean coating volume fraction ranging from 54 to 78 % in the dominating mass equivalent BC core diameter range of 200–220 nm. MAC_{BC} and E_{MAC} were strongly correlated with coating thickness of BC. By contrast, ~~while~~ other potential drivers of E_{MAC} variability ~~factors were found to have a potential minor influence as well, including~~such as ~~air mass origins (~~different BC sources (air mass origin and absorption Ångström exponent)~~)~~, ~~mixing morphology~~coating composition (ratio of inorganics to organics)~~,~~ and BC core size distribution had minor effects only ~~and absorption Ångström exponent (AAE)~~. These results for ambient BC measured at Melpitz during winter show that the lensing effect caused by coatings on BC is the main driver of the variations in MAC_{BC} and E_{MAC}, while changes in other BC particle properties such as source, BC core size or coating composition play only minor roles at this rural background site with a large fraction of aged particles. Indirect evidence suggests that

potential dampening of the lensing effect due to unfavorable morphology was most likely small or even negligible.

1 Introduction

Black carbon (BC), which commonly refers to graphitic elemental carbon (Petzold et al., 2013), is a major component of atmospheric aerosols. BC-containing particles are emitted from incomplete combustion processes. BC is highly refractory, insoluble and a strong light absorber across the whole solar spectrum (Corbin et al., 2019). The latter makes BC the dominant light-absorbing component of atmospheric aerosols and causes a substantial positive radiative forcing through aerosol-radiation interactions (Bond et al., 2013). Two parameters are required to quantify the light absorption coefficient of BC ($b_{ap,\,BC}$; [Mm^{-1}]) in climate models: the mass absorption cross section of black carbon (MAC_{BC}; [$m^2\ g^{-1}$]) and the BC mass concentration (m_{BC}; [$\mu g\ m^{-3}$]), as shown in Eq. (1),

$$b_{\mathrm{ap,BC}} = \mathrm{MAC}_{\mathrm{BC}} \times m_{\mathrm{BC}}\,, \quad (1)$$

BC mass concentrations are simulated with chemical transport models taking BC emission inventories as input. MAC_{BC} values must be assumed or calculated from simplified optical models based on knowledge gained from laboratory and field measurements.

The term "aerosol mixing state" refers to the distribution of different particulate species among particles, where an internally mixed particle contains multiple species and an externally mixed particle only contains a single species~~is used to describe the morphology of a particulate species of interest, including externally and internally mixed states~~. For example, when BC is freshly emitted, it is often separated from other species, which refers to the externally mixed state. During the atmospheric aging of BC, non-BC ~~species~~ particles coagulate (e.g. particulate sulfate, nitrate, organics) with or gaseous species condense ~~(gas vapors)~~ onto BC particles to form a variety of internal mixing states.

The mixing state of BC with other particulate matter in the same particle – the internal mixing state – is relevant because it influences the light absorption by the BC in this particle. Based on a simple configuration of concentric spheres core-shell morphology, Mie theory provides a solution to predict light absorption by coated BC particles (Bohren and Huffman, 1998). According to this theory, if a BC particle is coated with non-absorbing species, more light is ~~refracted~~ focused towards the BC core, enhancing the amount of light it absorbs, and

thereby increasing its MAC_{BC} value (Eq. 1). This is known as the "lensing effect" (van de Hulst, 1957). The MAC_{BC} enhancement factor, E_{MAC}, due to lensing is conceptually defined as the MAC value of the mixed particle, $MAC_{BC,mixed}$, divided by the MAC value of the bare BC core:

$$E_{\mathrm{MAC}} = \frac{\mathrm{MAC}_{\mathrm{BC,mixed}}}{\mathrm{MAC}_{\mathrm{BC,bare}}}, \quad (2)$$

The lensing effect cannot result in unlimited enhancement of light absorption. Instead, a saturation point occurs, above which E_{MAC} does not increase any further with continued increase in coating thickness. The maximal MAC enhancement factor that can be reached for a ~~particle~~ BC core depends on particle morphology and size, with greater values for smaller ~~particles~~cores. Mie theory (Bohren and Huffman, 1998) predicts that the lensing effect saturates at an enhancement factor of 2–3 for concentric coatings around BC cores with mass equivalent diameters in the range between 100 and 300 nm, which is the diameter range where ambient BC mass size distributions typically peak (Bond et al. (2006). Therefore, E_{MAC} factors of up to ~ 3 are plausible for ambient BC particles (Bond et al., 2006; Zhang et al., 2017).

Particle morphology, i.e. the shape of the particle and the core, as well as the position of the BC core within a particle, also affect absorption enhancement. More sophisticated numerical simulations of light absorption by BC particles of variable morphology indicate that the fractal dimension, the location inside the particle and the refractive index of BC aggregates also influence E_{MAC}. Considering these factors typically results in smaller E_{MAC} than would be expected with simpler core-shell morphologies (Adachi et al., 2010; Zhang et al., 2017).

As well as being theoretically predicted, the lensing effect has also been observed in laboratory experiments. For example Shiraiwa et al. (2010) coated colloidal graphite particles (compact, near-spherical shape) with volatile organic species (oleic acid and glycerol, boiling points are 290 °C and 360 °C, respectively) and measured their BC core size distribution, coating thickness and light absorption properties of both untreated and thermo-denuded samples (at 400 °C) . They observed that E_{MAC} at 532 nm increased from 1.3 to 2 as the coating volume fraction was increased from 42 % to 88 %. In contrast, Qiu et al. (2012) observed a negligible lensing effect when they coated 150 nm combustion soot particles with secondary organic aerosol formed by the OH-initiated oxidation of toluene in an environmental chamber. The observed E_{MAC} values at 532 nm only reached 1.1 for volume equivalent coating fractions from 54 % to 70 %. It should be noted that the results of Qiu et al. (2012) are outliers among the more numerous laboratory studies showing notable absorption enhancements.

The BC lensing effect and its relationship to internal mixing state have also been investigated with field measurements of atmospheric aerosols. Some studies have used a soot-particle aerosol mass spectrometer (SP-AMS, Aerodyne Inc.) to measure relative coating masses as an indicator for BC internal mixing state. The SP-AMS is a modified form of the aerosol mass spectrometer (AMS) performed by coupling a 1064 nm laser source to an AMS instrument, making it possible to measure both BC and non-refractory aerosol components. Using this instrument one can measure the chemical composition of BC-containing particles (specifically, the average ratio of non-BC to BC core mass, referred to as $R_{coat\text{-}BC}$). However, ~~the instrument is not quantitative in an absolute sense because~~ the detection efficiency of BC cores in an SP-AMS is sensitive to ~~depends on~~ BC mixing state, since coatings affect the focusing of BC-containing particles within the instrument, and consequently the degree of overlap between the instrument's laser and particle beams (Willis et al., 2014; Taylor et al., 2015). This complicates the quantification of absolute BC core and coating mass concentrations with the SP-AMS, particularly in ambient campaigns where a wide variety of BC mixing states might be encountered (e.g. Collier et al., 2018).

Other field studies have employed traditional single-particle soot photometer (SP2) instruments to measure absolute BC coating thicknesses. Unlike the SP-AMS, the detection efficiency of BC particles in the SP2 does not depend on particle mixing state. Therefore, SP2 measurements are more quantitative than SP-AMS measurements in terms of both rBC mass and BC core diameter. In addition, incandescence measurements are combined with optical measurements of particle size in the SP2, allowing quantitative measurement of the BC coating thickness under the assumptions of a core-shell morphology for BC-containing particles as well as certain material properties (Gao et al., 2007; Laborde et al., 2012a). The derived coating thickness values are sensitive to these assumptions as discussed in detail below in Sect. 4.2.1 and by Taylor et al. (2015), which necessitates the exercise of considerable care when using the SP2 to perform quantitative coating thickness measurements.

Cappa et al. (2019) summarized the most recent ambient observations of BC mixing state and the lensing effect. In some studies (Liu et al., 2015b; Peng et al., 2016) a strong lensing effect was observed, with E_{MAC} reaching above 2 for mean ratios of coating to core mass ($R_{coat\text{-}BC}$) values up to 6. However, in other studies, only a weak or negligible lensing effect was observed ($E_{MAC} < 1.2$ for $R_{coat\text{-}BC}$ in the range 0.6 to 20) (Healy et al., 2015; Cappa et al., 2019). Cappa et al. (2019) formulated two hypotheses to explain the large difference in E_{MAC} values observed in these two different groups of studies: 1) the diversity of coating mass fraction among individual particles (e.g., Fierce et al., 2016); and 2) different mixing morphologies (e.g. off-center behavior of BC within a particle caused reduced E_{MAC}, Adachi et al., 2010). Furthermore, the composition of the coating material may, via composition dependence of ~~mixing~~ mixed particle morphology (Moffet et al., 2016), also affect the resulting

lensing effect (e.g. Zhang et al., 2018; Wei et al., 2013). However, the relative importance and interplay of these effects in atmospheric aerosols remain poorly understood.

Zanatta et al. (2016) reported MAC_{BC} values inferred from long-term observations at various European sites of the European Research Infrastructure for the observation of aerosol, clouds and trace gases (ACTRIS), additionally providing indirect evidence that the lensing effect occurs. In this study, we performed an intensive field experiment at one of these sites - the Melpitz observatory in Germany - with the goal to directly quantify the main drivers behind variations of MAC_{BC}, with a particular focus on mixing state and lensing effect.

2 Method

2.1 Methods to quantify the lensing effect

To explore the light absorption and the coating induced enhancement by the same BC mass, the mass absorption cross section of BC (MAC_{BC}) is a key parameter to start with. Inverse to the modeling calculation shown in Eq. (1) in Sect. 1, the MAC_{BC} ([m^2 g^{-1}]) is defined in Eq. (3). To infer MAC_{BC}, the BC absorption coefficient ($b_{ap,BC}$; [Mm^{-1}]) at 870 nm and the BC mass concentration (m_{BC}; [µg m^{-3}]) need to be measured.

$$\mathrm{MAC_{BC}} = \frac{b_{\mathrm{ap,BC}}}{m_{\mathrm{BC}}}, \quad (3)$$

Two independent approaches were chosen in this study to quantify the lensing effect on the MAC_{BC} of atmospheric BC-containing particles. The first approach, hereafter referred to as the correlation method, is based on a correlation analysis of concurrent quantitative measurements of both MAC_{BC} and BC particle mixing state. The mixing state is inferred as coating thickness resulting from the difference of measured diameters between the entire particle and the BC core based on an assumed core-shell configuration. The relationships between this specific metric of BC mixing state and more general measures of aerosol mixing state (e.g. the mixing state index χ) are discussed in the review of Riemer et al. (2019). The second approach, hereafter referred to as the denuding method, is based on modifying the mixing state of atmospheric BC-containing particles, i.e. to remove the coatings present on atmospheric BC using a catalytic stripper. Measurements of the MAC_{BC} in both the untreated ambient aerosols and the corresponding denuded aerosols make it possible to establish the causal relationship between the lensing effect and BC mixing state. For this purpose, the E_{MAC} is calculated with Eq. (4) under the assumption that the MAC_{BC} of the denuded aerosol represents the properties of bare BC.

$$E_{\mathrm{MAC}} = \frac{\mathrm{MAC}_{\mathrm{BC,ambient}}}{\mathrm{MAC}_{\mathrm{BC,denuded}}}, \quad (4)$$

The two approaches described above were applied during a field experiment, described in details in the following.

2.2 The Melpitz site

The intensive field campaign was conducted at the research site of the Leibniz Institute for Tropospheric Research (TROPOS) in Melpitz (12°56′ E, 51°32′ N, 86 m a.s.l.). The Melpitz site is a rural and regional background site, belonging to many international (GAW, ACTRIS and EMEP) and domestic (GUAN) observational networks (Birmili et al., 2016; Poulain et al., 2014; Spindler et al., 2010; Spindler et al., 2013). The station is located near the town of Torgau with 20 000 inhabitants in eastern Germany and 50 km northeast from the city of Leipzig, with 600 000 inhabitants. The observational containers are situated on the flat and semi-natural meadow surround by agricultural land. A federal main road (B 87) is 1.5 km north from the station and two conservative forests are located 2.5 km and 1 km in the north and south direction, respectively. The Melpitz site is about 130 km from the Polish border and anthropogenic emissions between Melpitz and Poland are negligible (Spindler et al., 2013). The measurements here are regarded as representative of the lowland background atmosphere in central Europe (Asmi et al., 2011; Aas et al., 2012; Birmili et al., 2009). The two main wind directions for Melpitz are South-West (SW) and East (E) with the different air masses arriving at Melpitz: air masses crossing the western part of central Europe including the city of Leipzig and continental air masses with anthropogenic emissions from countries in the east of Europe via long-range transport. Seasonally, the particulate mass concentration is highest with the East wind direction in winter and lowest with the West wind direction in summer (Spindler et al., 2013).

The field experiment was conducted from 01 to 23 February in 2017. Contributions from different BC sources are expected during the winter season. Furthermore, the higher pollution level makes it possible to achieve higher time resolution with the online instruments.

2.3 Experimental setup

The sampling set-up including the instruments is shown in Fig. 1. The ambient air was passed through a PM_{10} inlet followed by a Nafion dryer (RH<30 %) and a flow splitter. A first branch fed the instruments permanently probing untreated ambient aerosol, including a multi-angle absorption photometer; MAAP (aerosol absorption coefficient at 637 nm wavelength), an Aethalometer AE33 (spectral dependence of the aerosol absorption coefficient), and an aerosol chemical speciation monitor, ACSM. The ACSM (Aerodyne Research, MA, US; Ng et

al., 2011) measured the near-PM1 bulk chemical composition of ~~the~~ non-refractory aerosol ~~components~~species including organics (Org), nitrate (NO_3), sulfate (SO_4), ammonium (NH_4) and chloride (Chl). The ACSM measurements are described as near-PM_1 since the~~(The~~ instrument inlet has an upper cut-off at an aerodynamic diameter of around 1 µm~~)~~.

A second branch directed sample to a 3-way valve, from which the aerosol passed through either a catalytic stripper or a bypass line. The valve was automatically switched every 15 minutes alternately delivering untreated ambient or denuded aerosol to a photo-acoustic extinctiometer (PAX) and a single-particle soot photometer, which measured the aerosol absorption coefficient at 870 nm wavelength and BC properties, respectively. The measurements were averaged to 3 h intervals (separately for each branch behind the switching inlet), as the signal-to-noise ratio of the 15 min data was insufficient for some instruments.

Beside the aerosol measurements, co-located trace gas measurements (including SO_2, NO and NO_2) were also performed (not shown in Fig. 1), which were used to indicate air mass origins combined with the patterns of meteorology and aerosol chemical properties (Sect. 3.1). Concentrations of SO_2 were measured with a UV-Fluorescence instrument (Type APSA 360A, HORIBA Jobin Yvon GmbH, Germany) and NO and NO_2 (NO_x) concentrations were measured with a Trace Level NOx Analyzer (Type 42i-TL, Thermo Fischer Scientific GmbH, Germany).

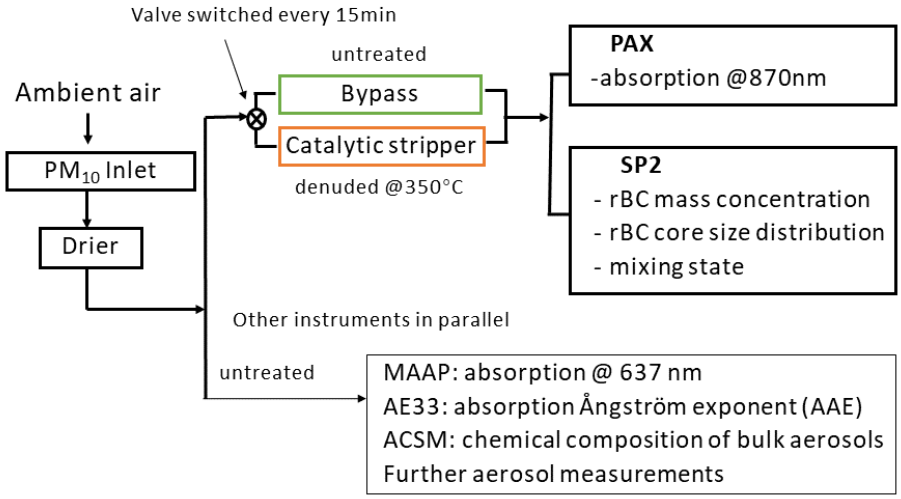

Figure 1. Schematic of the sampling system, instruments and target quantities related to this study. PAX is photoacoustic extinctiometer and SP2 is single particle soot photometer. PAX and SP2 analyzed both ambient and denuded samples. The other instruments only analyzed the untreated ambient aerosol, including a multi-angle absorption photometer (MAAP), an Aethalometer (AE33), an aerosol chemical speciation monitor (ACSM) and further instruments, which are not shown here.

2.4 Instrumentation

2.4.1 The single particle soot photometer (SP2)

The SP2 is based on the laser induced incandescence technique (LII) and the principles have been described in previous studies (Stephens et al., 2003; Schwarz et al., 2006). Briefly, particles pass through an intra-cavity, continuous-wave laser beam (Nd: YAG at 1064 nm). Since BC is the most strongly light absorbing and refractory aerosol material in the atmosphere (Pöschl, 2003; Schwarz et al., 2006), BC can absorb infrared light (Schwarz et al., 2010) and be heated to its boiling point as high as around 4230-4325 K (Moteki and Kondo, 2010), emitting thermal radiation as measurable incandescence before sublimation. The emitted incandescent light is optically filtered before being detected by a photomultiplier tube (PMT), which is sensitive to a wide wavelength range (broadband between ~ 350 and 800 nm), equipped with high gain and low gain. The peak intensity of the

incandescent light is proportional to the BC mass in the particle regardless of its mixing state (Slowik et al., 2007) since non-BC species evaporate at temperatures much lower than the BC sublimation temperature. Based on this operational characteristic, BC quantified by the LII method is termed as refractory BC (rBC) hereafter, following the terminology recommended by Petzold et al. (2013).

The inherent limitation for detection of BC by the SP2 is that for very small rBC mass in a single particle or insufficient lower laser intensities the conductive cooling dominates over BC absorption and thus BC cannot be heated to sublimation (Schwarz et al., 2010). The SP2 used in this study has 100 % number-detection efficiency on a single particle basis when the rBC mass per particle is above ~0.5 fg, which corresponds to an rBC mass equivalent diameter, D_{rBC}, of ~80 nm using a void-free material density of 1.8 g cm^{-3}. For BC cores greater than the upper limit of detection of the SP2, the particles are detected while the rBC mass cannot be quantified due to the signal saturation from the A/D converter. Therefore, the upper quantification limit (LOQ) is ~200 fg rBC mass per particle, corresponding to an rBC mass equivalent core diameter (D_{rBC}) of ~600 nm. Note that the SP2 is also equipped with a narrow band incandescence detector (NB: 630~800 nm; Schwarz et al., 2006). However, we did not further use these signals as the upper LOQ was at similar BC core mass as for the broadband detectors, and because two-color pyrometry is out of scope of this manuscript.

As discussed by Pileci et al. (2020), there are a number of different methods for quantifying and correcting for the mass of BC outside the SP2 size detection limits (if the user decides to apply a correction at all). These methods are based on extrapolation of SP2-measured BC core mass size distributions. In this study we used the lognormal fit approach. Further, to better represent the upper portion of the size distributions where most of the missing mass appeared to lie (Fig. S5), we fitted lognormal functions separately to the lower ($80 < D_{rBC} < 300$ nm) and upper portions ($230 < D_{rBC} < 600$ nm) of the measured size distributions. The extrapolated portions of these two types of fits are displayed in Fig. S5 for each of the four main periods of the campaign (which are introduced and described in Sect. 3.1). From the extrapolated sections of the fitted curves we estimate the missing mass percentages below the lower LOQ were 1.1, 0.4, 1.6, and 0.8 % for periods 1, 2, 3, and the short plume case, respectively. The corresponding percentages for the missing mass above the upper LOQ were 1.3, 4.9, 4.0, and 26 %. Since these estimated percentages are low (less than 5 % excepting the small portion of the dataset represented by the short plume case), we chose not to apply correction factors to account for the BC mass potentially missed by the SP2. Some possible consequences of this decision are discussed in Sect. 3.3.

~~The BC mass of cores outside the size detection limits of the SP2 was corrected by using a lognormal fit of the mass size distribution. For the campaign averaged rBC mass size distribution, the missing mass was 2.5 ± 1.4 %~~

~~below the lower LOQ and 1.1 ± 0.4 % above the upper LOQ. The details of the missing mass correction are described in a separate paper (Pileci et al., in preparation).~~

The recommended calibration of the incandescence channels with an aerosol particle mass analyzer (APM) is described elsewhere (Laborde et al., 2012a; Baumgardner et al., 2012; Moteki and Kondo, 2010). Briefly, an empirical calibration of the relationship between BC mass in a particle and resulting incandescence signal amplitude is required. Mass selected fullerene soot from Alfa Aesar (stock #40971, lot #FS12S011) was shown to provide calibration curves that match the response of the SP2 to BC from diesel exhaust (Laborde et al., 2012a) and atmospheric BC (Moteki and Kondo, 2010). In this study we used a different batch of fullerene soot (Alfa Aesar; stock #40971, lot W08A039) for SP2 calibration. The SP2 response to this batch was later shown to be equal to that of the batch FS12S011, and therefore this calibration is in full agreement with the recommended approach. The reproducibility of rBC mass using this calibration approach is estimated to be better than ±10 % and to represent BC mass in atmospheric aerosols from different sources within ±20 %.

Particles passing the laser beam also elastically scatter laser light, which is detected by avalanche photodetectors (APD). BC-free non-absorbing particles do not evaporate within the laser beam and remain unperturbed, and the scattering signal is determined by a standard APD. The amplitude of the scattering signal is proportional to the partial scattering cross section of the detected particle for the solid angle covered by the detector optics. From the measured scattering cross section the optical diameter of the particles (D_{opt}) is inferred using Mie theory (Bohren and Huffman, 1998, i.e. assuming spherical particle shape). The refractive index of the particles is assumed to be 1.50+0i, which typically provides optical ~~diameters~~ size distributions that agree ~~on average~~ within ~~a few percent~~20 % with ~~the~~ corresponding mobility ~~diameter of the particle~~size distributions, excepting some outlying cases when the total aerosol load was very low (Fig. S1). Unit detection efficiency for the standard optical sizing was achieved for optical diameters D_{opt} > ~150 nm and the upper LOQ, which is restricted by detector saturation, was at D_{opt} = 500 nm. Absolute calibration of the scattering cross section measurement was done using spherical polystyrene latex (PSL) size standards of 269 nm (Thermo Scientific) and calculation based on Mie theory with known scattering cross section.

The BC containing particles are heated to above 4000 K due to BC core absorption, such that the non-refractory coating materials evaporate within the laser beam. Therefore, the measured scattering amplitude is not proportional to the scattering cross section of the unperturbed particle. However, the leading edge of the light scattering signal still contains information on the scattering cross section of the unperturbed particle.

Interpretation of the leading edge signal is only possible if the laser intensity profile is known and if the time axis of the scattering signal can be related to the position of the particle in the laser beam. This is achieved with an additional position sensitive detector (PSD) introduced by Gao et al. (2007). Knowing the particle position in the laser beam makes it possible to infer the optical diameter of the unperturbed particle before evaporation onset in the leading edge of the laser beam, commonly referred to as leading-edge-only (LEO) method. Details on the LEO optical sizing approach can be found in previous studies (Gao et al., 2007; Laborde et al., 2012a; Taylor et al., 2015).

Accurate optical sizing with the LEO method requires several validations. A first one is to verify that the position dependent laser intensity is correctly accounted for. This is done by comparing the LEO results from the scattering detector with the corresponding standard optical sizing for BC-free particles (see Fig. S2 (a) for details). The LEO sizing can also be done with the PSD signal, in which case an adjustable factor is used to make the LEO results match the results of a normal scattering detector, as shown in Fig. S2 (b). This approach implicitly ties the PSD detector to the calibration of the normal scattering detector. We used the PSD detector instead of the normal scattering detector for the LEO sizing because the 10 % and 90 % percentiles are much narrower for the former, as shown in Fig. S2 c and d.

The principle behind the LEO sizing can be applied to the time-resolved signal of the normal scattering signal at any position in the laser beam (Laborde et al., 2012a). The scattering signal of a BC-containing particle at incandescence onset represents that of the bare BC core, which makes it possible to infer its optical diameter ($D_{opt,BC}$). This is done with assuming spherical shape and a certain BC refractive index (RI_{BC}). Figure S3 shows a comparison of the optical diameter of the BC core with the BC mass equivalent diameter inferred from the incandescence signal. The refractive index of the bare BC core was chosen to be 1.75+0.43i, which made the two diameters match in this study. This value is lower than the value most commonly used for ambient soot in other studies with SP2 measurement at various sites (RI_{BC} = 2.26+1.26i; Moteki et al., 2010; Laborde et al., 2012b; Laborde et al., 2013; Zanatta et al., 2018; Dahlkötter et al., 2014). The reason for achieving the BC diameter match with a lower than usual refractive index is not known, nor should this approach be interpreted as an accurate refractive index measurement. However, choosing it in this manner ensures bias-free measurements of the coating thickness of ~~uncoated~~ bare BC particles (i.e., this choice results in coating thickness histograms for bare BC particles that are centered around 0 nm).

The optical size of the individual BC-containing particle (D_{total}) can be inferred from the combination of Mie model calculation, the measured scattering signal of the entire particle and the core diameter (D_{rBC}) (Taylor et al., 2015; Schwarz et al., 2008). Briefly, based on a concentric core-shell configuration, the Mie model is able to calculate the scattering cross-section of the BC core with the input of D_{rBC} and RI_{BC}. Then D_{total} can be inferred by the Mie model with the input of the refractive index of the coating (RI_{coat}) with scattering by coating (difference between measured scatter signal of entire particle and Mie calculated BC core scattering signal). The particle scattering cross-sections with fixed D_{rBC}, D_{total}, RI_{BC} and RI_{coat} inputs by the Mie model are stored in a series of 2-D lookup tables for data analysis in the PSI SP2 toolkit run with Igor Pro (Wavemetrics, OR, USA). Finally, the coating thickness (T_{coat}) can be calculated with the reconstructed D_{total} and D_{rBC}:

$$T_{\mathrm{coat}} = (D_{\mathrm{total}} - D_{\mathrm{rBC}})/2\,, \quad (5)$$

The coating thickness is more sensitive to RI_{core} than RI_{coat}, which is consistent with previous sensitivity evaluation (Taylor et al., 2015). The precision of the coating thickness retrieved by the LEO method was estimated to be about ±20 % (Laborde et al., 2012b) for D_{rBC} ranging from 150 to 400 nm.

2.4.2 Absorption measurements

2.4.2.1 Instruments

A MAAP (ThermoFisher Scientific, MA, USA; Petzold and Schönlinner, 2004) was used to measure the aerosol absorption coefficient at 637 nm. The MAAP measures both the light radiation transmitted and back scattered from a particle-loaded fiber filter, and determines the fraction of light absorption by absorbing aerosol components via a radiative transfer program. To minimize the interference by the light scattering aerosol components on the angular distribution of the back scattered radiation, the measurements are performed with three detectors at different angles. For the data analysis in this study, a factor of 1.05 has been applied for the required wavelength correction (from 660 to 637 nm) according to Müller et al. (2011).

A PAX (Droplet Measurement Technologies, CO, USA) was used to measure the aerosol absorption coefficient at 870 nm, which minimizes interference from light absorbing particulate matter other than BC such as brown carbon or dust. It applies photo-acoustic spectroscopy, which is described in detail in Arnott et al. (1999). Photo-acoustic spectroscopy has been widely used in recent years as it is an in situ measurement without perturbing particle morphology (Lack et al., 2006). The PAX was calibrated following the manufacturer instructions. However, the precision of these calibrations was insufficient and the absorption coefficients measured with application of these calibration coefficients were inconsistent with the results from the MAAP, as further discussed in Sect. 2.4.2.2 (Müller et al., 2011).

An Aethalometer (Model AE33, Magee Scientific, CA, USA; Hansen et al., 1984) was also used to measure the aerosol absorption coefficients at seven wavelengths (370, 470, 520, 590, 660, 880, and 950 nm). The AE33 is also a filter-based instrument, with associated limitations in quantifying the absorption coefficient absolutely. However, in this study we only applied the AE33 to infer the relative spectral dependence of light absorption. For this purpose we used the default instrument output, which includes a loading compensation and a correction for the effects of multiple scattering within the filter matrix (Drinovec et al., 2015). Note that the absolute value of the multiple scattering correction is irrelevant for our purpose, except for the fact that it is assumed to be independent of wavelength.

The spectral dependence of the aerosol absorption coefficient, b_{ap}, often follows a power law $b_{ap}(\lambda) \sim \lambda^{-AAE}$ in good approximation. The exponent AAE is commonly referred to as the absorption Ångström exponent. In this study we use absorption coefficients measured by the AE33 at two different wavelengths (λ_1 and λ_2) to infer the AAE using the following equation (Moosmüller et al., 2011):

$$\mathrm{AAE}\,(\lambda_1, \lambda_2) = \frac{-\ln(b_{\mathrm{ap}}(\lambda_1)/b_{\mathrm{ap}}(\lambda_2))}{\ln(\lambda_1/\lambda_2)}\,, \qquad (6)$$

BC absorbs light broadly from near-UV to near-infrared wavelengths and thus has a weak spectral dependence (AAE ≈ 1; van de Hulst, 1957). By contrast, light absorbing organics (Corbin et al., 2019), can exhibit substantial light absorption at near-UV and blue wavelengths while being negligible at red to near-infrared wavelengths, which normally results in AAE larger than 1.

Typical AAE values for traffic emissions are close to unity since BC is the only light absorbing component. However, AAE values are significantly larger than unity in biomass burning emissions due to co-emission of BC and brown carbon. The difference of the two branches of AAE values can be used for source apportionment via an "AAE model" (Zotter et al., 2017 Liu et al., 2014; Elser et al., 2016). Note that the application of the model is only precise under favorable conditions, in which traffic and biomass burning are the only sources.

2.4.2.2 Absorption coefficient

The absorption coefficient was quantified with a combination of PAX, MAAP and AE33 data. The absorption coefficient measured by the MAAP at λ=637 nm was adjusted to λ=870 nm, using the 3h-averaged AAE data obtained from the AE33:

$$b_{\mathrm{ap,MAAP,870nm}} = b_{\mathrm{ap,MAAP,637nm}} \times (637/870)^{\mathrm{AAE}(637,870)} \quad (7)$$

The correlation between wavelength-adjusted MAAP data and PAX data is excellent in the range above ~1 Mm^{-1} (Fig. 2). However, the $b_{ap,PAX,870nm}$ measurements are biased systematically lower than the $b_{ap,MAAP,870nm}$ measurements by 31 %, which is most likely a result of imprecise and hence inaccurate PAX calibration (Sect. 2.4.2.1). The MAAP demonstrated good accuracy in several inter-comparison studies and it has been shown to have a low instrument-to-instrument variability of less than 5 % (Müller et al., 2011). Therefore, we decided to scale the PAX data by a constant scaling factor of 1.44 [=1/(1-0.31)] to match $b_{ap,MAAP,870nm}$ as shown in Fig. 2. Application of this constant scaling factor brings the scaled PAX and MAAP measurements into good agreement at absorption coefficients greater than ~15 Mm^{-1}, while the scaled PAX measurements are up to 10 % lower than the corresponding MAAP measurements in the range down to 1 Mm^{-1} (as shown by the green crosses in Fig. 2). The scaled PAX data provide absorption coefficients with high time resolution and for both ambient and denuded inlets, with absolute calibration referenced to the MAAP.

~~As mentioned above, the PAX provides high time resolution in situ measurements. Moreover, the PAX measured both ambient and denuded samples in this study. The MAAP provides absolute quantification since the differences among different instruments are less than 5 % (Müller et al., 2011). The AE33 provides wavelength dependence. In order to have quantitative absorption measurements, the absorption coefficient measured by the PAX ($b_{ap,PAX,870nm}$; [Mm^{-1}]) needs to be scaled to that of the MAAP ($b_{ap,MAAP,870nm}$; [Mm^{-1}]) at 870 nm. The original absorption coefficients measured by the MAAP were at 637 nm ($b_{ap,MAAP,637nm}$; [Mm^{-1}]). To compare b_{ap} by the PAX and the MAAP at the same wavelength of 870 nm, $b_{ap,MAAP,637nm}$ values were adjusted to that of 870 nm by the measured AAE values within the range of 637 to 870 nm as shown in Eq. (7):~~

~~$$b_{\mathrm{ap,MAAP,870nm}} = b_{\mathrm{ap,MAAP,637nm}} \times (637/870)^{\mathrm{AAE}(637,870)}, \quad (7)$$~~

~~The correlation between the PAX measurements and the MAAP measurements scaled to 870 nm is excellent above ~1 Mm^{-1} (Fig. 2). However, there is 31 % systematic bias between $b_{ap,PAX,870nm}$ and $b_{ap,MAAP,870nm}$, which is more likely an issue of inaccurate PAX calibration at high absorption coefficients. Since the MAAP is more robust as an absolute reference, the $b_{ap,PAX,870nm}$ values were scaled by a factor of 1.44 to match $b_{ap,MAAP,870nm}$ as show in Fig. 2.~~

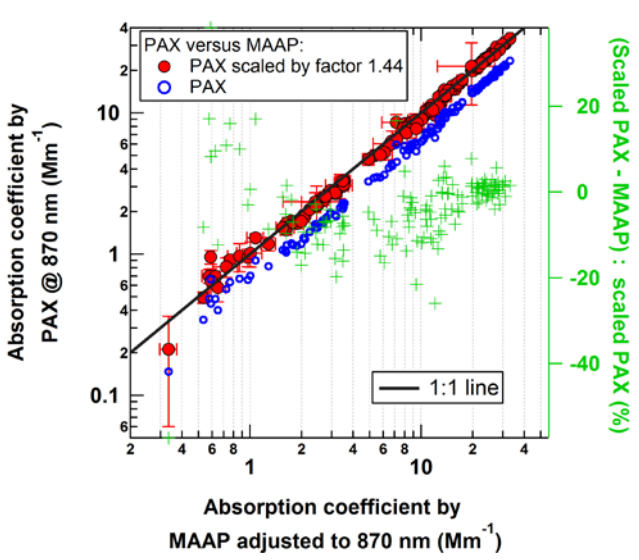

405

Figure 2. Comparison of the absorption coefficients measured by the PAX and the MAAP. The MAAP data measured at 637 nm were adjusted to 870 nm using the spectral dependence of the absorption measured by the aethalometer. The PAX data measured at 870 nm are shown with original calibration and after scaling by a factor 1.44 to match the MAAP data on average. The percentage difference between the scaled PAX and MAAP measurements is plotted on the right-hand y-axis (green crosses).

410

2.4.3 The Catalytic Stripper (CS)

The basic principle and inner structure of the catalytic stripper (CS; Catalytic Instruments; Model CS015) has been described in Amanatidis et al. (2013). The residence time of the CS used in this study was approximately 0.35 s with the flow rate of 1.5 L min^{-1}, and the temperature was set to 350 °C. As shown in Figure S5, the
415 denuding process by the catalytic stripper did not influence the shape of the rBC core size distribution in the range ~60 to 600 nm. The fractional loss of rBC mass was up to 20 % for D_{rBC} below 300nm. The losses ~~did not introduce any~~likely introduced only negligible ~~-~~bias in the MAC_{BC} values since the absorption measurement by the PAX was also behind the CS. The median coating thickness was 58 and 32 nm before and after denuding, respectively, indicating that the CS did not remove the coating completely. Denuding could potentially cause

Commented [MRL1]: This figure has been replaced with a n version to show the residual fractions on the right y-axis

some compaction of the BC cores. However, the denuded sample data were only used to determine the MAC_{BC} of the bare BC cores – more precisely an upper limit of it due to residual coating – and hence such denuding does not significantly affect the interpretation of our results.

3 Results and discussion

3.1 Periods with distinct air mass origin

The time series of wind direction and wind speed as well as chemical information are shown in Fig. 3. Three distinct periods and a short plume case were identified based on these data and on air mass back trajectory analyses (Fig. 4; calculated for an air mass arrival altitude of 100 m). The exact time windows and characteristics of the different periods are summarized in Table S1. In period 1 (02 Feb 2017 09:00 to 05 Feb 2017 21:00, UTC time), the local wind speed at Melpitz was low (median=1.2 m s^{-1}; IQR: 0.8 to 1.7 m s^{-1}) and the local wind direction at the site varied frequently. Back trajectory analysis showed that most of the air masses came from south to southwest (S to SW) of the sampling site, passing through the high Alps region. The local wind directions were generally not consistent with the air mass origin sector according to the back trajectory analysis. However, given the low and variable local winds during this time period, the back trajectory result is more relevant for interpreting the aerosol and gas phase composition. The gas phase mixing ratios were usually strongly dominated by NO_x (except for period 2, see Table S1). The median SO_2 to NO_x ratio was 0.08 (interquartile range IQR 0.05–0.11). Similarly, the aerosol properties were comparable among the periods except for period 2. For period 1, the median value of the total aerosol mass concentration from the integrated ACSM data (non-BC) and the SP2 (BC) was 10.6 (IQR 8.7–11.7) µg m^{-3} (Table S1), the mass ratio of particulate inorganics to organics was 1.45 (IQR 1.22–1.55), and the sulfate to nitrate mass ratio was 0.60 (IQR 0.39–0.71). Note, these mass concentrations approximately correspond to PM_1 composition due to the intrinsic upper detection limits of the ACSM and SP2. The aerosol composition measured in this study is consistent with previous observations from Melpitz and indicate that NO_x-rich vehicle emissions were a dominant source of pollution in these air masses (Spindler et al., 2013).

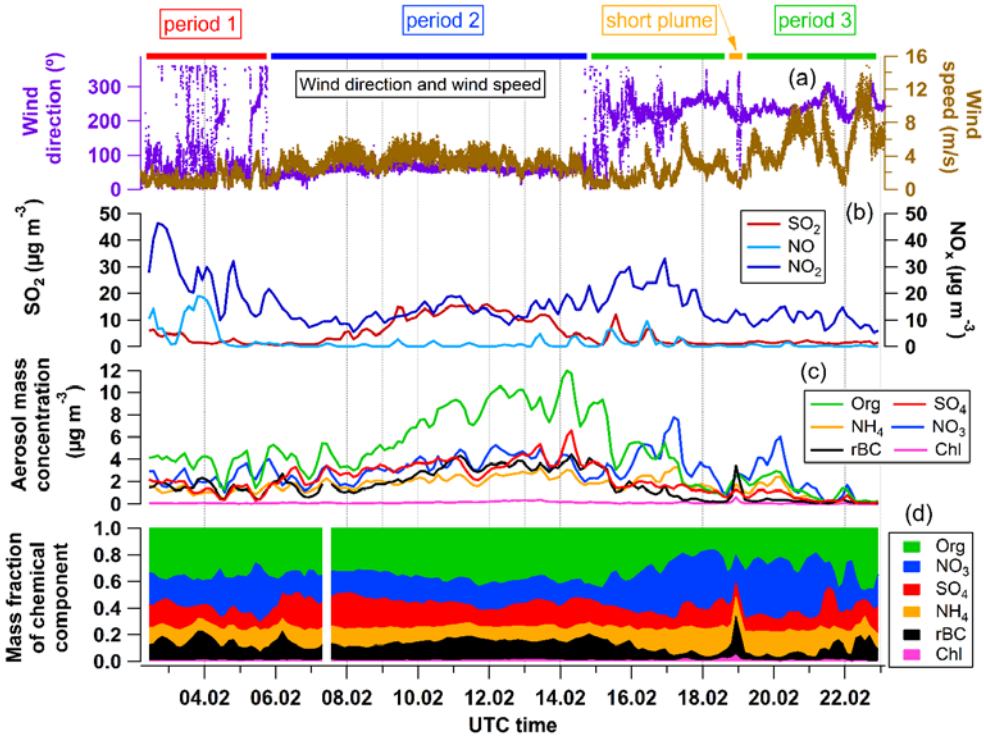

Figure 3. Time series of (a) wind direction and wind speed at 10 min time resolution measured 6 m above ground, (b) concentrations of gas phase species SO_2, NO, and NO_2 at 3 h time resolution, (c) mass concentrations of aerosol phase chemical components measured by the ACSM and the SP2 at 3 h time resolution, and (d) relative mass fractions of the measured aerosol chemical components.

Commented [GBM2]: One small change has been made in th figure: the % symbol was incorrectly placed in the y-axis label of panel (d). This has now been removed.

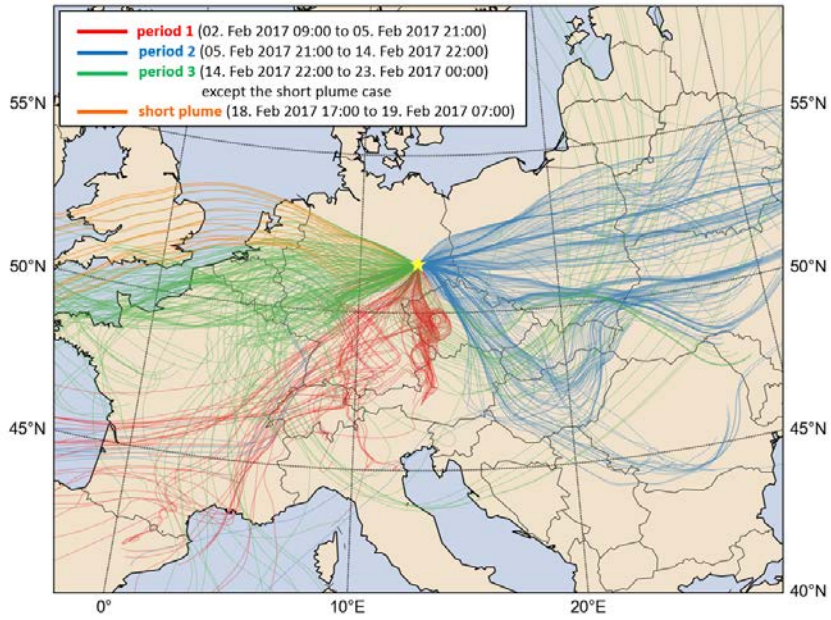

Figure 4. Map of air mass back trajectories: 96-hour air mass back trajectories terminating at Melpitz site (yellow star) at an altitude of 100 m for every hour of the campaign. Trajectories terminating at altitudes of 10 m and 500 m were similar to those shown here. The map is based on the HYSPLIT atmospheric transport and dispersion modeling system provided by Air Resources Laboratory (ARL) (Stein et al., 2015).

In period 2 (05 Feb 2017 21:00 to 14 Feb 2017 22:00), the local wind speed at the site (median 3.4, IQR 2.7–4.1 m s^{-1}) was higher than that of period 1 with constant local wind direction from the northeast to southeast (Fig. 3a). Back trajectory analysis indicated that the air masses arriving at the site had traveled from north-eastern, eastern and south-eastern Europe (Fig. 4), consistent with the local wind directions. In the gas phase, the most striking feature of the measurements is that SO_2 was present at significantly higher levels than in the other periods, with a median concentration of 9.2 (IQR 3.2–13.2) µg m^{-3} (Fig. 3b). The SO_2 to NO_x ratio was also much higher with a median value of 0.63 (IQR 0.28–0.83). The PM_1 aerosol mass concentration from integrated ACSM (non-BC) and SP2 (BC) also showed the highest levels observed during the whole campaign period, with a median mass concentration of 23.0 (IQR 20.4–27.2) µg m^{-3} (Table. S1), which was almost twice as high compared to the other periods. Despite the higher concentrations of chemical components (Fig. 3c), the relative

composition of organic and total inorganic components (Fig. 3d) was similar to that of the period 1 and remained relatively stable within period 2. However, within the inorganic fraction, the sulfate to nitrate mass ratio was remarkably high with a median value of 1.1 (0.9–1.2) during this period. The source of sulfur leading to the high concentrations of SO_2 and sulfate in period 2 was likely residential and industrial solid fuel burning in east and south-east Europe, where coal with a high sulfur content is still used as a fuel source. For example, Poland, located 150 km east of the Melpitz site, has the highest SO_2 emissions among EU countries (Glasius et al., 2018). Previous studies have shown that combustion of coal and biomass (wood) are significant sources of carbonaceous aerosols in Poland in winter (Spindler et al., 2013; Ciarelli et al., 2017; Glasius et al., 2018).

In period 3 (14 Feb 2017 22:00 to 23 Feb 2017 00:00), the local wind at the site was dominated by westerly winds with generally higher and more variable wind speeds (median 4 m s^{-1}, IQR 2.5–6.3 m s^{-1}) than those of period 1 and 2. The majority of the back trajectories originate from western Europe (Fig. 4), consistent with local wind direction. In the particle phase, total aerosol mass concentrations decreased steadily throughout period 3 to the lowest values observed during the whole campaign. The median total aerosol mass concentration was 10.9 (IQR 8.1–15.8) µg m^{-3} during the period (Table S1). Among the aerosol components, substantially higher mass fractions of nitrate (35 %, 25–41 %) were found compared to the other periods, while rBC mass concentrations (0.6, 0.3–1.4 µg m^{-3}) and rBC mass fractions (7 %, 4–11 %) reached their lowest levels for the whole campaign (Fig. 3c and d, Table. S1). Organic mass fractions were less than 30 % (Table. S1), lower than the fractions observed in periods 1 and 2.

A short plume of BC aerosol passed over the sampling site between 18 Feb 17:00 and 19 Feb 07:00. Given the stagnant air conditions and low wind speed during this period, this plume likely resulted from a local emission. As shown in Fig. 3c, the 3-hourly averaged rBC mass concentration peaked at ~ 4 µg m^{-3} during this event, which was the highest value reached during the campaign. The organic aerosol concentration was stable during the event (2.3, 2.1–2.5 µg m^{-3}), which suggests that the plume did not come from a forest fire or biomass burning event since such events would emit large amounts of organics. A coal burning source for the plume is also not evident since the SO_2 did not increase as shown in Fig. 3b. The fact that the AAE_{470_950} dropped to around 1.0 during the period within the absorbing aerosol plume may indicate fresh emissions from a combustion engine as BC source. In addition, the observed much larger BC core diameters (above 300 nm, Fig. 5b) in the plume compared to the other periods likely indicated a super-polluter. Very dirty trucks or cars are known to produce larger BC particles than typical engines do (Schneider et al., 2015); however, the persistence of the plume rather indicates a nearby stationary rather than multiple mobile sources. In summary, the short plume seems to have resulted from a local event but the exact source is not apparent.

3.2 Physical and optical properties of BC

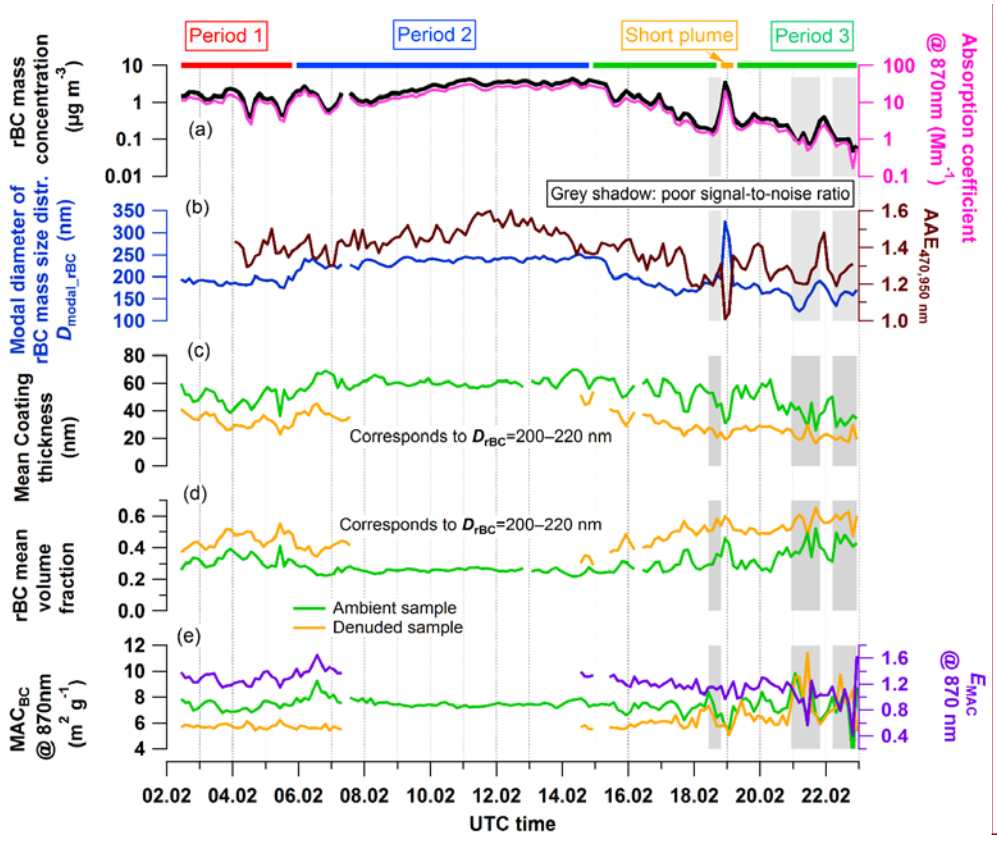

505

Figure 5. Time series of the physical and optical parameters of BC in the dried aerosol sample at 3 h time resolution: (a) ambient rBC mass concentration measured by SP2 (left axis) and absorption coefficient of bulk aerosol measured by PAX at 870 nm (right axis), (b) model BC core diameter of rBC mass size distributions determined with log-normal fits shown in Fig. S6 (left axis) and AAE_{470_950} (right axis), (c) mean thickness of non-BC coatings on ambient and denuded rBC cores with mass equivalent diameters in the range 200 to

Commented [MRL3]: One small change has been made in th figure: the % symbol was incorrectly placed in the y-axis label of panel (d). This has now been removed.

220 nm, calculated from single particle data, (d) mean rBC volume fractions for ambient and denuded rBC particles calculated from the coating thickness data shown in (c), (e) mean MAC_{BC} of ambient and denuded samples (left axis) and corresponding E_{MAC} calculated with Eq. (4) (right axis). The gap in the denuded time series in (c) and (d) (and corresponding gap in the E_{MAC} time series in (e)) from 06 to 14 Feb is due to malfunction of the valve switching system. The time periods when rBC mass was less than 0.2 µg m^{-3} are marked with a grey shading due to poor signal-to-noise ratio.

Time series of the physical and optical properties of BC in the essentially water-free aerosol sample as present after drying to low RH are shown in Fig. 5. The BC mass concentration and absorption coefficient measurements were highly uncertain during periods of low aerosol loading (grey shaded periods occurring at the end of the campaign) due to the SP2 data acquisition settings (the SP2 was set to save data from only one out of every 200 particles) and instrumental limits (the ~~lower quantification limit for the~~manufacturer-reported sensitivity of the PAX ~~during the campaign was~~is ~~≈~~<1 Mm^{-1} at 60 secs averaging time, which is consistent with instrument performance demonstrated in Fig. 2). Therefore, based on these considerations, a criterion of rBC mass concentrations < 0.2 µg m^{-3} was used to filter out data from further statistical analysis.

The ambient rBC mass concentration ranged between 1.00 and 3.03 µg m^{-3} (IQR) throughout the whole campaign, but with systematic differences between the distinct campaign periods. Overall, the rBC mass concentration was higher in air masses from eastern Europe, consistent with previous observations at Melpitz in winter (Spindler et al., 2013). Specifically, the rBC mass concentration ranged from 1.79 to 3.48 µg m^{-3} during period 2, increasing from ~ 0.5 to 4 µg m^{-3} over the first four days of the period and then maintaining a relatively stable level at around 3.5 µg m^{-3}. In contrast, the rBC mass concentrations only ranged from 1.21 to 1.73 µg m^{-1} during period 1 with air masses from southern and south-western Europe (Fig. 4). In period 3, the rBC mass concentration varied from 0.60 to 2.19 µg m^{-3}. At the beginning of this period, the rBC mass concentration decreased rapidly from ~4 to 1 µg m^{-1} in a single day, as a result of the rapid switching of air arriving from eastern to western Europe. Following this sharp change, the rBC mass concentration was generally less than 1 µg m^{-3} for the remainder of the period, which was likely the result of stronger dilution of emissions due to higher wind speeds and possibly also lower emissions in western Europe compared to eastern Europe.

The modal diameter of rBC mass equivalent diameter, calculated as the geometric mean of three-hourly averaged lognormal rBC mass size distributions (D_{modal_rBC}), is shown in Fig. 5b. D_{modal_rBC} ranged from 186 to 240 nm throughout the whole campaign, which is a typical level for aged BC particles in continental remote or urban areas. For example, previous studies have observed D_{modal_rBC} values of ~240 nm in the European Arctic region (Zanatta et al., 2018), ~200 nm in continental air masses from eastern Europe measured in Paris (Laborde et al.,

2013), and ~210-220 nm in Asian outflow measured at a remote site in Japan (Ueda et al., 2016). During this campaign, systematically larger median D_{modal_rBC} values were measured in period 2 (239 nm) than in periods 1 (190 nm) and 3 (181 nm). The larger BC particles measured in period 2 might be related to coal burning emissions (e.g. lignite coal burning in Poland): while the burning of hard coal briquette emits particles that lie mostly in the nuclei and Aitken mode (20-100 nm), the number size distribution of lignite emissions peaks in the accumulation mode (100-1000 nm) (Bond et al., 2002). Therefore, it is possible that BC cores from lignite burning are larger than BC from other common sources such as traffic. Wood burning emissions from domestic heating are also expected to generate larger BC cores than those emitted by traffic, and thus could also be partly responsible for the generally larger BC cores observed during period 2. ~~According to a summary in , the production of lignite (60-70 million tons) has been almost the same as that of hard coal (70-80 million tons) in Poland from 2010 to 2015~~. During the short/distinct plume, D_{modal_rBC} ranged from 192 to 298 nm, substantially larger than the values measured in remote background air, which supports the interpretation that the plume resulted from local emissions.

3.3 BC mixing state, MAC_{BC} and the lensing effect

The ambient MAC_{BC} at 870 nm ranged from 7.2 to 7.9 $m^2\ g^{-1}$ during the whole campaign, with a geometric mean value of 7.4 $m^2\ g^{-1}$. These values are slightly higher than the MAC_{BC} values calculated over 3 winter seasons in Melpitz and reported by Zanatta et al. (2016). These authors applied a MAAP and thermal-optical elemental carbon mass measurements, and reported a MAC_{BC} at 637 nm of 8.2 $m^2\ g^{-1}$. This values corresponds to a MAC_{BC} at 870 nm value of 5.3 to 5.7 $m^2\ g^{-1}$, assuming $AAE_{637\text{-}870nm}$ values of 1.2 and 1.4, respectively. Nordmann et al. (2013) previously reported 7.4 $m^2\ g^{-1}$ for MAC_{BC} at 637 nm based on a week-long measurement combining MAAP and Raman spectroscopy, which is 10 % lower than the value from Zanatta et al. (2016). The discrepancies between the values measured in this study and those reported by Zanatta et al. (2016) and Nordmann et al. (2013) could be related to the fact that the studies were conducted over different time periods, or they might be due to the different techniques that were used to measure the BC mass concentration in each study. Pileci et al. (2020) showed from multiple field campaigns that co-located rBC and EC concentrations measurements can differ by as much as ~50 % in European background air. Given this fact, the agreement between the MAC_{BC} values reported in this study and those previously reported is well within expectations.

The degree of internal mixing, expressed as the thickness of non-BC material coating the BC cores ('coating thickness'), was measured by the SP2 as described in Sect. 2.4.1. The modal diameters of the BC core mass distribution (D_{modal_rBC}) were around 200–220 nm mass equivalent diameter during the campaign (Fig. 5b).

Fortunately, these modal diameters were in the range of diameters for which the LEO-fit analysis described in Sect. 2.4.1 could be successfully applied to all types of internally mixed BC particles (i.e., all types of BC particles ranging from uncoated to thickly coated particles). Therefore, to obtain a representative indicator of BC internal mixing state that is applicable to the mode of the BC mass size distributions, coating thicknesses are presented here for BC cores with diameters between 200–220 nm. For simplicity we hereafter refer to this parameter as 'coating thickness' without specifying the range of BC core diameters over which it has been calculated. The mean coating thickness at 3 h time resolution (Fig. 5c~~a~~) was calculated from single particle data as shown in Fig. S7. The coating thickness for ambient particles ranged from 51 to 61 nm (IQR) over the whole campaign, which corresponds to rBC volume fractions between 25 and 30 % (Fig. 5d).

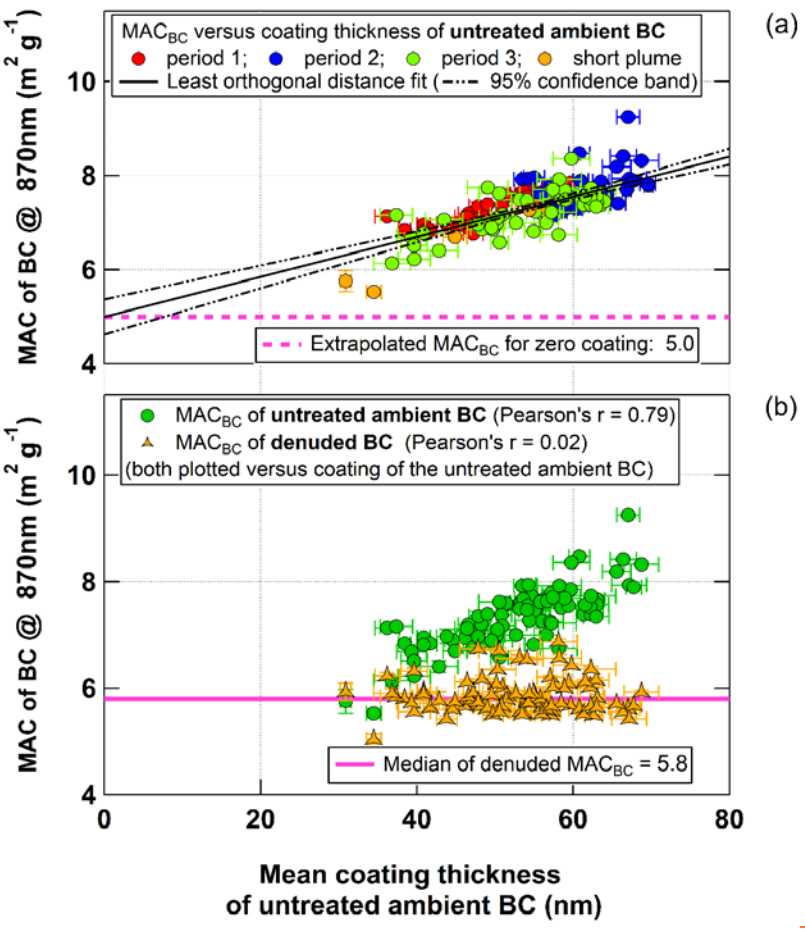

Figure 6. (a) MAC$_{BC}$ of the aerosol sample dried to low RH against the mean coating thickness of ambient rBC particles with core diameters in the range 200–220 nm mass equivalent diameter. (b) MAC$_{BC}$ of ambient and thermo-denuded samples against the mean coating thickness of ambient rBC particles. Each data point represents an average value over a 3-h time period with error bars representing the standard error of the mean (these averages were performed with 1 min resolution data in the case of the MAC$_{BC}$ values and 1 sec resolution data in the case of the mean coating thicknesses). An orthogonal distance linear regression was applied to the ambient data to calculate a y-intercept value which represents an estimate of the MAC for zero coating, i.e., MAC$_{BC,bare}$. Note that

Commented [GBM4]: A minor update was made to this figu two erroneous data points of "MAC$_{BC}$ of denuded BC" were remo (these were not measured downstream of denuder).

the number of ambient MAC_{BC} data points in (b) is smaller than in (a) due to the gap of missing data in the denuded MAC_{BC} time series from 07 to 14 Feb shown in Fig. 5e.

It is apparent from the time series in Fig. 5c and e that the ambient MAC_{BC} and BC coating thickness correlated well. These two ~~quantities~~ properties of the dried aerosol ~~dried to low RH~~ are plotted as a scatter plot in Fig. 6a, indicating that ambient MAC_{BC} and coating thickness were positively correlated with a Pearson correlation coefficient of 0.73. This provides evidence that there was indeed a lensing effect during the campaign and that the BC mixing state was the main driver of MAC_{BC} variability. We hereafter refer to this method of directly evaluating the dependence of MAC_{BC} on the internal mixing state as the correlation method. To investigate the robustness of the results of the correlation method, Fig. S10 displays versions of Fig. 6a with different scaling factors applied to the underlying quantities used to calculate MAC_{BC}. In particular, we investigated the effect of applying a loading-dependent scaling factor to PAX data in Fig. S10b (as motivated by Fig. 2 and the discussion in Sect. 2.4.2.2), as well as the effect of applying separate missing rBC mass correction factors for each time period of the campaign in Fig. S10c (as discussed in Sect. 2.4.1). In these cases (as well as the case when both types of scaling factors are applied, Fig. S10d), the positive correlation between MAC_{BC} and the mean coating thickness remains, supporting the evidence for an observed lensing effect.

In order to estimate the MAC_{BC} of bare, uncoated BC ($MAC_{BC,bare}$) a linear function was fit to the measurements in Fig. 6a (via orthogonal distance regression, ODR fit) to obtain a y-intercept of 5.0 $m^2\ g^{-1}$. Since the relationship between MAC_{BC} and coating thickness may not be linear for lightly coated BC (the lensing effect appears to be weaker for lightly coated than moderately to heavy coated BC; Peng et al., 2016; Liu et al., 2017), this extrapolated intercept is regarded as a lower limit estimate of $MAC_{BC,bare}$.

A second, more direct approach was also applied to investigate the lensing effect – we refer to this as the denuding method. In this method a catalytic stripper (CS) was used to remove BC coating material (Fig. 5c) before the MAC_{BC} measurement. Fig. 5e shows that this process resulted in lower MAC_{BC} for the denuded samples relative to the corresponding ambient samples. In Fig. 6b, the ambient and denuded MAC_{BC} values are plotted against the mean coating thickness of the unperturbed, ambient BC particles (i.e., before denuding by the CS). It is seen that most of the denuded-MAC_{BC} values ~~all~~ fall in the range from 5.6 to 6.0 $m^2\ g^{-1}$ (median= 5.8 $m^2\ g^{-1}$) and that the values are largely independent of the original coating thickness, with a Pearson correlation coefficient of only 0.02 (the denuded-MAC_{BC} values are also largely independent of the coating thickness of the denuded particles as shown in Fig. S4, with a Pearson correlation coefficient of -0.29). This is in contrast to the trend observed for the ambient MAC_{BC} measurements, which showed strong correlation with the coating

thickness of the unperturbed BC particles. These results suggest that the coating material removed from the BC particles by the CS was largely responsible for the lensing effect displayed by the ambient BC particles.

The results displayed in Fig. 5c and Fig. S8 indicate that the CS did not remove all coating material from the BC particles, likely due to the short residence time of around 0.35 s only. The denuded particles retained thin coatings which might still be responsible for a lensing effect. However, such a lensing effect is not apparent when plotting the denuded-MAC_{BC} values against the coating thickness of the denuded particles (Fig. S10). ~~Therefore~~In any case, we consider the median denuded MAC_{BC} of 5.8 $m^2 g^{-1}$ to represent an upper limit estimate of $MAC_{BC,bare}$. The true value of $MAC_{BC,bare}$ likely falls within the range of 5.0 to 5.8 $m^2 g^{-1}$ defined by the lower and upper limit estimates arising from the correlation and denuding methods, respectively. Still, the results of the two methods are roughly consistent with each other, strengthening the conclusion that the internal mixing of BC drove the variability of MAC_{BC} in this campaign.

3.4 Influence of other BC particle properties on MAC_{BC}

In this section, the importance of BC particle properties other than the internal mixing state is explored in relation to MAC_{BC} variability.

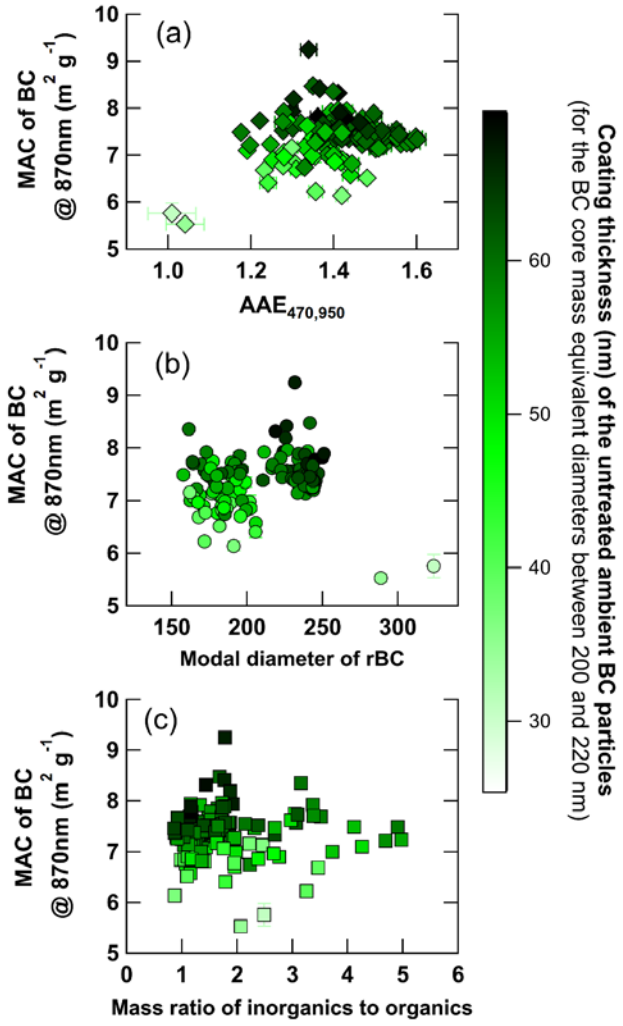

Figure 7. Time-resolved MAC_{BC} values of untreated ambient BC particles at 870 nm wavelength calculated at 3 h resolution plotted against (a) the absorption Ångström exponent, $AAE_{470,950}$, between 470 and 950 nm wavelength, (b) the modal diameter of the BC

core mass size distributions (D_{rBC}) (expressed as mass equivalent diameter), and (c) the ratio of non-refractory inorganic to organic components measured in near-PM1 by the ACSM.

First, we address the question if the ambient MAC_{BC} is dependent on the BC "source". In a qualitative manner, the air mass origins characterized in Sect. 3.1 can be used to indicate different emission sources of BC particles in order to answer this question. In Fig. 6a, it is seen that the MAC_{BC} measurements from all air mass origin periods (Fig. 6a) scatter around the same regression fitting line. This suggests that the differences in MAC_{BC} between the periods are driven by differences in coating thickness, rather than the air mass origins or the characteristics of BC from different sources.

As introduced in Sect. 2.4.2.2, the absorption Ångström exponent (AAE) can indicate different BC sources (e.g. traffic emissions typically display AAE ~1, while wood burning emissions generally have AAE >1). Therefore, in a more quantitative manner, the correlation of MAC_{BC} and AAE can be calculated to explore a possible source dependence for MAC_{BC}. Time series of AAE values calculated between different pairs of wavelengths are shown in Fig. S9a, indicating similar behavior for all wavelength pairs. Given this fact, $AAE_{470,950}$ was chosen to explore the correlation with MAC_{BC} in Fig. 5b in order to have the wavelength dependence of absorption across a wide range of wavelengths (from blue to near-infrared).

$AAE_{470,950}$ ranged from approximately 1.2 to 1.6 during the campaign, except for the short plume period where values around 1 were observed. This indicates that there were contributions from emission sources other than traffic to BC during the campaign. Wood burning is performed in winter in central Europe for heating purposes, and it is likely that brown carbon emissions from this activity resulted in absorption at shorter wavelengths, contributing to high $AAE_{470,950}$ values (>1). If it is assumed that additional emission sources such as coal burning did not contribute to the sample, the aethalometer model for source apportionment (Zotter et al., 2017) can be used to separate the contributions of wood burning and traffic emissions to total absorption (and therefore equivalent BC). The results of this model are shown in Fig. S9b. During periods 1 and 3, the model suggests that traffic and wood burning emissions contributed roughly equally to the observed total BC mass concentration. In contrast, during period 2, the modeled wood burning contribution dominated over the traffic contribution.

It is important to stress, however, that the AAE model can only apportion the measured absorption to two sources. As discussed in Sec. 3.1 , it is likely that a third source – coal burning emissions – also contributed to

the BC measured during the campaign, at least in period 2 when the SO_2 to NOx ratio was significantly higher. Bond et al. (1999) observed that the industrial burning of lignite coal produced a yellowish, carbonaceous aerosol with strong absorption wavelength dependence. More generally, Bond et al. (2002) observed $AAE_{435,880}$ values between 1 and 3 for aerosol produced from the burning of different types of coal. Given the wide range of observed AAE for coal burning emissions, and the lack of knowledge regarding a specific value that is appropriate for central Europe (e.g. as is the case for biomass burning aerosols; Zotter et al., 2017), it is not possible to use measured AAE values to apportion a specific fraction of equivalent BC to coal emissions. Still, the $AAE_{470,950}$ values found here were mostly above 1.4 during period 2, which is consistent with the assumption that coal burning (lignite) emissions were relevant during this period. Therefore, we conclude that coal burning emissions likely contributed to the BC measured during the campaign, however, without being able to quantify this contribution. In this case, the contributions of wood burning and traffic to BC as calculated with the aethalometer model and displayed in Fig. S9b should be considered as upper limit estimates, since these contributions would likely be lower if a third source was included in the model.

Independent of a precise BC source apportionment the correlation of AAE with MAC_{BC} can still be assessed to explore a potential source dependence for MAC_{BC}. Fig. 7a indicates there was no clear relationship between MAC_{BC} and $AAE_{470,950}$ during the campaign. This supports the conclusion of the analysis displayed in Fig. 6a that MAC_{BC} variability was driven by coating thickness, and not by the characteristics of BC from different sources.

Second, we address the question if the MAC_{BC} depends on the BC core diameter. Figure 7b shows that there was no clear relationship between MAC_{BC} and BC core diameter (R^2=0.01, or 0.09 with the two outlying points with the largest modal diameters removed), which indicates that the variation in BC size was not responsible for the MAC_{BC} variability. This is because the modal diameters of the BC core mass size distributions only varied within a relatively narrow range during the campaign (D_{rBC} from 150 to 250 nm). This corresponds to dimensionless size parameters x (= $\pi D_{rBC}/\lambda$) in the range from 0.5 to 0.9. In both the Rayleigh (x<<1) and Mie regime (x~1), the size-distribution-weighted MAC_{BC} is relatively independent of D_{rBC}. For much greater D_{rBC} (x >> 1, known as the geometric regime) incident light is unable to penetrate through the whole particle: absorption only occurs in the outer layer of the particle, which results in a strong negative relationship between MAC_{BC} and D_{rBC} in this regime. The modal diameters of the BC core mass size distributions observed during this campaign were not large enough to reach the geometric regime, which is why no clear relationship was observed between MAC_{BC} and D_{rBC}.

Third, the dependence of the ambient MAC_{BC} on the coating composition is evaluated. Moffet et al. (2016) indicated that the chemical composition of the BC coating material may affect the optical properties of BC by influencing the location of a BC core within its hosting particle. These authors observed in a field study in central California that BC cores in particles with organic-rich coatings were located near particle centers while BC cores in particles with inorganic coatings were located near particle edges. They hypothesized that the latter case occurs due to crystallization of the inorganic species. In terms of light absorption enhancement, a few laboratory and field studies have found evidence that E_{MAC} values depend on whether BC is internally mixed with organic or inorganic species. Wei et al. (2013) found that glycerol-coated BC had E_{MAC} at 532 nm of ~1.4 while BC cores coated with solid ammonium sulfate and ammonium nitrate had E_{MAC} at 532 nm of only 1.10 and 1.06, respectively. However, it should be noted that the amount of coating could not be quantified conclusively in these experiments, and therefore it ~~cannot be verified~~ must be considered likely that the coating volume fractions ~~was equal for the~~differed for the different coating compositions. Zhang et al. (2018) applied a multi-linear regression analysis to positive matrix factorization (PMF) source apportionment results to conclude that highly oxidized secondary organic aerosol was the major chemical component responsible for aerosol light absorption enhancement observed at an urban background site in Paris, France. These authors showed that E_{MAC} at 870 nm displayed a positive relationship with the mass ratio of bulk secondary organic to secondary inorganic aerosol, with E_{MAC} at 870 nm increasing from 1 to 2 as the mass ratio of organics to inorganic increased from 2 to 8. However, it should also be noted here that coating amounts were not measured, and therefore the observed relationship could potentially be the result of cross-correlation between coating composition and coating thickness.

In this study, the chemical composition was measured for bulk aerosols by an ACSM. No chemical or mixing state information is available at the single particle level. Therefore, we used the bulk ratio of measured inorganic to organic particulate matter as a proxy variable to investigate a possible dependence of MAC_{BC} on coating composition. In Fig. 7c it is seen that MAC_{BC} displays no clear relationship with the inorganic to organic ratio. By contrast, darker points are systematically higher up than brighter points, indicating that the amount of coating (coating thickness) had a large effect on absorption enhancement through the lensing effect, whereas variations in coating composition only had a negligible effect during this campaign. However, it cannot be ruled out that a relationship between coating chemical composition and absorption enhancement did in fact exist, but that the relationship is not apparent in Fig. 7c because the bulk ratio of inorganic to organic aerosol mass is a poor indicator of the composition of coatings on individual particles.

Despite the fact that atmospheric aging processes tend to make aerosols more homogeneous during transport away from sources, e.g. by increasing the degree of internal mixing, some dependence of MAC_{BC} on BC source

could be retained. Possible drivers for such source dependence include differences in BC core size and morphology, in chemical microstructure of the BC, in morphology of the coated BC due to differences in coating processes and/or coating composition. The MAC_{BC} of denuded aerosol samples exhibited very limited variability (Fig. S4b) suggesting that potential differences in MAC_{BC} of bare cores from different sources are small. The analyses presented above further suggest that BC source related differences in MAC_{BC}, which may or may not exist close to sources, largely disappear during transport to the rural background site. The only exception are variations in coating thickness, which have been shown to drive MAC_{BC} variations, and which may have retained some residual relation with BC source.

3.5 Absorption enhancement factors (lensing effect) and their comparison with previous studies

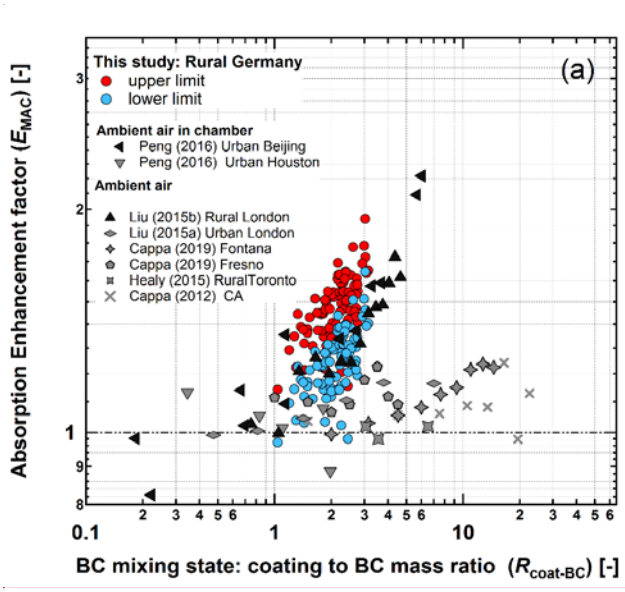

Commented [MRL5]: This figure has been updated. The Ued (2016) data have been removed from the figure.

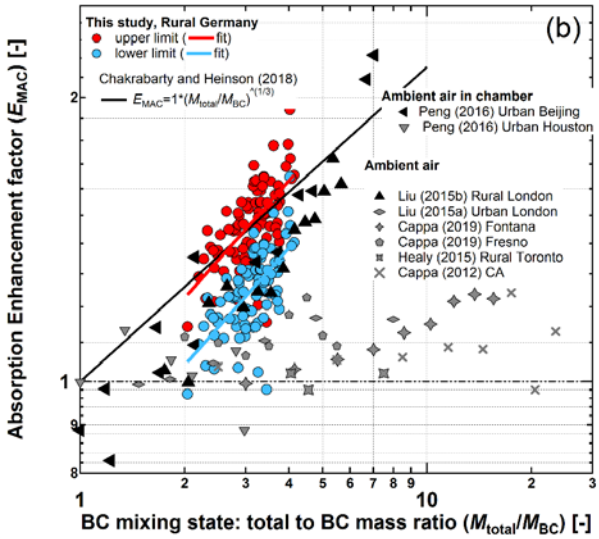

Commented [MRL6]: This figure has been updated. The Ued (2016) data have been removed from the figure.

Figure 8. Summary of E_{MAC} values and their dependence on BC mixing state from this study compared with literature data measured at wavelengths from 532 nm to 870 nm. The E_{MAC} values are plotted versus the ratio of coating to BC core mass (a) and versus the ratio of total particle mass to BC core mass (only considering BC-containing particles) (b). Panel (a) is an updated version of a figure from Cappa et al. (2019), while in ~~and~~ panel (b) the abscissa has been changed to M_{total}/M_{BC} to additionally include~~s~~ the simple power-law ~~dependence~~ parameterization of the lensing effect proposed by Chakrabarty and Heinson (2018), which uses M_{total}/M_{BC} as the~~free~~ input parameter to represent BC mixing state (where M_{total} refers to the mass of the total particle, such that $M_{total}/M_{BC} = 1 + R_{coat\text{-}BC}$). The two approaches applied to obtain the lower and upper limit E_{MAC} values presented for this study are discussed in Sect. 3.3). Note: the data points ~~of the studies by Ueda et al. (2016) and~~from the study of Liu et al. (2015a) deviate marginally from those in the original figure by Cappa et al. (2019), as the abscissa values were recalculated from the original data using ~~equal~~ material densities for BC and coating material of 1.8 and 1.6 g cm^{-3}, respectively, as applied in this study.

The relationship between E_{MAC} and the internal mixing state of BC is shown in Fig. 8a. In order to directly compare the results of this study with those from previous studies, the BC mixing state is represented in Fig. 8a by the mean ratio of coating to core mass ($R_{coat\text{-}BC}$) for BC cores with mass equivalent diameter between 200 and 220 nm, rather than mean coating thickness over this same size range as in Fig. 6. Two sets of data points from this study are shown in Fig. 8a: lower limit estimates of E_{MAC} that were obtained with constraining the MAC_{BC} of

bare BC cores by the denuding method (i.e., E_{MAC} = $MAC_{BC,amb}$/5.8 m^2 g^{-1}), and upper limit estimates of E_{MAC} that were obtained with constraining the MAC_{BC} of bare BC cores by the correlation method (i.e., E_{MAC} = $MAC_{BC,amb}$/5.0 m^2 g^{-1}), as described in Sect. 3.3. The differences between these two sets of measurements is at least partly due to the fact that the thermodenuding process at 350 °C employed here was not sufficient to completely remove all coating material from the BC particles (Figs. 5c and S8). This is an important point to consider in all studies that employ similar types of thermodenuders in order to remove coatings from BC particles.

E_{MAC} measurements from previous studies are also displayed in Fig. 8a in order to place the results from this study in context. The most striking aspect of this comparison is that ambient E_{MAC} measurements tend to cluster into two main branches of points, as was recently pointed out by Cappa et al. (2019). One branch of measurements, indicated by light grey markers in Fig. 8a, suggest that E_{MAC} has little or no relationship to $R_{coat\text{-}BC}$ (i.e. a weak lensing effect). By contrast, the second branch of measurements (black markers in Fig 8a) indicate a strong positive relationship between E_{MAC} and $R_{coat\text{-}BC}$ (i.e. a clear lensing effect). The results from this study populate the latter branch of points, indicating the occurrence of a clear lensing effect.

The reasons why a strong lensing effect is observed in some ambient studies but not in others remain elusive and hypothetical. Firstly, it's important to note that there are methodological differences between the studies summarized in Fig. 8a. Some studies employed an SP-AMS to measure BC mixing state (Cappa et al., 2012; Cappa et al., 2019; Healy et al., 2015; Liu et al., 2015b), while others used alternative instruments such as SP2, ~~transmission electron microscopy (TEM)~~ and a V-TDMA (volatility tandem differential mobility analyzer) for this purpose (Liu et al., 2015a; Peng et al., 2016 and this study). It is noteworthy that the majority of SP-AMS-based studies observed only a weak lensing effect~~, which suggests that this result may be related to instrument characteristics, such as the fact that the instrument collection efficiency depends on BC mixing state (as discussed in the Introduction section)~~. However, a weak lensing effect was also observed in one SP2 based study (Liu et al., 2015a) and a strong lensing effect in one SP-AMS based study (Liu et al., 2015b), which suggests that the discrepancies between studies are not only due to this methodological reason. Nevertheless, dedicated SP-AMS and SP2 instrument inter-comparison experiments should be conducted to directly compare $R_{coat\text{-}BC}$ measurements from these two instruments to see to what extent discrepancies between the methods can explain the divergence of results in Fig. 8a.

Secondly, there are plausible physical explanations to explain the clustering of measurements into the two branches of points displayed in Fig. 8a, as discussed by Cappa et al. (2019). One hypothesis is that the ~~distribution~~ relative location of BC and other aerosol components within the BC-containing particles ~~on a per-particle level~~ determines whether a lensing effect occurs or not. Theoretical studies (Adachi et al., 2010; Zhang et al., 2017) and laboratory measurements (Schnaiter, 2005) indicate that BC particles encapsulated in a core-shell configuration display substantial absorption enhancement, while BC particles that are only partially encapsulated or 'attached' to the edge of other particles display little or no absorption enhancement. TEM studies have found that both of these types of mixed BC particles can be found in the ambient atmosphere (Ueda et al., 2016; Liu et al., 2015b), and some studies have even linked the presence of concentrically coated BC particles to higher observed E_{MAC} (Ueda et al., 2016). Recent studies indicate that a threshold value of $R_{coat\text{-}BC}$ appears to exist beyond which particles collapse to a core-shell-like configuration and display a substantial lensing effect (Peng et al., 2016; Liu et al., 2017). Aside from ~~individual-particle-level~~typical morphology and average mixing state, the distribution of coating material across an ensemble of particles is also an important determinant of the average absorption enhancement displayed by that ensemble (Fierce et al., 2016). This is another potential hypothesis for why some studies have measured lower than expected E_{MAC} values for aerosols with large $R_{coat\text{-}BC}$.

During the Melpitz campaign, neither measurements of BC particle morphologies nor single-particle-level coating thickness measurements over the full size range of BC particles are available (representative LEO-fit measurements only cover a limited range, see Sect. 2.4.1). Therefore, we are unable to say definitively why a clear lensing effect was observed in this study and not in other studies. However, given the fact that a clear lensing effect was observed, we assume that the majority of BC particles were above the threshold of absorption enhancement and were fully coated in a core-shell like configuration. This in turn suggests that BC particles measured at the rural background site of Melpitz during winter were in a relatively aged state.

Recently, Chakrabarty and Heinson (2018) proposed that the absorption enhancement of BC particles as a function of the total particle to BC core mass ratio follows a simple power law with an exponent of 1/3. This finding is based on numerically exact electromagnetic calculations of simulated BC aggregates with variable degree of internal mixing with non-absorbing matter, and it is also in agreement with some previous experimental studies. The E_{MAC} results from this study and selected ambient literature studies are plotted against BC mixing state expressed as M_{total}/M_{BC} in Fig. 8b (where $M_{total}/M_{BC} = 1 + R_{coat\text{-}BC}$). Our results and some of the other studies having clear lensing effect (black markers) are generally consistent with the proposed power-function scaling law. However, other studies having weak lensing effect (light gray markers) disagree with the scaling law, which could be due to the hypotheses mentioned previously. It is noteworthy that the

upper limit E_{MAC} estimates of this study appear to more closely follow the scaling law than the lower-limit estimates. This may suggest that the upper limit E_{MAC} estimates are more realistic, which could be reasonable considering that the lower limit estimates were derived from the denuding measurements which failed to completely remove the BC coatings. However, quantitative comparison of ambient results should be treated with care, given the limited range of mass ratios that were observed and the potential influence of other minor factors on E_{MAC} as described in Sect. 3.4. Nevertheless, the agreement of the observation of this study with a model based on coated BC particles with morphologies favorable for occurrence of the lensing effect provides indirect evidence that dampening of the lensing effect due to particle shapes with unfavorable morphologies was only minor or negligible for the rural background aerosol at Melpitz in winter.

4 Conclusions

Field measurements of BC particle properties and additional aerosol characteristics were performed at the rural background site of Melpitz, Germany during winter (February 2017). Two independent methods (the denuding and correlation methods) were used to show that the variability of MAC_{BC} at this site was driven by the degree of BC internal mixing state (i.e. a clear lensing effect was observed). The enhancement of light absorption by BC due to coatings varied from 1.0 to 1.6 (lower limit estimates), or 1.2 to 1.9 (higher limit estimates), for mean BC volume fractions ~~in the internally mixed particles varying from~~that varied from 46 to 22 ~~to 46~~ % (for BC core sizes from 200 to 220nm). The lower and higher limit estimates were determined using two different approaches, one of them involving denuding by means of a catalytic stripper, and the difference between the two may potentially be caused by incomplete coating removal. All these results apply for essentially water-free aerosol as present after drying to low RH.

The strong lensing effect observed in this study agrees well with a theoretical relationship recently published and with a subset of previous ambient studies. No evidence was found for cases with absence of lensing effect despite internally mixed BC, as reported in other previous studies. By contrast, evidence suggests that potential dampening of the lensing effect due to unfavorable morphology was most likely small or even negligible. Additional potential drivers of MAC_{BC} variations including dominant BC source, average BC core size and coating composition were also investigated. None of these was found to have a substantial effect at the rural background site Melpitz with a large fraction of aged particles. However, such effects could potentially be obscured by the lack of single particle composition and morphology information that would be required for ~~more~~ a single-particle level quantitative assessment.

Overall, the results of this study support that knowing the BC mixing state in terms of BC volume fraction in the internally mixed particles is sufficient to describe the lensing effect and MAC_{BC} in good approximation. By

contrast, the influence of coating composition appears to be minor for atmospheric aerosols. However, future field studies addressing the coating composition effect would have to combine ~~quantitative mixing state measurements with~~ coating composition ~~measurements~~and quantification with~~, and also mixing state~~ morphology measurements, which remains an experimental challenge. In addition to this challenge, follow up studies should aim to intercompare different techniques for measuring BC volume fractions (e.g. SP2 versus SP-AMS measurements of $R_{coat\text{-}BC}$).

Data availability. Data will be made available on Zenodo if the manuscript was accepted for publication.

Author contributions. MGB acquired the funding and designed the experiment jointly with RLM and JY. BW coordinated the campaign. JY, RM, MZ, TM, LP, BW and TT took the measurements and/or ~~analysed~~analyzed the raw data. JY interpreted the results and wrote the manuscript together with RLM and MGB. All co-authors reviewed and commented the manuscript.

Competing interests. The authors declare that they have no conflict of interest.

Acknowledgements. The authors gratefully acknowledge Achim Grüner and Gerald Spindler for regular operation of the Melpitz observatory and the NOAA Air Resources Laboratory (ARL) for the provision of the HYSPLIT transport and dispersion model. Financial support was received from the ERC (grant agreement no. 615922-BLACARAT). Further support was received from the ACTRIS2 project funded by the EU (H2020 grant agreement no. 654109) and the Swiss State Secretariat for Education, Research and Innovation (SERI; contract number 15.0159-1). The opinions expressed and arguments employed herein do not necessarily reflect the official views of the Swiss Government. MZ and ABH gratefully acknowledge the funding by the Deutsche Forschungsgemeinschaft (DFG, German Research Foundation) – Projektnummer 268020496 – TRR 172, within the Transregional Collaborative Research Center "ArctiC Amplification: Climate Relevant Atmospheric and SurfaCe Processes, and Feedback Mechanisms (AC)³".

References

Aas, W., Tsyro, S., Bieber, E., Bergström, R., Ceburnis, D., Ellermann, T., Fagerli, H., Frölich, M., Gehrig, R., Makkonen, U., Nemitz, E., Otjes, R., Perez, N., Perrino, C., Prévôt, A. S. H., Putaud, J. P., Simpson, D., Spindler, G., Vana, M., and Yttri, K. E.: Lessons learnt from the first emep intensive measurement periods. Atmos. Chem. Phys., 12, 8073-8094, https://doi.org/10.5194/acp-12-8073-2012, 2012.

Adachi, K., Chung, S., and R. Buseck, P.: Shapes of soot aerosol particles and implications for their effects on climate. 115, https://doi.org/10.1029/2009JD012868, 2010.

Amanatidis, S., Ntziachristos, L., Giechaskiel, B., Katsaounis, D., Samaras, Z., and Bergmann, A.: Evaluation of an oxidation catalyst ("catalytic stripper") in eliminating volatile material from combustion aerosol. J. Aerosol Sci., 57, 144-155, https://doi.org/10.1016/j.jaerosci.2012.12.001, 2013.

Arnott, W. P., Moosmüller, H., Rogers, C. F., Tianfeng, J., and Bruch, R.: Photoacoustic spectrometer for measuring light absorption by aerosol: Instrument description. Atmos. Environ., 33, 2845-2852, https://doi.org/https://doi.org/10.1016/S1352-2310(98)00361-6, 1999.

Asmi, A., Wiedensohler, A., Laj, P., Fjaeraa, A. M., Sellegri, K., Birmili, W., Weingartner, E., Baltensperger, U., Zdimal, V., Zikova, N., Putaud, J. P., Marinoni, A., Tunved, P., Hansson, H. C., Fiebig, M., Kivekäs, N., Lihavainen, H., Asmi, E., Ulevicius, V., Aalto, P. P., Swietlicki, E., Kristensson, A., Mihalopoulos, N., Kalivitis, N., Kalapov, I., Kiss, G., de Leeuw, G., Henzing, B., Harrison, R. M., Beddows, D., amp, apos, Dowd, C., Jennings, S. G., Flentje, H., Weinhold, K., Meinhardt, F., Ries, L., and Kulmala, M.: Number size distributions and seasonality of submicron particles in europe 2008–2009. Atmos. Chem. Phys., 11, 5505-5538, https://doi.org/10.5194/acp-11-5505-2011, 2011.

Baumgardner, D., Popovicheva, O., Allan, J., Bernardoni, V., Cao, J., Cavalli, F., Cozic, J., Diapouli, E., Eleftheriadis, K., Genberg, P. J., Gonzalez, C., Gysel, M., John, A., Kirchstetter, T. W., Kuhlbusch, T. A. J., Laborde, M., Lack, D., Müller, T., Niessner, R., Petzold, A., Piazzalunga, A., Putaud, J. P., Schwarz, J., Sheridan, P., Subramanian, R., Swietlicki, E., Valli, G., Vecchi, R., and Viana, M.: Soot reference materials for instrument calibration and intercomparisons: A workshop summary with recommendations. Atmos. Meas. Tech., 5, 1869-1887, https://doi.org/10.5194/amt-5-1869-2012, 2012.

Birmili, W., Weinhold, K., Nordmann, S., Wiedensohler, A., Spindler, G., Müller, K., Herrmann, H., Gnauk, T., Pitz, M., Cyrys, J., Flentje, H., Nickel, C., Kuhlbusch, T. A. J., and Löschau, G.: Atmospheric aerosol measurements in the german ultrafine aerosol network (guan): Part 1 – soot and particle number size distribution. Gefahrst. Reinh. Luft, 69, 137–145, 2009.

Birmili, W., Weinhold, K., Rasch, F., Sonntag, A., Sun, J., Merkel, M., Wiedensohler, A., Bastian, S., Schladitz, A., Löschau, G., Cyrys, J., Pitz, M., Gu, J., Kusch, T., Flentje, H., Quass, U., Kaminski, H., Kuhlbusch, T. A. J., Meinhardt, F., Schwerin, A., Bath, O., Ries, L., Gerwig, H., Wirtz, K., and Fiebig, M.: Long-term observations of tropospheric particle number size distributions and equivalent black carbon mass concentrations in the german ultrafine aerosol network (guan). Earth System Science Data, 8, 355-382, https://doi.org/10.5194/essd-8-355-2016, 2016.

Bohren, C. F. and Huffman, D. R.: Absorption and scattering by a sphere, in Absorption and scattering of light by small particles, pp. 82-129, WILEY-VCH Verlag GmbH & Co. KGaA, Weinheim, Germany, 1998.

Bond, T. C., Bussemer, M., Wehner, B., Keller, S., Charlson, R. J., and Heintzenberg, J.: Light absorption by primary particle emissions from a lignite burning plant. Environ. Sci. Technol., 33, 3887-3891, https://doi.org/10.1021/es9810538, 1999.

Bond, T. C., Covert, D. S., Kramlich, J. C., Larson, T. V., and Charlson, R. J.: Primary particle emissions from residential coal burning: Optical properties and size distributions. Journal of Geophysical Research: Atmospheres, 107, ICC 9-1-ICC 9-14, https://doi.org/10.1029/2001jd000571, 2002.

Bond, T. C., Doherty, S. J., Fahey, D. W., Forster, P. M., Berntsen, T., DeAngelo, B. J., Flanner, M. G., Ghan, S., Kärcher, B., Koch, D., Kinne, S., Kondo, Y., Quinn, P. K., Sarofim, M. C., Schultz, M. G., Schulz, M., Venkataraman, C., Zhang, H., Zhang, S., Bellouin, N., Guttikunda, S. K., Hopke, P. K., Jacobson, M. Z., Kaiser, J. W., Klimont, Z., Lohmann, U., Schwarz, J. P., Shindell, D., Storelvmo, T., Warren, S. G., and Zender, C. S.: Bounding the role of black carbon in the climate system: A scientific assessment. Journal of Geophysical Research: Atmospheres, 118, 5380-5552, https://doi.org/10.1002/jgrd.50171, 2013.

Bond, T. C., Habib, G., and Bergstrom, R. W.: Limitations in the enhancement of visible light absorption due to mixing state. J. Geophys. Res., 111, https://doi.org/10.1029/2006jd007315, 2006.

Cappa, C. D., Onasch, T. B., Massoli, P., Worsnop, D. R., Bates, T. S., Cross, E. S., Davidovits, P., Hakala, J., Hayden, K. L., Jobson, B. T., Kolesar, K. R., Lack, D. A., Lerner, B. M., Li, S. M., Mellon, D., Nuaaman, I., Olfert, J. S., Petaja, T., Quinn, P. K., Song, C., Subramanian, R., Williams, E. J., and Zaveri, R. A.: Radiative absorption enhancements due to the mixing state of atmospheric black carbon. Science, 337, 1078-81, https://doi.org/10.1126/science.1223447, 2012.

Cappa, C. D., Zhang, X., Russell, L. M., Collier, S., Lee, A. K. Y., Chen, C.-L., Betha, R., Chen, S., Liu, J., Price, D. J., Sanchez, K. J., McMeeking, G. R., Williams, L. R., Onasch, T. B., Worsnop, D. R., Abbatt, J., and Zhang, Q.: Light absorption by ambient black and brown carbon and its dependence on black carbon coating state for two california, USA, cities in winter and summer. Journal of Geophysical Research: Atmospheres, 124, 1550-1577, https://doi.org/10.1029/2018jd029501, 2019.

Chakrabarty, R. K. and Heinson, W. R.: Scaling laws for light absorption enhancement due to nonrefractory coating of atmospheric black carbon aerosol. Phys Rev Lett, 121, 218701, https://doi.org/10.1103/PhysRevLett.121.218701, 2018.

Ciarelli, G., Aksoyoglu, S., El Haddad, I., Bruns, E. A., Crippa, M., Poulain, L., Äijälä, M., Carbone, S., Freney, E., amp, apos, Dowd, C., Baltensperger, U., and Prévôt, A. S. H.: Modelling winter organic aerosol at the european scale with camx: Evaluation and source apportionment with a vbs parameterization based on novel wood burning smog chamber experiments. Atmos. Chem. Phys., 17, 7653-7669, https://doi.org/10.5194/acp-17-7653-2017, 2017.

Collier, S., Williams, L. R., Onasch, T. B., Cappa, C. D., Zhang, X., Russell, L. M., Chen, C.-L., Sanchez, K. J., Worsnop, D. R., and Zhang, Q.: Influence of emissions and aqueous processing on particles containing black carbon in a polluted urban environment: Insights from a soot particle-aerosol mass spectrometer. Journal of Geophysical Research: Atmospheres, 123, 6648-6666, https://doi.org/10.1002/2017jd027851, 2018.

Corbin, J. C., Czech, H., Massabò, D., de Mongeot, F. B., Jakobi, G., Liu, F., Lobo, P., Mennucci, C., Mensah, A. A., Orasche, J., Pieber, S. M., Prévôt, A. S. H., Stengel, B., Tay, L. L., Zanatta, M., Zimmermann, R., El Haddad, I., and Gysel, M.: Infrared-absorbing carbonaceous tar can dominate light absorption by marine-engine exhaust. npj Clim. Atmos. Sci., 2, 12, https://doi.org/10.1038/s41612-019-0069-5, 2019.

Dahlkötter, F., Gysel, M., Sauer, D., Minikin, A., Baumann, R., Seifert, P., Ansmann, A., Fromm, M., Voigt, C., and Weinzierl, B.: The pagami creek smoke plume after long-range transport to the upper troposphere over europe – aerosol properties and black carbon mixing state. Atmos. Chem. Phys., 14, 6111-6137, https://doi.org/10.5194/acp-14-6111-2014, 2014.

Drinovec, L., Močnik, G., Zotter, P., Prévôt, A. S. H., Ruckstuhl, C., Coz, E., Rupakheti, M., Sciare, J., Müller, T., Wiedensohler, A., and Hansen, A. D. A.: The "dual-spot" aethalometer: An improved measurement of aerosol black carbon with real-time loading compensation. Atmos. Meas. Tech., 8, 1965-1979, https://doi.org/10.5194/amt-8-1965-2015, 2015.

Elser, M., Huang, R.-J., Wolf, R., Slowik, J. G., Wang, Q., Canonaco, F., Li, G., Bozzetti, C., Daellenbach, K. R., Huang, Y., Zhang, R., Li, Z., Cao, J., Baltensperger, U., El-Haddad, I., and Prévôt, A. S. H.: New insights into pm2.5 chemical composition and sources in two major cities in china during extreme haze events using aerosol mass spectrometry. Atmos. Chem. Phys., 16, 3207-3225, https://doi.org/10.5194/acp-16-3207-2016, 2016.

Fierce, L., Bond, T. C., Bauer, S. E., Mena, F., and Riemer, N.: Black carbon absorption at the global scale is affected by particle-scale diversity in composition. Nat. Commun., 7, 12361, https://doi.org/10.1038/ncomms12361, 2016.

Gao, R. S., Schwarz, J. P., Kelly, K. K., Fahey, D. W., Watts, L. A., Thompson, T. L., Spackman, J. R., Slowik, J. G., Cross, E. S., Han, J. H., Davidovits, P., Onasch, T. B., and Worsnop, D. R.: A novel method for estimating light-scattering properties of soot aerosols using a modified single-particle soot photometer. Aerosol Sci. Technol., 41, 125-135, https://doi.org/10.1080/02786820601118398, 2007.

Glasius, M., Hansen, A. M. K., Claeys, M., Henzing, J. S., Jedynska, A. D., Kasper-Giebl, A., Kistler, M., Kristensen, K., Martinsson, J., Maenhaut, W., Nøjgaard, J. K., Spindler, G., Stenström, K. E., Swietlicki, E., Szidat, S., Simpson, D., and Yttri, K. E.: Composition and sources of carbonaceous aerosols in northern europe during winter. Atmos. Environ., 173, 127-141, https://doi.org/10.1016/j.atmosenv.2017.11.005, 2018.

Hansen, A. D. A., Rosen, H., and Novakov, T.: The aethalometer — an instrument for the real-time measurement of optical absorption by aerosol particles. Sci. Total Environ., 36, 191-196, https://doi.org/10.1016/0048-9697(84)90265-1, 1984.

Healy, R. M., Wang, J. M., Jeong, C. H., Lee, A. K. Y., Willis, M. D., Jaroudi, E., Zimmerman, N., Hilker, N., Murphy, M., Eckhardt, S., Stohl, A., Abbatt, J. P. D., Wenger, J. C., and Evans, G. J.: Light-absorbing properties of ambient black carbon and brown carbon from fossil fuel and biomass burning sources. Journal of Geophysical Research: Atmospheres, 120, 6619-6633, https://doi.org/10.1002/2015jd023382, 2015.

Laborde, M., Crippa, M., Tritscher, T., Jurányi, Z., Decarlo, P. F., Temime-Roussel, B., Marchand, N., Eckhardt, S., Stohl, A., Baltensperger, U., Prévôt, A. S. H., Weingartner, E., and Gysel, M.: Black carbon physical properties and mixing state in the european megacity paris. Atmos. Chem. Phys., 13, 5831-5856, https://doi.org/10.5194/acp-13-5831-2013, 2013.

Laborde, M., Mertes, P., Zieger, P., Dommen, J., Baltensperger, U., and Gysel, M.: Sensitivity of the single particle soot photometer to different black carbon types. Atmos. Meas. Tech., 5, 1031-1043, https://doi.org/10.5194/amt-5-1031-2012, 2012a.

Laborde, M., Schnaiter, M., Linke, C., Saathoff, H., Naumann, K. H., Möhler, O., Berlenz, S., Wagner, U., Taylor, J. W., Liu, D., Flynn, M., Allan, J. D., Coe, H., Heimerl, K., Dahlkötter, F., Weinzierl, B., Wollny, A. G., Zanatta, M., Cozic, J., Laj, P., Hitzenberger, R., Schwarz, J. P., and Gysel, M.: Single particle soot photometer intercomparison at the aida chamber. Atmos. Meas. Tech., 5, 3077-3097, https://doi.org/10.5194/amt-5-3077-2012, 2012b.

Lack, D. A., Lovejoy, E. R., Baynard, T., Pettersson, A., and Ravishankara, A. R.: Aerosol absorption measurement using photoacoustic spectroscopy: Sensitivity, calibration, and uncertainty developments. Aerosol Sci. Technol., 40, 697-708, https://doi.org/10.1080/02786820600803917, 2006.

Liu, D., Allan, J. D., Young, D. E., Coe, H., Beddows, D., Fleming, Z. L., Flynn, M. J., Gallagher, M. W., Harrison, R. M., Lee, J., Prevot, A. S. H., Taylor, J. W., Yin, J., Williams, P. I., and Zotter, P.: Size distribution, mixing state and source apportionment of black carbon aerosol in london during wintertime. Atmos. Chem. Phys., 14, 10061-10084, https://doi.org/10.5194/acp-14-10061-2014, 2014.

Liu, D., Taylor, J. W., Young, D. E., Flynn, M. J., Coe, H., and Allan, J. D.: The effect of complex black carbon microphysics on the determination of the optical properties of brown carbon. Geophys. Res. Lett., 42, 613-619, https://doi.org/10.1002/2014gl062443, 2015a.

Liu, D., Whitehead, J., Alfarra, M. R., Reyes-Villegas, E., Spracklen, Dominick V., Reddington, Carly L., Kong, S., Williams, Paul I., Ting, Y.-C., Haslett, S., Taylor, Jonathan W., Flynn, Michael J., Morgan, William T., McFiggans, G., Coe, H., and Allan, James D.: Black-carbon absorption enhancement in the atmosphere determined by particle mixing state. Nat. Geosci., 10, 184-188, https://doi.org/10.1038/ngeo2901, 2017.

Liu, S., Aiken, A. C., Gorkowski, K., Dubey, M. K., Cappa, C. D., Williams, L. R., Herndon, S. C., Massoli, P., Fortner, E. C., Chhabra, P. S., Brooks, W. A., Onasch, T. B., Jayne, J. T., Worsnop, D. R., China, S., Sharma, N., Mazzoleni, C., Xu, L., Ng, N. L., Liu, D., Allan, J. D., Lee, J. D., Fleming, Z. L., Mohr, C., Zotter, P., Szidat, S., and Prevot, A. S. H.: Enhanced light absorption by mixed source black and brown carbon particles in uk winter. Nat Commun, 6, 8435, https://doi.org/10.1038/ncomms9435, 2015b.

Moffet, R. C., amp, apos, Brien, R. E., Alpert, P. A., Kelly, S. T., Pham, D. Q., Gilles, M. K., Knopf, D. A., and Laskin, A.: Morphology and mixing of black carbon particles collected in central california during the cares field study. Atmos. Chem. Phys., 16, 14515-14525, https://doi.org/10.5194/acp-16-14515-2016, 2016.

Moosmüller, H., Chakrabarty, R. K., Ehlers, K. M., and Arnott, W. P.: Absorption ångström coefficient, brown carbon, and aerosols: Basic concepts, bulk matter, and spherical particles. Atmos. Chem. Phys., 11, 1217-1225, https://doi.org/10.5194/acp-11-1217-2011, 2011.

Moteki, N. and Kondo, Y.: Dependence of laser-induced incandescence on physical properties of black carbon aerosols: Measurements and theoretical interpretation. Aerosol Sci. Technol., 44, 663-675, https://doi.org/10.1080/02786826.2010.484450, 2010.

Moteki, N., Kondo, Y., and Nakamura, S.-i.: Method to measure refractive indices of small nonspherical particles: Application to black carbon particles. J. Aerosol Sci., 41, 513-521, https://doi.org/10.1016/j.jaerosci.2010.02.013, 2010.

Müller, T., Henzing, J. S., de Leeuw, G., Wiedensohler, A., Alastuey, A., Angelov, H., Bizjak, M., Collaud Coen, M., Engström, J. E., Gruening, C., Hillamo, R., Hoffer, A., Imre, K., Ivanow, P., Jennings, G., Sun, J. Y., Kalivitis, N., Karlsson, H., Komppula, M., Laj, P., Li, S. M., Lunder, C., Marinoni, A., Martins dos Santos, S., Moerman, M., Nowak, A., Ogren, J. A., Petzold, A., Pichon, J. M., Rodriquez, S., Sharma, S., Sheridan, P. J., Teinilä, K., Tuch, T., Viana, M., Virkkula, A., Weingartner, E., Wilhelm, R., and Wang, Y. Q.: Characterization and intercomparison of aerosol absorption photometers: Result of two intercomparison workshops. Atmos. Meas. Tech., 4, 245-268, https://doi.org/10.5194/amt-4-245-2011, 2011.

Ng, N. L., Herndon, S. C., Trimborn, A., Canagaratna, M. R., Croteau, P. L., Onasch, T. B., Sueper, D., Worsnop, D. R., Zhang, Q., Sun, Y. L., and Jayne, J. T.: An aerosol chemical speciation monitor (acsm)

for routine monitoring of the composition and mass concentrations of ambient aerosol. Aerosol Sci. Technol., 45, 780-794, https://doi.org/10.1080/02786826.2011.560211, 2011.
Nordmann, S., Birmili, W., Weinhold, K., Müller, K., Spindler, G., and Wiedensohler, A.: Measurements of the mass absorption cross section of atmospheric soot particles using raman spectroscopy. Journal of Geophysical Research: Atmospheres, 118, 12,075-12,085, https://doi.org/10.1002/2013jd020021, 2013.
Peng, J., Hu, M., Guo, S., Du, Z., Zheng, J., Shang, D., Levy Zamora, M., Zeng, L., Shao, M., Wu, Y.-S., Zheng, J., Wang, Y., Glen, C. R., Collins, D. R., Molina, M. J., and Zhang, R.: Markedly enhanced absorption and direct radiative forcing of black carbon under polluted urban environments. P. Natl. Acad. Sci. USA, https://doi.org/10.1073/pnas.1602310113, 2016.
Petzold, A., Ogren, J. A., Fiebig, M., Laj, P., Li, S. M., Baltensperger, U., Holzer-Popp, T., Kinne, S., Pappalardo, G., Sugimoto, N., Wehrli, C., Wiedensohler, A., and Zhang, X. Y.: Recommendations for reporting "black carbon" measurements. Atmos. Chem. Phys., 13, 8365-8379, https://doi.org/10.5194/acp-13-8365-2013, 2013.
Petzold, A. and Schönlinner, M.: Multi-angle absorption photometry—a new method for the measurement of aerosol light absorption and atmospheric black carbon. J. Aerosol Sci., 35, 421-441, https://doi.org/10.1016/j.jaerosci.2003.09.005, 2004.
Pileci, R. E., Modini, R. L., Bertò, M., Yuan, J., Corbin, J. C., Marinoni, A., Henzing, B. J., Moerman, M. M., Putaud, J. P., Spindler, G., Wehner, B., Müller, T., Tuch, T., Trentini, A., Zanatta, M., Baltensperger, U., and Gysel-Beer, M.: Comparison of co-located rbc and ec mass concentration measurements during field campaigns at several european sites. Atmos. Meas. Tech. Discuss., 2020, 1-32, https://doi.org/10.5194/amt-2020-192, 2020.
Pöschl, U.: Aerosol particle analysis: Challenges and progress. Anal Bioanal Chem, 375, 30-2, https://doi.org/10.1007/s00216-002-1611-5, 2003.
Poulain, L., Birmili, W., Canonaco, F., Crippa, M., Wu, Z. J., Nordmann, S., Spindler, G., Prévôt, A. S. H., Wiedensohler, A., and Herrmann, H.: Chemical mass balance of 300 °c non-volatile particles at the tropospheric research site melpitz, germany. Atmos. Chem. Phys., 14, 10145-10162, https://doi.org/10.5194/acp-14-10145-2014, 2014.
Qiu, C., Khalizov, A. F., and Zhang, R.: Soot aging from oh-initiated oxidation of toluene. Environ Sci Technol, 46, 9464-72, https://doi.org/10.1021/es301883y, 2012.
Riemer, N., Ault, A. P., West, M., Craig, R. L., and Curtis, J. H.: Aerosol mixing state: Measurements, modeling, and impacts. Rev. Geophys., 57, 187-249, https://doi.org/10.1029/2018rg000615, 2019.
Schnaiter, M.: Absorption amplification of black carbon internally mixed with secondary organic aerosol. J. Geophys. Res., 110, https://doi.org/10.1029/2005jd006046, 2005.
Schneider, I. L., Teixeira, E. C., Silva Oliveira, L. F., and Wiegand, F.: Atmospheric particle number concentration and size distribution in a traffic–impacted area. Atmospheric Pollution Research, 6, 877-885, https://doi.org/10.5094/apr.2015.097, 2015.
Schwarz, J. P., Gao, R. S., Fahey, D. W., Thomson, D. S., Watts, L. A., Wilson, J. C., Reeves, J. M., Darbeheshti, M., Baumgardner, D. G., Kok, G. L., Chung, S. H., Schulz, M., Hendricks, J., Lauer, A., Kärcher, B., Slowik, J. G., Rosenlof, K. H., Thompson, T. L., Langford, A. O., Loewenstein, M., and Aikin, K. C.: Single-particle measurements of midlatitude black carbon and light-scattering aerosols from the boundary layer to the lower stratosphere. J. Geophys. Res., 111, https://doi.org/10.1029/2006jd007076, 2006.

Schwarz, J. P., Spackman, J. R., Fahey, D. W., Gao, R. S., Lohmann, U., Stier, P., Watts, L. A., Thomson, D. S., Lack, D. A., Pfister, L., Mahoney, M. J., Baumgardner, D., Wilson, J. C., and Reeves, J. M.: Coatings and their enhancement of black carbon light absorption in the tropical atmosphere. J. Geophys. Res., 113, https://doi.org/10.1029/2007jd009042, 2008.

Schwarz, J. P., Spackman, J. R., Gao, R. S., Perring, A. E., Cross, E., Onasch, T. B., Ahern, A., Wrobel, W., Davidovits, P., Olfert, J., Dubey, M. K., Mazzoleni, C., and Fahey, D. W.: The detection efficiency of the single particle soot photometer. Aerosol Sci. Technol., 44, 612-628, https://doi.org/10.1080/02786826.2010.481298, 2010.

Shiraiwa, M., Kondo, Y., Iwamoto, T., and Kita, K.: Amplification of light absorption of black carbon by organic coating. Aerosol Sci. Technol., 44, 46-54, https://doi.org/10.1080/02786820903357686, 2010.

Slowik, J. G., Cross, E. S., Han, J.-H., Davidovits, P., Onasch, T. B., Jayne, J. T., Williams, L. R., Canagaratna, M. R., Worsnop, D. R., Chakrabarty, R. K., Moosmüller, H., Arnott, W. P., Schwarz, J. P., Gao, R.-S., Fahey, D. W., Kok, G. L., and Petzold, A.: An inter-comparison of instruments measuring black carbon content of soot particles. Aerosol Sci. Technol., 41, 295-314, https://doi.org/10.1080/02786820701197078, 2007.

Spindler, G., Brüggemann, E., Gnauk, T., Grüner, A., Müller, K., and Herrmann, H.: A four-year size-segregated characterization study of particles pm10, pm2.5 and pm1 depending on air mass origin at melpitz. Atmos. Environ., 44, 164-173, https://doi.org/10.1016/j.atmosenv.2009.10.015, 2010.

Spindler, G., Grüner, A., Müller, K., Schlimper, S., and Herrmann, H.: Long-term size-segregated particle (pm10, pm2.5, pm1) characterization study at melpitz -- influence of air mass inflow, weather conditions and season. J. Atmos. Chem., 70, 165-195, https://doi.org/10.1007/s10874-013-9263-8, 2013.

Stein, A. F., Draxler, R. R., Rolph, G. D., Stunder, B. J. B., Cohen, M. D., and Ngan, F.: Noaa's hysplit atmospheric transport and dispersion modeling system. Bull. Am. Meteor. Soc., 96, 2059-2077, https://doi.org/10.1175/bams-d-14-00110.1, 2015.

Stephens, M., Turner, N., and Sandberg, J.: Particle identification by laser-induced incandescence in a solid-state laser cavity. Appl. Opt., 42, 3726-3736, https://doi.org/10.1364/AO.42.003726, 2003.

Taylor, J. W., Allan, J. D., Liu, D., Flynn, M., Weber, R., Zhang, X., Lefer, B. L., Grossberg, N., Flynn, J., and Coe, H.: Assessment of the sensitivity of core / shell parameters derived using the single-particle soot photometer to density and refractive index. Atmos. Meas. Tech., 8, 1701-1718, https://doi.org/10.5194/amt-8-1701-2015, 2015.

Ueda, S., Nakayama, T., Taketani, F., Adachi, K., Matsuki, A., Iwamoto, Y., Sadanaga, Y., and Matsumi, Y.: Light absorption and morphological properties of soot-containing aerosols observed at an east asian outflow site, noto peninsula, japan. Atmos. Chem. Phys., 16, 2525-2541, https://doi.org/10.5194/acp-16-2525-2016, 2016.

van de Hulst, H. C.: Light scattering by small particles. J. Wiley ; Chapman and Hall, New York : London, 1957.

Wei, Y., Ma, L., Cao, T., Zhang, Q., Wu, J., Buseck, P. R., and Thompson, J. E.: Light scattering and extinction measurements combined with laser-induced incandescence for the real-time determination of soot mass absorption cross section. Anal Chem, 85, 9181-8, https://doi.org/10.1021/ac401901b, 2013.

Willis, M. D., Lee, A. K. Y., Onasch, T. B., Fortner, E. C., Williams, L. R., Lambe, A. T., Worsnop, D. R., and Abbatt, J. P. D.: Collection efficiency of the soot-particle aerosol mass spectrometer (sp-ams) for internally mixed particulate black carbon. Atmos. Meas. Tech., 7, 4507-4516, https://doi.org/10.5194/amt-7-4507-2014, 2014.

Zanatta, M., Gysel, M., Bukowiecki, N., Müller, T., Weingartner, E., Areskoug, H., Fiebig, M., Yttri, K. E., Mihalopoulos, N., Kouvarakis, G., Beddows, D., Harrison, R. M., Cavalli, F., Putaud, J. P., Spindler, G., Wiedensohler, A., Alastuey, A., Pandolfi, M., Sellegri, K., Swietlicki, E., Jaffrezo, J. L., Baltensperger, U., and Laj, P.: A european aerosol phenomenology-5: Climatology of black carbon optical properties at 9 regional background sites across europe. Atmos. Environ., 145, 346-364, https://doi.org/10.1016/j.atmosenv.2016.09.035, 2016.

Zanatta, M., Laj, P., Gysel, M., Baltensperger, U., Vratolis, S., Eleftheriadis, K., Kondo, Y., Dubuisson, P., Winiarek, V., Kazadzis, S., Tunved, P., and Jacobi, H. W.: Effects of mixing state on optical and radiative properties of black carbon in the european arctic. Atmos. Chem. Phys., 18, 14037-14057, https://doi.org/10.5194/acp-18-14037-2018, 2018.

Zhang, X., Mao, M., Yin, Y., and Wang, B.: Absorption enhancement of aged black carbon aerosols affected by their microphysics: A numerical investigation. Journal of Quantitative Spectroscopy and Radiative Transfer, 202, 90-97, https://doi.org/10.1016/j.jqsrt.2017.07.025, 2017.

Zhang, Y., Favez, O., Canonaco, F., Liu, D., Močnik, G., Amodeo, T., Sciare, J., Prévôt, A. S. H., Gros, V., and Albinet, A.: Evidence of major secondary organic aerosol contribution to lensing effect black carbon absorption enhancement. npj Clim. Atmos. Sci., 1, https://doi.org/10.1038/s41612-018-0056-2, 2018.

Zotter, P., Herich, H., Gysel, M., El-Haddad, I., Zhang, Y., Močnik, G., Hüglin, C., Baltensperger, U., Szidat, S., and Prévôt, A. S. H.: Evaluation of the absorption ångström exponents for traffic and wood burning in the aethalometer-based source apportionment using radiocarbon measurements of ambient aerosol. Atmos. Chem. Phys., 17, 4229-4249, https://doi.org/10.5194/acp-17-4229-2017, 2017.

Supplement

Table S1. Characteristics of the campaign Periods (median and IQR)

periods parameters	period 1 (02. Feb 09:00 - 05. Feb 21:00)	period 2 (05. Feb 21:00 - 14. Feb 22:00)	period 3 (14. Feb 22:00 - 23. Feb 00:00)	short plume (18. Feb 17:00 - 19. Feb 07:00)
Dominant air mass origin	S to SW	NE to SE	W	NW
Local wind speed (m/s)	1.2 (0.8–1.7)	3.4 (2.7–4.1)	4 (2.5–6.3)	1.5 (1.2–1.7)
Gas ratio of SO_2 to NO_X	0.08 (0.04– 0.11)	0.63 (0.28– 0.83)	0.12 (0.09– 0.19)	0.09 (0.08– 0.09)
D_{modal_rBC} (nm)	190 (183–193)	239 (232–242)	181 (169–199)	242 (192–298)
Total aerosol concentration (µg m^{-3})	10.6 (8.7–11.7)	23.0 (20.4–27.2)	10.9 (8.1–15.8)	8.1 (6.6–10.2)
Mass fractions of organics (%)	36 (35–38)	37 (33–39)	29 (23–35)	28 (25–31)
Mass fractions of BC (%)	12 (10–16)	14 (12–15)	7 (4–11)	14 (9–21)
Mass fractions of nitrate (%)	24 (20–28)	18 (17–20)	35 (25–41)	27 (25–30)
Mass fractions of sulfate (%)	13 (11–17)	19 (17–22)	12 (11–15)	11 (10–12)

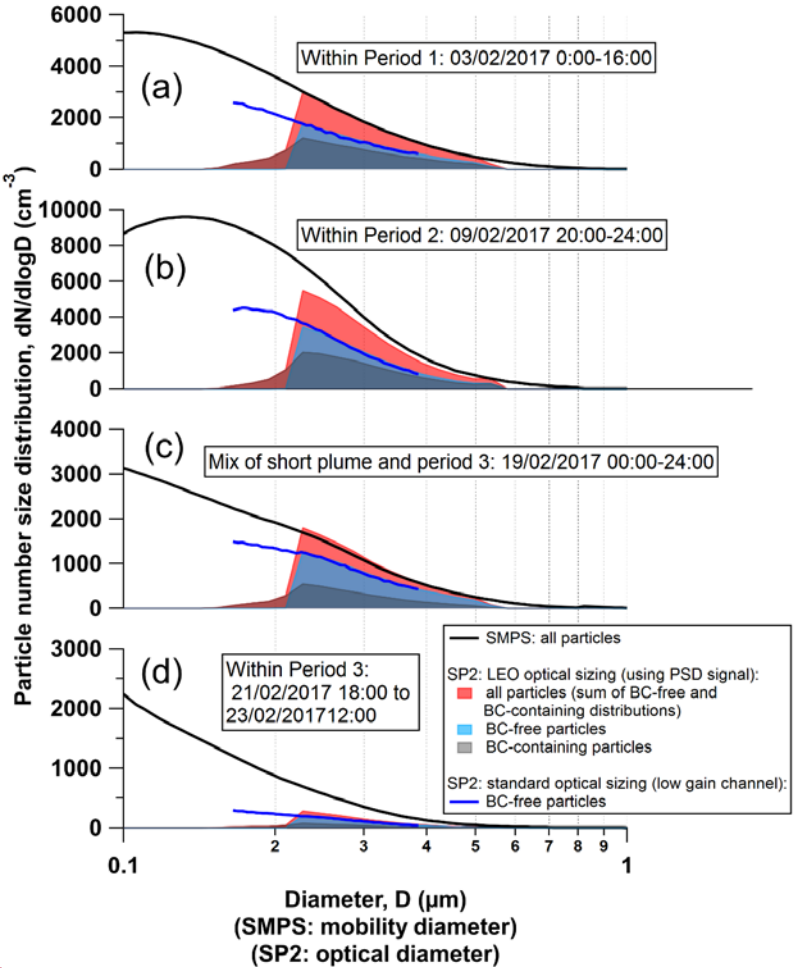

Figure S1. Cross check of total particle number size distribution measured by SP2 compared with that from SMPS.

Commented [MRL7]: This is a new version of this figure: colored areas have been made semi-transparent so that full distributions are visible

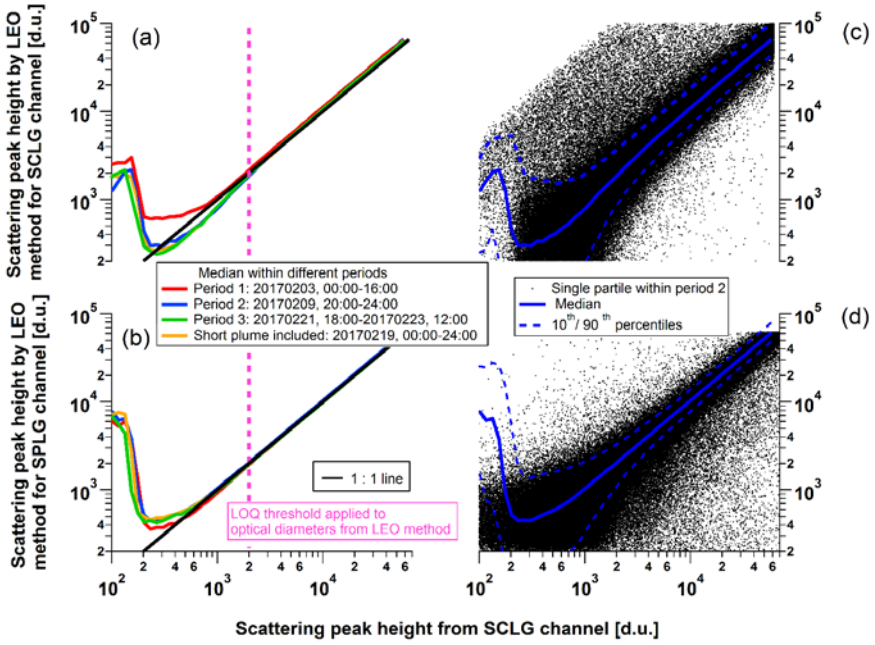

Figure S2. Verification of LEO method by BC-free particles. (a) Median of LEO scattering peak height vs standard scattering peak height from low gain scattering detector (SCLG) for four example days during different periods of the campaign. Scaling factors were applied to correct minor bias in the LEO fit analysis, i.e. to make the LEO fit results match the standard peak analysis. (b) LEO scattering peak height retrieved from the low gain position sensitive detector (SPLG) vs standard scattering peak height from the low gain scattering channel. (Adjustable scaling factors were applied to tie the LEO-fit to the calibration of the low gain scattering channel. (c) and (d) show single particle data corresponding to (a) and (b), respectively.

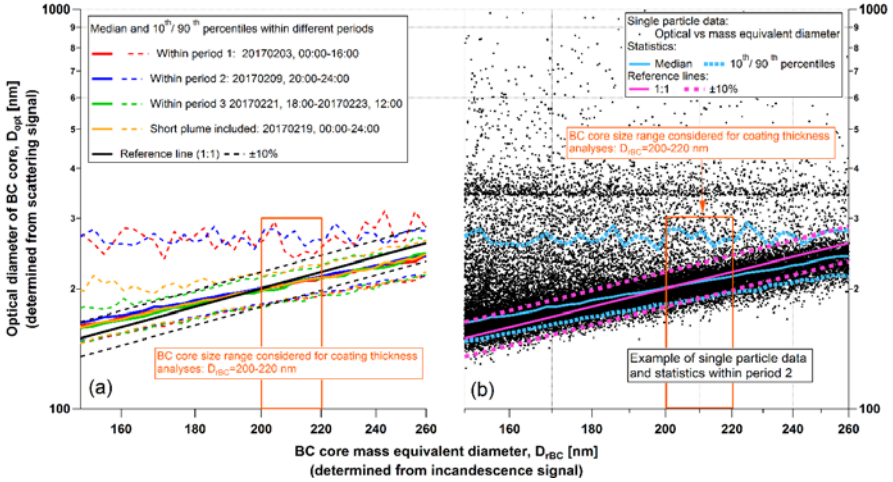

Figure S3. Verification of LEO fit: Optical diameter of the bare BC core compared with the rBC mass equivalent diameter. (a) Median and 10th and 90th percentiles of the single particle data. (b) Single particle data and corresponding statistics for period 2 as an example. The LEO fit results were used for the BC core diameter range from 200 nm to 220 nm, in which uncoated and coated particles can be sized optically. Within this size range the median values fall on the1 to 1 line within 2 %. This ensures accuracy of the reported coating thickness for bare BC particles, i.e. that particle reported to have a coating thickness of zero indeed represent uncoated BC, except for the random noise present on single particle level.

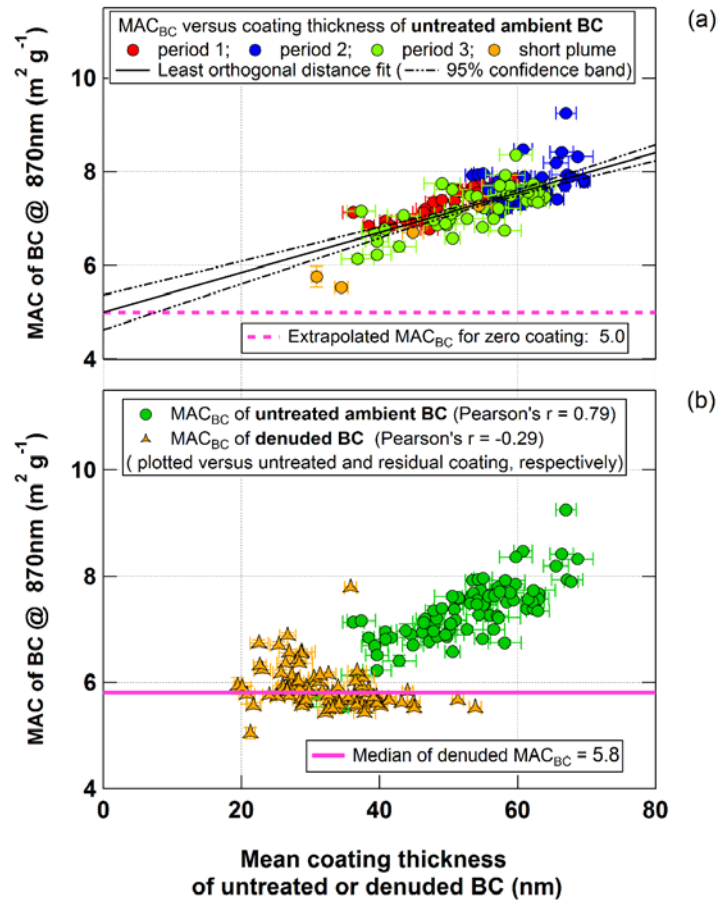

Figure S4. Repeated version of Fig. 6 in the main text with one change made: in panel b) the denuded MAC_{BC} values are plotted against the coating thickness of the denuded particles, rather than the coating thickness of the untreated particles as in Fig. 6.

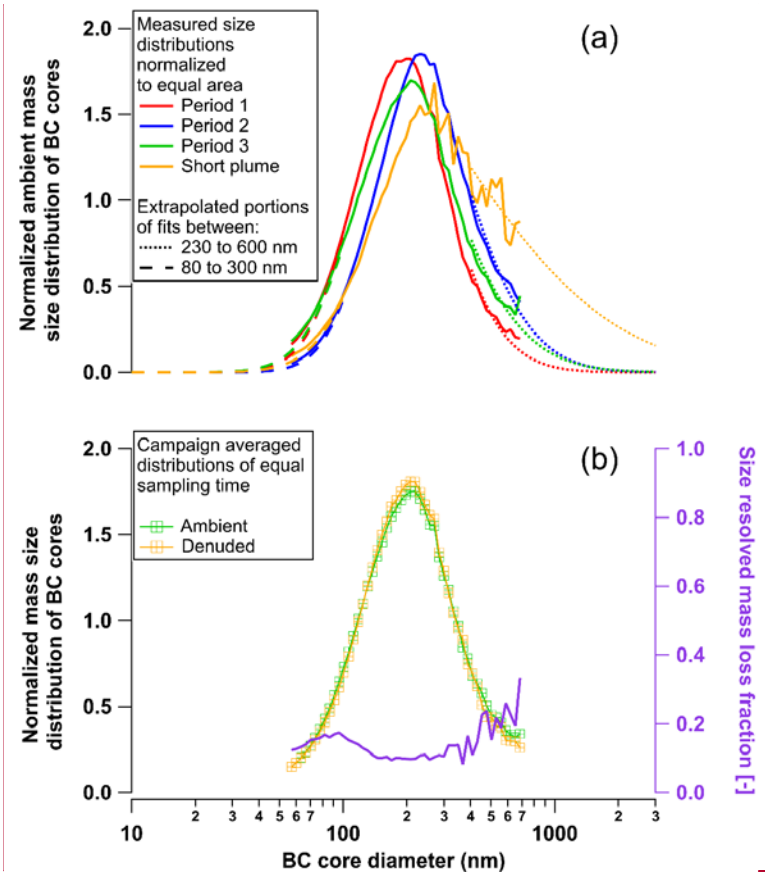

Figure S5. Normalized rBC mass size distributions as a function of BC core mass equivalent diameter. ~~Ambient averaged~~Average distributions measured during ambient conditions for each of the different campaign periods are shown in (a), and ambient ~~compared with~~ and denuded ~~data for complete common measurement period~~distributions averaged over the full campaign period (with equal sampling times) are shown in (b). The size resolved mass loss fraction within the catalytic stripper, computed from ~~comparing~~ the denuded ~~with~~ and ambient size distributions, is also shown in (b). Panel (a) displays the extrapolated portions of two different types

Commented [MRL8]: This is a new version of this figure: extrapolated portions of the two different types of lognormal fits that were calculated for each period are now displayed in the up panel

of lognormal fits that were applied to the measured distributions for each period in order to estimate the missing BC mass beyond the lower and upper SP2 detection limits.

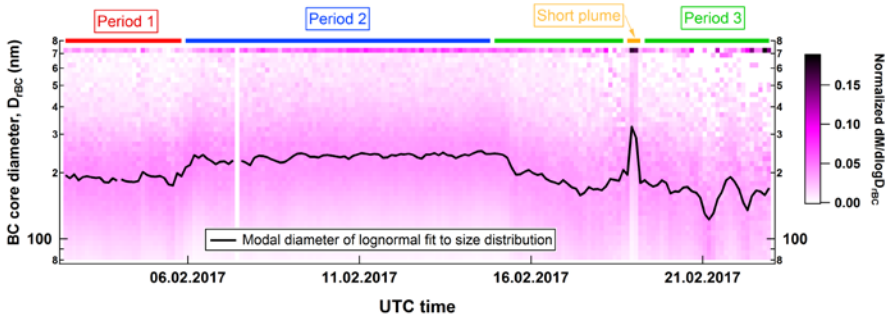

Figure S6. Time series of the normalized ambient rBC mass size distribution (at 3 h time resolution) as a function of BC core mass equivalent diameter (D_{rBC}). The overflow size bin including all BC particles D_{rBC} greater than ~700 nm is also shown.

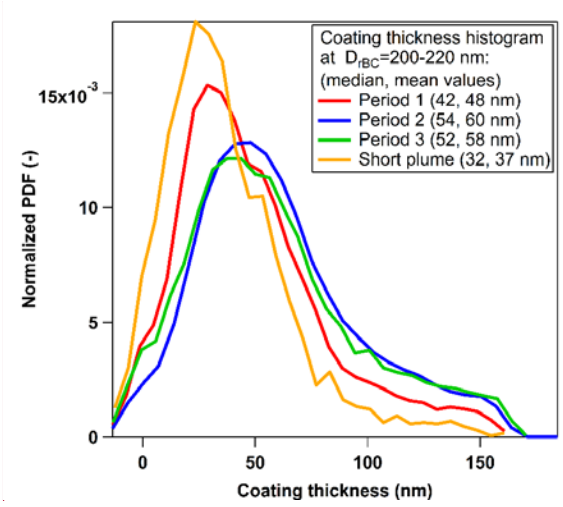

Figure S7. Histograms of BC particle coating thickness on single particle level separately shown for the three periods and the short plume.

Commented [MRL9]: This is a new version of this figure: me values have been added to the figure legend

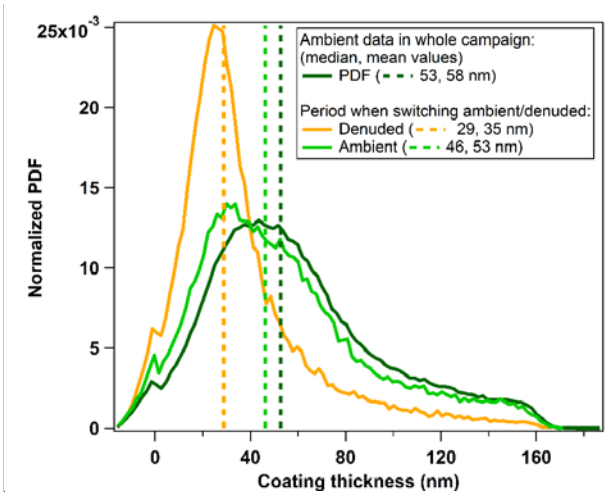

1215

Figure S8. Histograms of BC particle coating thickness on single particle level for rBC mass equivalent core diameters between 200 nm to 220 nm. Histograms are separately shown for the whole campaign (ambient sample only) and for the period when the denuder was
1220 **operated (ambient and denuded samples).**

Commented [MRL10]: This is a new version of this figure: m values have been added to the figure legend

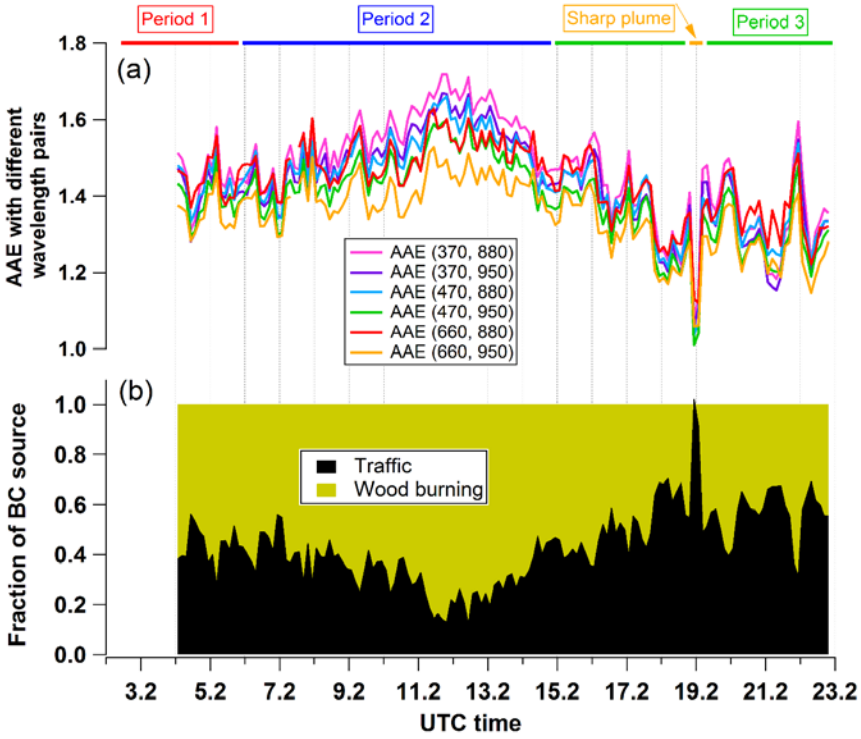

Figure S9. (a) Time series at 3 h time resolution of AAE of different pairs of wavelengths, and (b) the estimated fractional contribution of traffic and wood burning emissions to BC mass. The attribution of sources was done using the so-called "aethalometer model" using the coefficients reported in Zotter et al. (2017). Note that traffic and wood burning fractions are upper limits as BC from coal burning, which is potentially present, could be assigned to either source.

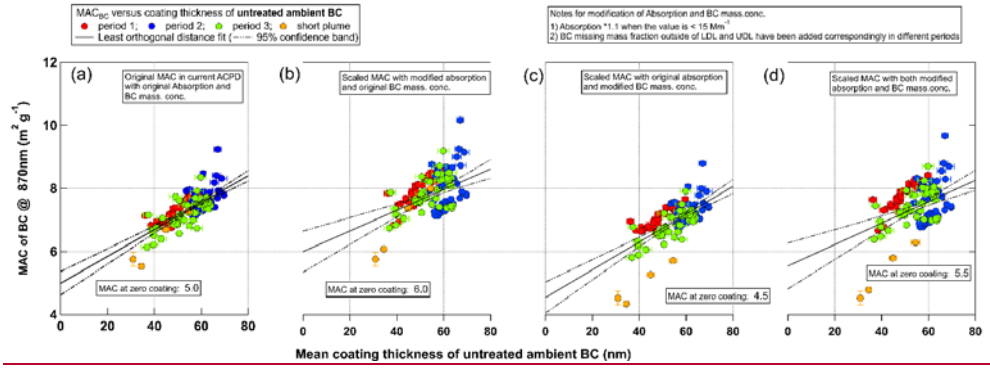

Figure S10. Panel a) is a repeated version of Fig. 6a in the main text. Panel b) displays the same quantities but with an additional correction factor of 1.1 applied to the MAC of BC values corresponding to absorption coefficients less than 15 Mm^{-1} (as motivated by Fig. 2 and the discussion in Sect. 2.4.2.2), panel c) displays the same quantities but with period-dependent missing mass correction factors applied to the MAC of BC values (as discussed in Sect. 2.4.1), and panel d) displays the same quantities but with both the loading-dependent absorption scaling factors and period-dependent missing mass correction factors applied to the MAC of BC values